The Role of SHORT HYPOCOTYL UNDER BLUE 1 in *Arabidopsis* Seed and Seedling Development

A DISSERTATION
SUBMITTED TO THE FACULTY OF THE GRADUATE SCHOOL
OF THE UNIVERSITY OF MINNESOTA
BY

Yun Zhou

IN PARTIAL FULFILLMENT OF THE REQUIREMENTS
FOR THE DEGREE OF
DOCTOR OF PHILOSOPHY

Advised by Dr. Min Ni

January 2010

Acknowledgements

I would like to sincerely appreciate my advisor Dr. Min Ni for his exceptional and enormous guidance during my Ph.D. thesis research. With great passion, insightful views, and the creative use of scientific approaches, he has been a great model for me in my scientific career. I am always encouraged by his dedication and persistence for research, which helped me get through all the difficulties and frustrations. And I very much appreciate his patient corrections and suggestions on my scientific writings and presentations, shaping me into a more and more professional scientist.

I would like to sincerely thank faculty members of my advisory committee, Dr. Jane Glazebrook, Dr. William Gray, Dr. Pete Lefebvre, and Dr. Neil Olszewski for their valuable suggestions and continuous encouragement on my thesis research. Their critical comments on my thesis proposal made me think about my research more broadly and carefully, and their helpful suggestions on my experimental designs and result interpretation saved my time and get me out of confusions. In particular, I greatly appreciate Dr. Gray for generously providing me the Superdex 200 gel filtration column and the ÄKTA FPLC system for my research, as well as his suggestion on the protein purification and antibody generation.

I thank the Arabidopsis Biological Resource Center (ABRC, Columbus, OH) for *Arabidopsis* T-DNA insertion mutant seeds. I am grateful to Dr. David Marks for the pEZT-NL vector and the help on microscopes; Dr. Olszewski for providing me the agrobacterium strain Agl1; Dr. Scott D. Michaels for providing me the *flc-3* mutant, and Dr. Sibum Sung for valuable suggestions on flowering experiments. I thank Gilbert

Ahlstrand from CBS imaging center for his help with scanning electron microscopy, and Tom Krick from the Center for Mass Spectrometry and Proteomics for his help in fatty acid analysis.

I would like to express my appreciation to the Plant Biological Sciences Graduate Program for offering me the graduate assistantship to pursue my degree. Thanks to the lab members especially Xiaojun Kang and Xiaodong Sun in Ni lab who have helped my research all the time. Thanks to Kai-Ting Fan for lots of technical help from her with the gel-filtration experiments. Thanks to Dr. Nora Plesofsky and Dr. Bob Brambl for generously providing me the sonication system. I also would like to thank many faculty, postdoctoral associates, and graduate students in the department for their help and support during the course of my study, research, and life for which I did not mention above. Additionally, I acknowledge the contribution of Dr. Xiansheng Zhang lab, especially Xiangyu Zhao and Xiaojuan Zhang, from Shandong Agriculture University in China to section (Figure 28) and *in situ* hybridization experiments (Figure 32). Last but not the least, I thank my parents and many friends for their continuous encouragements and inspirations that accompanied me during the years of my graduate study, through all the good days and bad days.

This research was supported by the National Science Foundation (NSF), the National Research Initiative of the USDA, the College of Food, Agriculture, and Natural Sciences (CFANS) graduate research fellowship, the Microbial and Plant Genomics Institute (MPGI) graduate research fellowship, the Philip C. Hamm Memorial Graduate Student Scholarship, and the Plant Biological Sciences Graduate Program summer fellowship and travel awards at the University of Minnesota, Twin Cites.

Abstract

SHORT HYPOCOTYL UNDER BLUE 1 or SHB1 was previously identified as a negative regulator of the cryptochrome-mediated blue light response in *Arabidopsis* early seedling development. *shb1*, a T-DNA insertional loss-of-function allele, showed a short hypocotyl phenotype only under blue light, whereas *shb1-D*, a gain-of-function over-expression allele, showed a long hypocotyl phenotype under blue as well as red or far red light. SHB1 is a nuclear protein and contains a N-terminal SPX domain and a C-terminal EXS homologous to yeast SYG1 protein family. Using a biochemical approach, I found that SHB1 is anchored to a large protein complex through both of its SPX and EXS domains. In a genetic screen, I identified five mis-sense mutations within or nearby its N-terminal SPX domain and these mutation impaired its biological function and proper assembly into a protein complex. In contrast, the C-terminal EXS domain, when over-expressed, created a dominant negative phenotype and interfered with the assembly of the endogenous SHB1 into a native protein complex. SHB1 also functions in flowering timing control and this involvement is likely related to its light signaling activity. In addition, SHB1 plays a specific role in a quite different developmental phase, seed development. SHB1 regulates the timing of endosperm cellularization and promotes the subsequent embryo development through its control over both cell division and cell expansion. SHB1 associates with the promoters of *MINISEED3* (*MINI3*), a WRKY transcription factor gene, and *HAIKU2* (*IKU2*), an LRR receptor kinase gene *in vivo*, and activates the expression of these two genes required for endosperm development. In summary, SHB1 plays a novel signaling role in both *Arabidopsis* seed and early seedling

development, and this conserved function may be implicated for some SHB1-like proteins in many other organisms.

Table of Contents

List of Figures

Chapter I

Literature Review

I. Light Signaling in Arabidopsis

Light signals trigger de-etiolation or photomorphogenic responses in most plants, including the inhibition of hypocotyl elongation, the opening of the cotyledons and hypocotyl hook, the expansion of cotyledons, and the development of chloroplasts (Chen et al., 2004). The effective wavelengths that regulate photomorphogensis are red and far-red light perceived by phytochromes and UV-A/blue light perceived by cryptochromes. Among the five phytochrome members in *Arabidopsis*, phytochrome A (phyA) mainly regulates far-red light-mediated de-etiolation responses, and phyB together with phyC, phyD, and phyE regulate red light-mediated de-etiolation responses (Neff et al., 2000; Huq and Quail, 2005). Cryptochrome1 (cry1) and cryptochrome2 (cry2) specifically regulate photomorphogensis under blue light (Ahmad et al., 1993; Lin et al., 1998). Blue light triggers the phosphorylation of cry1 and cry2 and activates a series of signaling events or activities downstream of the blue light perception (Shalitin et al., 2002, 2003). Recently, a basic-helix-loop-helix transcription factor has been shown to interact with photo-activated cry2, suggesting its function in early photoreceptor signaling in response to blue light (Liu et al., 2008).

Other components downstream of crys include SUB1 (SHORT UNDER BLUE1) and PP7 (PHOSPHATASE 7). SUB1 is a cytosolic calcium-binding protein and acts in both blue and far-red light pathways since *sub1* showed a short hypocotyl phenotype under both blue and far-red light (Guo et al., 2001). PP7 is a Ser/Thr phosphatase and

down-regulation of *PP7* caused a long hypocotyl phenotype under blue light (Mφller et al., 2003). Recently, Genoud et al. (2008) have reported possible involvement of PP7 in phytochrome-mediated responses. HFR1 (LONG HYPOCOTYL IN FAR-RED1) is an atypical basic helix-loop-helix transcription factor and was shown previously for its function in far-red light signaling (Fairchild et al., 2000). HFR1 also plays a role in the regulation of several blue light–mediated responses (Duek and Fankhauser, 2003; Zhang et al., 2008). In addition, PIF4 (PHYTOCHROME INTERATING FACTOR 4), HRB1 (HYERSENSTIVE TO RED AND BLUE1), and OBP3 (OBF BINDING PROTEIN3) are all involved in red and blue light-mediated de-etiolation responses (Huq and Quail, 2002; Kang et al., 2005; Ward et al., 2005)

It has been previously shown that SHB1 (SHORT HYPOCOTYL UNDER BLUE 1) acts negatively in cryptochrome-mediated blue light responses in *Arabidopsis* (Kang and Ni, 2006). *shb1*, a T-DNA insertion loss-of-function allele, showed a short hypocotyl phenotype only under blue light, whereas *shb1-D* (short hypocotyl under blue 1, Dominant), a gain-of-function overexpression allele, showed a long hypocotyl phenotype under blue as well as red or far red light (Kang and Ni, 2006). Obviously, over-accumulation of SHB1 protein expands its signaling activity to a broader spectrum of light wavelengths. SHB1 contains an N-terminal SPX domain and a C-terminal EXS domain homologous to yeast SYG1 and mouse XPR1 protein (Kang and Ni, 2006). The SPX domain (pfam03105 family) is named after SYG1, PHO81, and XPR1, whereas as the EXS domain (pfam03124 family) is named after ERD1, XPR1 and SYG1. In yeast, the SPX domain in SYG1 (SUPPRESSOR OF YEAST GPA1) protein can rescue the

lethal phenotype caused by a mutation in a G-protein a subunit. The truncated SYG1 protein can also directly interact with a G-protein ß subunit to inhibit signal transduction in yeast (Spain et al., 1995). PHO81 (PHOSPHATASE 81) is involved in inhibition of cyclin dependent kinase (CDK) activity to regulate the phosphate homeostasis in yeast and *Arabidopsis* (Schneider et al., 1994; Neef and Kladde, 2003; Hamburger et al., 2002). XPR1 (XENOTROPIC AND POLYTROPIC RETROVIRUS RECEPTOR) works as putative xenotropic and polytropic retrovirus receptor in G protein-coupled signal transduction in humans (Battini et al., 1999; Tailor et al., 1999; Yang et al., 1999). ERD1 (ER RETENTION DEFECTIVE 1) is required for the targeting and processing of glycoproteins in yeast (Hardwick et al., 1990). To date, the function of most SPX and EXS domains remain largely unknown with respect to signal transduction, growth, and developmental regulation. In general, most of the SHB1 homologs from other organisms may have a membrane destination while as some SPX domain containing proteins in higher plants localize in nucleus (Wang et al., 2009). SHB1 is localized to the nucleus (Kang and Ni, 2006) and is associated in vivo with the promoters of two genes that function in endosperm development (Chapter IV; Zhou et al., 2009). Therefore, SHB1 may play quite a unique biochemical role compared to the signaling transduction functions of its homologs across various organisms.

II. Photoperidic flowering in Arabidopsis

Plant flowering time is controlled by the integration of environmental signals with the developmental status of a plant (Searle and Coupland, 2004). The exogenous

regulations include day-length sensing, light quality perception, and temperature response or vernalization. The internal signaling cascades in response to certain development stages or leave numbers are defined as autonomous pathway. In addition, gibberellic acid (GA) pathway seems to act independently of either exogenous regulations or autonomous pathway (Mouradov et al., 2002; Boss et al., 2004). *Arabidopsis* is a facultative long-day plant, and thus flower initiation is accelerated under long days but delayed under short days (Searle and Coupland, 2004).

CONSTANS (CO), which encodes a zinc finger protein, is a key component in the photoperiodic flowering pathway (Putterill et al., 1995). The expression of *CO* is regulated by both the circadian clock and the plant photoreceptors. Among the photoreceptors, phyB mediates a red light inhibition of flowering under both long days and short days. phyA promotes flowering possibly through two independent mechanisms: suppressing phyB function and promoting flowering independent of phyB (Lin, 2000; Mockler et al., 2003). In response to extended photoperiods, cry2-deficient *Arabidopsis* plants have a delayed flowering phenotype (Guo et al., 1998). The abundance of *CO* mRNA was reduced in *phyA* but was slightly increased in *phyB* under long days (Cerdán and Chory, 2003; Putterill et al., 1995; Tepperman et al., 2001). The expression of *FT* was also reduced in the *phyA* and *cry2* mutants under long days (Yanovsky and Kay, 2002). In addition, CO protein is subject to posttranscriptional regulation by light signals of various wavelengths (Valverde et al., 2004). crys and phyA stabilize CO protein under blue or far-red light, whereas phyB promotes the degradation of CO under red light, generating a daily rhythm in the abundance of CO. In turn, CO regulates the expression

of *FT* (*FLOWERING LOCUS T*) or *SOC1* (*SUPPRESSOR OF OVEREXPRESSION OF CONSTANS 1*), integrators of several flowering pathways (Cerdán and Chory, 2003; Samach et al., 2000; Suárez-López et al., 2001; Yanovsky and Kay, 2002).

The autonomous pathway mutants display photoperiod-independent late flowering and strong acceleration of flowering in response to prolonged exposure to cold (Koornneef et al., 1991). The central quantitative floral repressor *FLC (FLOWERING LOCUS C)* encodes a MADS-domain transcription factor and integrates vernalization and autonomous pathway in *Arabidopsis* (Michaels and Amasino, 1999; Sheldon et al., 1999; Michaels and Amasino, 2001). FLC represses flowering, at least partly, by directly binding to specific regulatory elements in the *FT* and *SOC1* loci (Hepworth et al., 2002; Helliwell et al., 2006; Searle et al., 2006). Several genes upstream of *FLC* in this pathway including *FVE*, *FLD*, *LD* (*LUMINIDEPENDENS*), *FLK*, *FY*, *FCA* and *FPA* have also been isolated (Koornneef et al., 1991; Lee et al., 1994; Chou and Yang, 1998; Schomburg et al., 2001; Lim et al., 2004; Mockler et al., 2004). *ld-3* mutant flowers late in both longs and short days but the delay of flowering is more extreme in short days (Lee et al., 1994). The flowering of the *ld* mutants can be accelerated by vernalization in both long and short days. *LD* encodes a nuclear protein, and LD along with other autonomous pathway components negatively regulates the expression of *FLC* (Michaels and Amasino, 1999).

The regulation of chromatin structure via diverse histone modifications is a crucial molecular mechanism in the control of *FLC* expression (He and Amasino, 2005). Histone acetylation and trimethylation at lysine 4 of histone 3 (triMeH3K4) are correlated with active transcription of *FLC* (He and Amasino, 2005). The enrichment in the

triMeH3K4 histone mark depends on the activity of the PAF1 complex, which consists of ELF7 (EARLY FLOWERING 7), ELF8, VIP4 (VERNALIZATION INDEPENDENCE 4) and VIP5 (He and Amasino, 2005). The expression of *FLC* was increased in *ld* mutant, and a strong increase was observed in triMeH3K4 in region IV that corresponds to the 5' UTR and the first exon of the *FLC* locus (Lee et al., 1994). The histone H3 acetylation (H3Ac) was also increased in the region around the translation initiation start, the first exon, and the 5' region around the first intron of the *FLC* locus in the *ld* mutant (Domagalska et al., 2007).

III. Seed development in *Arabidopsis*

In angiosperms, double fertilization leads to the formation of a diploid embryo and a triploid endosperm as the endosperm arises from the central cell that contains two identical haploid genomes. The endosperm constitutes the major volume of the mature seed in monocots and some dicots. In *Arabidopsis* and many other dicots, seed development is marked by two distinct phases and the embryo grows to full size and replaces most of the endosperm at maturity (Sundaresan, 2005). In an initial phase, a rapid growth and proliferation of the endosperm occurs to result in a large increase in size (Boisnard-Lorig et al., 2001). Then, the embryo growth takes place at the expense of endosperm during the second phase. At maturity, the seed contains only a single layer of endosperm cells, and the maternal integument ultimately becomes the seed coat (Scott et al., 1998; Garcia et al., 2003). The seed coat and endosperm growth in *Arabidopsis* precedes embryo growth, and the seed reaches almost its final size before the

enlargement of the embryo. Therefore, the seed size is determined by the coordinated growth of the diploid embryo, the triploid endosperm, and the diploid maternal ovule.

The molecular mechanisms that underlie the control over seed size remain elusive. Both maternal and non-maternal factors are involved in seed size regulation and crosstalk occurs between maternal and zygotic tissue to coordinate the mature seed size (Garcia et al., 2005). In *Arabidopsis*, increased dosage of paternal genome in endosperm increases seed size, whereas increased dosage of maternal genome has the opposite effect (Scott et al., 1998). This imbalance shows characteristic endosperm phenotypes such as delayed cellularization of the peripheral endosperm and hypertrophy of the chalazal endosperm and associated nodules (Scott et al., 1998). Mutations in *DNA METHYLTRANSFERASE1* and *DECREASE IN DNA METHYLATION1* dramatically reduce DNA methylation and cause parent-of-origin effects on F1 seed size (Xiao et al., 2006). Pollination of *met1-6* or *ddm1-2* pistils with wild-type pollens produced large F1 seeds, and reciprocal crosses generated small F1 seeds. The endosperm of the small seeds with a hypomethylated paternal genome has an early endosperm cellularization and an ultimate smaller endosperm volume. By contrast, larger F1 seeds with a hypomethylated maternal genome show delayed endosperm development and a larger endosperm volume.

The seeds of triple cytokinin receptor mutant are enlarged as twice the size of the wild-type seeds, and genetic analysis suggests that cytokinin may act through a maternal and/or endospermal control of embryo size (Hutchison et al., 2006; Riefler et al., 2006). Mutations in the transcription factor *APETALA2* increase seed size due to an increase in both embryo cell number and cell size (Jofuku et al., 2005; Ohto et al., 2005). *ap2*

mutants also accumulate more seed oil and proteins, and the seed trait is passed through the maternal sporophyte and the endosperm genomes (Jofuku et al., 2005; Ohto et al., 2005). The mechanism by which AP2 regulates seed size is still unclear, but it may act through alteration of sugar metabolism or the ratio of hexose to sucrose during seed development (Ohto et al., 2005).

In contrast, mutations in either *IKU2* (*HAIKU2*) or *MINI3* (*MINISEED3*) reduce seed size, and the seed phenotypes of the mutants depend on the genotype of the embryo and endosperm but not on the genotype of the maternal ovule (Luo et al., 2005). *MINI3* encodes a WRKY family transcription factor, and is expressed in both the endosperm and the embryo. *IKU2* encodes a leucine-rich repeat (LRR) receptor kinase, and is expressed in the endosperm but not in the embryo or elsewhere of the plant. Interestingly, *IKU2* expression is down-regulated in the *mini3* mutant and *MINI3* may therefore act upstream of *IKU2* (Luo et al., 2005). The reduced seed size of the *iku* mutants is closely associated with a reduced growth of endosperm and a reduced proliferation of embryo after the early torpedo stage (Garcia et al., 2003). The reduced growth of endosperm is correlated with a premature cellularization of the endosperm, and IKU2 and MINI3 may regulate endosperm size through the timing of cellularization (Garcia et al., 2003; Luo et al., 2005). AGL62 is another regulator of endosperm cellularization as the endosperm cellularizes prematurely in *agl62* seeds (Kang et al., 2008). *EXS/EMS* also encodes a putative LRR receptor kinase and is expressed in both embryo and endosperm (Canales et al., 2002; Zhao et al., 2002). The seeds of *exs-2* are smaller at maturity due to reduced cell size but not cell number (Canales et al., 2002).

Integument, which contains whole maternal genome, also plays role in seed size determination independent of fertilization in *Arabidopsis*. For example, *Arabidopsis mnt*/*arf2* (*megaintegumenta*/*auxin response factor 2*) mutant causes extra cell division in the integuments surrounding the mutant ovules, enlarges seed coats, and increases seed size (Schruff et al., 2005). Another player in seed development, TTG2, also modulates seed size through its regulation on integument cell elongation (Johnson et al., 2002; Garcia et al., 2005).

Chapter II

SHB1 functions in light regulated seedling development

Introduction

In this chapter, I explore the function of SHB1 in light signal transduction. I conducted gain-of-function deletion analysis of SHB1 in transgenic *Arabidopsis* and identified several intragenic mutations through forward genetic screen (Zhou and Ni, *submitted*). The transgenic plants that overexpress SHB1 N-terminal SPX domain phenocopied *shb1-D* with a long hypocotyl phenotype under red, far-red, and blue light. In contrast, the transgenic plants that overexpress SHB1 C-terminal EXS domain showed a short hypocotyl phenotype under blue light, similar to that of the *shb1* knockout mutant. Six intragenic mis-sense mutations within or nearby the SPX domain were also identified from *shb1-D* suppressor screen, and the mutations fully or partially suppressed the long hypocotyl phenotype of *shb1-D* under blue light. With a gel filtration technique, the function of SHB1 domains and the consequence of the SHB1 mis-sense mutations in relation to the assembly of SHB1 into a large protein complex were further explored.

Materials and Methods

Plant materials, double mutants, and phenotypic analysis

The *Arabidopsis thaliana shb1-D* (Ws), *shb1* (Col), *pif4* (Ws), and *hfr1-201* (Col) mutants were described previously (Kang et al., 2005; Kang and Ni, 2006). *C225-1 hfr1-201* (Col) and *N320-2 pif4* (Ws) were generated by crossing and double homozygous

lines were genotyped based on their basta resistance for the transgenes and kanamycin resistance for either *pif4* or *hfr1-201* as previously described (Kang and Ni, 2006). The homozygous lines were further confirmed by PCR-genotyping. Monochromatic red, far-red, or blue light was generated through LED SNAP-LITE (Quantum Devices). The quantification of hypocotyl elongation, and chlorophyll and anthocyanin content were performed as described previously (Kang et al., 2005).

Constructs and plasmids

Full-length *SHB1* genomic DNA or truncated derivatives were amplified from BAC T30C3 with end-incorporated SalI and BamHI restriction sites and cloned into the XhoI and BamHI sites of pEZT-NL. The full-length, N320, N420, and N520 truncations shared the same forward primer 5'-ACGCGTCGACATGAGGTTTGGGAAAGAGT-3'. Reverse primers for N320, N420 and N520 truncations were 5'-CGCGGATCCGCATTGGAGAAATGTTCAATGA -3', 5'-CGCGGATCCGCTTGTTTGAATCCAAAGA -3', and 5'-CGCGGATCCGCTGTTAGTTGATCTCCCAAGA -3', respectively. The full-length, C225, C325, and C425 truncations shared the same reverse primer 5'-CGCGGATCCGCATTGTTATGATGATCTCCA -3'. The forward primers for C225, C325, C425 truncations were 5'-ACGCGTCGACATGCAACTAACAAGCCAGGTTCGA-3', 5'-ACGCGTCGACATGGGCACTGAACTTGGTTATA-3', and 5'-ACGCGTCGACATGGTTCAAGCACTGAGGAGTCTA- 3', respectively.

Real-time RT-PCR analysis

The RNA isolations, reverse transcription and real-time PCR analysis were performed as described previously (Zhou et al., 2009). The primers used in qRT-PCR analysis for *HFR1*, *PIF4*, *SHB1*, *CAB3*, and *UBQ10* were described previously (Kang and Ni, 2006; Zhou et al., 2009).

Protein extraction and gel filtration chromatography

Sample preparations for gel filtration chromatography were performed as described (Hardtke et al. 2000; Zhang et al. 2008). Briefly, 7-day-old *Arabidopsis* seedlings were homogenized in extraction buffer that contains 50 mM Tris-HCl pH 7.5, 150 mM NaCl, 10 mM $MgCl_2$, 1 mM EDTA, 10% glycerol, 1mM DTT, 1 mM PMSF (phenylmethylsulfonyl fluoride), and 1X Halt™ protease inhibitor cocktail (Pierce). The homogenates were centrifuged twice at 13,200 rpm for 15 min at 4°C, and the final supernatant was filtered through a 0.2 μm filter (Pall Corporation, MI). After the filtration, the total protein concentration of the extracts was determined by using the protein assay reagent kit from Bio-Rad with BSA (Bovine serum albumin) as a standard.

All gel filtration chromatography experiments were operated in the ÄKTA™ FPLC™ system (GE Healthcare, NJ), which automatically performs the fast protein liquid chromatography in a 4°C cooler, and monitors the progression through a 3.2 UNICORN™ software. Briefly, approximately 600 μg of total protein extracts were injected into the system and the proteins were fractioned through a Superdex 200 10/300

GL column (Amersham Biosciences, NJ). The proteins were eluted at a flow rate of 0.2 mL/min with elution buffer (extraction buffer without protease inhibitors, filtered through 0.22 μm Millipore membrane filter and degassed). After 6 mL of void volume, fractions of 0.5 mL each were collected and concentrated through StrataClean Resin (Stratagene, CA) for subsequent SDS-PAGE and western blot analysis. The Superdex 200 column was also calibrated with Gel Filtration Calibration Kits (Amersham Biosciences, NJ) and the molecular weight standards include ferritin (440 KDa), aldolase (158 KDa), albumin (67 KDa), ovalbumin (43 KDa), chymotrypsinogen A (25 KDa), and ribonuclease A (13.7 KDa) as described previously (Zhang et al., 2008).

Anti-SHB1 antiserum and western blot analysis

A PCR-generated 2-kb SHB1 C-terminal fragment was subcloned into the EcoR I and Sal I sites of pET-30a expression vector. Approximately 3 mg of SHB1 proteins were purified by using a His-tag affinity column (Novagen) and dialyzed, and injected into rabbits for polyclonal antibody production (Cocalico Biologicals, PA). The specificity of antibody was verified by using pre-immunoserum and the fourth bleeding serum in western blot analysis. The anti-GFP monoclonal antibody was purchased from Santa Cruz Biotechnology (Santa Cruz, CA). Protein samples were resolved on 10% SDS-PAGE gels (Bio-Rad, CA), and transferred to Polyvinylidene fluoride (PVDF) membrane (Millipore, MA). The membranes were stained with Poncue S to confirm the transfer efficiency and to serve as loading control. Western blot analysis was performed as described (Gray et al., 1999).

EMS mutagenesis and suppressor screens

EMS (Ethylmethane Sulphonate) mutagenesis was conducted as described (Wanger and Quail, 1995). M2 seeds were harvested into different groups, 50 plants per group. M2 seedlings were screened in agar plates for a shorter hypocotyl phenotype under blue light compared to that of *shb1-D*. Individual short hypocotyl plants were then propagated as putative suppressor mutants. Their phenotypes were further verified in the next generation, and backcrossed to Ws wild type to generate a F2 population for further genetics analysis.

Characterization of the mis-sense mutations

The intragenic mutants were backcrossed to Ws wild type to clean up their genetic background. The genomic DNAs were isolated from each mutant by using DNeasy plant mini kit (Qiagen, CA). Several fragments were amplified by PCR to cover the overall *SHB1* genomic sequence by using Advantage 2 PCR kit (Clontech, CA). The PCR products were purified and sequenced by using BigDye Terminator v3.1 Cycle sequencing Kit (Applied Biosystems, CA) on a ABI PRISM™ 3730xl DNA analyzer (Applied Biosystems, CA). The sequence alignment and data analyses were performed using 1.4.0 FinchTV software.

Site-directed Mutagenesis

SHB1 genomic DNA in the pEZTL-NL vector was mutagenized by using a Quikchange site-directed mutagenesis kit (Stratagene, CA). The PCR primer sequences to generate each specific mutation were: G81R 5' - GACACGGCTCGAAGAAAGGCTCGAGACGGCGGC-3' and 5'- GCCGCCGTCTCGAGCCTTTCTTCGAGCCGTGTC-3'; A94T 5'- CTACGTTTTTAAAGACCGGAGAAGCAGGTGG -3' and 5'- CCACCTGCTTCTCCGGTCTTTAAAAACGTAG -3'; G124E 5'- TTTACAGGCTGAAAGAGGAGACAGCTAGAAC -3' and 5'- GTTCTAGCTGTCTCCTCTTTCAGCCTGTAAA-3'; P156L 5'- GAATCAGAAGAACCTTTCTGTCTTTGATTC-3' and 5'- GAATCAAAGACAGAAAGGTTCTTCTGATTC -3'; P156S 5'- TCAGAATCAGAAGAACTCTTCTGTCTTTGAT -3' and 5'- ATCAAAGACAGAAGAGTTCTTCTGATTCTGA -3'; R421S 5'- AACGTCATCTTATAAAGTTTTCCACCGGTAT-3' and 5'- ATACCGGTGGAAAACTTTATAAGATGACGTT-3'.

Transient expression and SHB1 localization

SHB1:GFP or mutated SHB1:GFP was transiently expressed in *Nicotiana benthamiana* leaves through leaf injection with *Agrobacterium tumefaciens* strain Agl1. Following an incubation at 25 °C for 2 days, the leaf samples were examined with a Nikon Eclipse E800 microscope. The images were taken by a Cool Cam color CCD

camera (Cool Camera), and analyzed through a 3.0 Imago Pro Plus software (Media Cybermetics).

Results

Creation of SHB1 deletion lines in Arabidopsis

To explore the functional domains of SHB1, Six truncated *SHB1* genomic DNA sequence with their C-termini fused with GFP under the control of Cauliflower Mosaic Virus (CaMV) 35S promoter were constructed as described (Figure 1A). The N-terminal deletion constructs were designated as N320, N420 and N520 and contained the first 320, 420 and 520 amino acids, respectively (Figure 1A). Although the three N-terminal truncations varied in length, all contained the putative SPX domain. In parallel, three C-terminal truncations contained the EXS domain and were named as C425, C325 and C225 since the constructs contained the C-terminal 425, 325 or 225 amino acids (Figure 1A). All constructs were introduced into *Arabidopsis thaliana* Wassilewskija (Ws) wild type through floral dip methods (Clough and Bent, 1998). Over 30 homozygous transgenic lines for each construct, with a single T-DNA insertion, were identified in their T3 generations based on their basta resistance. The expressions of their transgenes were examined by using real-time RT-PCR and the accumulations of the truncated SHB1 transcript were shown for several independent transgenic lines in Figure 1B. In several lines, the accumulation of the fusion proteins was also examined in western-blot by using antibody against GFP (Figure 7A).

The SHB1 N-terminus retains the function of full-length SHB1

The phenotypes of all transgenic lines along with Ws wild type, segregated wild type, and empty vector controls were examined under various light wavelengths (Figures 2 and 3). Over-accumulation of the truncated SHB1 N-terminal 320 amino acid polypeptides (*N320 OE*) caused a long hypocotyl phenotype under red, far-red, and blue light compared to Ws wild type, but not in darkness (Figures 2A and 2B). The transgenic lines that carry the *N420 OE* and *N520 OE* constructs also showed a similar long hypocotyl phenotype (Figures 2A). Interestingly, the hypocotyl phenotypes of *N320 OE*, *N420 OE* and *N520 OE* transgenic lines under red, far-red, and blue light were very similar to that of *shb1-D*, a gain-of-function mutant or to that of the transgenic plants that overexpress full-length *SHB1* (Figures 2A and 2B). Therefore, the N-terminal SPX domain may be the major site to mediate the light signaling activity of SHB1.

The transgenic line that carries the shortest N-terminal truncation (*N320*) was examined for further genetic and phenotypic analyses. Consistent with the previous discoveries, the transgenic plants that overexpress the SHB1 *N320* truncation caused a mis-expression of *CHLOROPHYLL A/B BINDING PROTEIN 3* (*CAB3*) compared to Ws wild type, similar to *shb1-D* or the *SHB1 OE* lines (Figure 5A). The transgenic lines also showed a similar response in their accumulation of chlorophyll or anthocynins pigments and cotyledon expansion under red or blue light (Figures 5B to 5D).

Overaccumulation of SHB1 C-terminus caused a dominant negative phenotype

The transgenic plants that overexpress three SHB1 C-terminal truncations (C225, C325 and C425) with the EXS domain showed a short hypocotyl phenotype under blue light, resembling that of *shb1* (Figures 3A and 3B). Similar to *shb1*, the transgenic plants did no show any hypocotyl phenotypes under red or far-red light or in darkness (Figures 3A and 3B) (Kang and Ni, 2006). The *C225* transgenic lines, which contain the shortest region of EXS domain, were focused for further analyses. In the transgenic lines, the expression of *CAB3* gene was suppressed and the content of chlorophyll and anthocyanin pigments was reduced under red and blue light, similar to that of *shb1* (Figure 5A to 5C) (Kang and Ni, 2006). In addition, the size of their cotyledons was also reduced under blue light (Figure 5D). Since the accumulation of the endogenous SHB1 proteins was not affected in various C225 transgenic lines compared to that of Ws wild type (Figure 4), the possible co-suppression effect of these transgenic lines was excluded. Rather the dominant negative phenotype was caused by the over-accumulation of C225:GFP fusion proteins in transgenic lines *C225-1* and *C225-10* (Figure 7A).

Overexpression of SHB1 N- and C-terminus affects PIF4 and HFR1 expression

Overexpression of SHB1 N-terminal polypeptide of 320 amino acids also activated the expressions of its two downstream genes, *HFR1* and *PIF4,* in response to red or blue light (Figures 6A and 6B) (Kang and Ni, 2006). Moreover, *pif4 N320-2* double homozygous line showed a short hypocotyl phenotype like that of *pif4* under red or blue light (Figure 6C), suggesting that the function of the SPX domain was dependent on a functional PIF4. The expression of *HFR1* and *PIF4* was shown to be down-regulated

in *shb1* compared to wild type in response to red and blue light (Kang and Ni, 2006). In the current study, the expression of *HFR1* and *PIF4* was also suppressed in the *C225 OE* transgenic line (Figures 6A and 6B). Furthermore, the *hfr1-201 C225-1* double homozygous lines showed a long hypocotyl phenotype similar to that of *hfr1-201* under blue light (Figure 6D). The dominant negative phenotype caused by the over-accumulation of the SHB1 EXS domain apparently requires a functional HFR1.

SHB1 exists in a protein complex

The dominant-negative phenotype of the *C225 OE* transgenic lines leaded to the hypothesis that SHB1 is involved in protein-protein interaction or protein complex formation. To further investigate the mechanism underlying the dominant-negative phenotype, I prepared the protein extracts from the full-length *SHB1:GFP OE* transgenic line in Ws background, and the *N320:GFP OE* and *C225:GFP OE* transgenic lines either in Ws or *shb1* background. The accumulation of the full-length or truncated SHB1 fusion proteins was shown in Figure 7A. I further performed gel filtration analysis through superdex-200 gel filtration column in a ÄKTA fast protein liquid chromatography (FPLC) system. After fractionation of the crude protein extracts, multiple fractions were collected from the column and loaded on SDS-PAGE. Anti-GFP antibody was used to detect the full-length or truncated SHB1:GFP fusion proteins in a protein gel blot. It was shown that the full-length SHB1:GFP fusion protein peaked in fractions 10, 11, and 12, and fraction 11 corresponds to a protein complex of about 305 kD based on the calibration with the standard molecular weight marker (Figure 7B). Since the SHB1-GFP

fusion protein has a molecular weight of 110 kD, data from our gel filtration analysis suggest that SHB1:GFP mostly exists in a protein complex and SHB1 may not function in a monomeric form in vivo.

SHB1 associates with a protein complex through both its SPX and EXS domains

Compared to the full-length SHB1:GFP fusion protein, N320:GFP fusion protein was collected in fraction 12, 13 and 14, showing a size shift of the protein complex toward a lower molecular weight of 139 kD (Figure 7B). The difference in the molecular weight between the full-length SHB1:GFP and N320:GFP could not explain the size difference between the SHB1:GFP-containing protein complex and N320:GFP-containing protein complex (Figure 7B). It is likely that the N320:GFP-containing protein complex lost some regulatory components that are normally retained through its C-terminal EXS domain. However, the N320:GFP-containing protein complex was fully functional as overexpression of this N-terminal fragment caused a similar hypocotyl phenotype as that of full-length SHB1:GFP overexpression lines (Figure 2).

The C225:GFP fusion protein was detected in fractions 11, 12 and 13, with a slightly peak shift to fraction 12, a lower molecular mass of 179 kD (Figure 7B). As the shift in molecular mass is not dramatic, the size shift of the C225:GFP-containing complex may be due the loss of its N-terminal SPX domain and an associated protein of a smaller size. However, the protein complex solely formed through the C225:GFP fusion protein was not functional since we observed a dominant negative hypocotyl phenotype (Figures 3 and 7B). Nevertheless, both the SPX domain and the EXS domain are likely

involved in the assembly of the full-length SHB1-containing protein complex. As the gel filtration profiles of the N320:GFP or the C225:GFP fusion protein were exactly the same in either Ws or *shb1*, the protein complex that we detected for N320:GFP or C225:GFP was independent of the endogenous SHB1 protein (Figure 7B). This observation may also exclude a possibility that the endogenous full-length SHB1 forms a dimer with either the N320:GFP or the C225:GFP fusion protein.

Over-accumulation of C225:GFP displaces endogenous SHB1 from the protein complex

The endogenous SHB1 protein was further examined in the gel filtration fractions from Ws wild type, and the *N320-GFP OE* or *C225-GFP OE* transgenic plants by using anti-SHB1 antibody (Figure 7C). In Ws wild type, the endogenous SHB1 appeared in fractions 10, 11, and 12, a similar pattern as we have observed for SHB1:GFP fusion protein (Figure 7B and 7C). A similar gel filtration pattern of the endogenous SHB1 in the *N320:GFP OE* transgenic lines was shown, suggesting that the N320:GFP fusion protein does not interfere with the participation of the endogenous SHB1 protein into the native protein complex. By contrast, over-accumulation of C225:GFP fusion protein greatly altered the gel filtration pattern of the endogenous SHB1 (Figure 7C). The endogenous SHB1 protein was detected in multiple fractions of lower molecular mass from fraction 11 to fraction 15 in the *C225:GFP OE* transgenic lines (Figure 7C). The lower end of the fractions corresponds to monomeric SHB1 and the other fractions may represent partial protein complexes of smaller molecular weight (Figure 7C).

Intragenic SHB1 mutations defined five critical amino acids in the SPX domain

The forward genetic screen for suppressors of *shb1-D* was conducted under blue light from an EMS (Ethylmethane Sulphonate)-mutagenized *shb1-D* population. Of about 200,000 M2 plants screened, 58 suppressors were isolated and backcrossed the mutants to Ws wild type to determine if they are intragenic or extragenic. The hypocotyl phenotypes of about 250 F2 seedlings were examined for each putative suppressor under blue light and determined the segregation ratio of the long-hypocotyl individuals versus the short-hypocotyl individuals in the segregating F2 population. Of the 58 suppressors, six intragenic suppressors were identified that are tightly linked to the *shb1-D* locus. Out of 500 F2 siblings from two replicates, no long-hypocotyl individual in the segregating F2 population was observed. The *SHB1*genomic DNA from the intragenic mutants were PCR-amplified, purified, and sequenced. All six intragenic suppressors contained mis-sense mutations within or nearby the N-terminal SPX domain of the *SHB1* gene (Figure 8A). All mutations caused amino acid alterations: G81R conversion in intragenic mutant 1-12 with a change from glycine (GGG) to arginine (AGG), A94T conversion in intragenic mutant N13-3 with a change from alanine (GCC) to threonine (ACC), G124E conversion in intragenic mutant N5-13 with a change from glycien (GGG) to glutamic acid (GAG), P156L conversion in intragenic mutant N19-5 with a change from proline (CCT) to leucine (CTT), P156S conversion in intragenic mutant 11-9 with a change from proline CCT) to serine (TCT), and R421S conversion in intragenic mutant 36RS16 with a change from arginine (CGT) to serine (AGT) (Figure 8A). These mutations were all

consistent with G/C to A/T conversion caused by EMS mutagenesis (Ishii and Kondo, 1975; Kim et al., 2008).

The six intragenic suppressors were further examined under various light wavelengths. Compared to *shb1-D,* these six intragenic mutants all showed a shorter hypocotyl phenotype under red, far-red, and blue light compared to *shb1-D*, but a longer or slightly longer hypocotyl than that of Ws wild type under these light conditions (Figure 8B and 9). These mutations may all be partial loss-of-function mutations. These intragenic mutants did not show any hypocotyl phenotype compared to either *shb1-D* or Ws wild type in the dark (Figure 8B and 9). To further confirm the identification of these mis-sense mutations, one mutated version of SHB1:GFP (G81R) construct was generated by using a PCR-based site-directed mutagenesis kit. The mutated version of SHB1:GFP under the control of CaMV 35S promoter was transformed into Arabidopsis Ws, and the resultant transgenic plants accumulated a comparable level of SHB1:GFP fusion protein to that of *SHB1-GFP OE* transgenic line (Figure 10A). However, the hypocotyl lengths of these G81R transgenic lines were similar to or slightly longer than that of Ws wild type, but much shorter than that of *SHB1-GFP OE* transgenic line under red, far-red, or blue light (Figure 10B).

Mis-sense mutations in SPX domain affected its association with the protein complex

The mis-sense mutations in the SPX domain may affect the accumulation or the stability of SHB1 protein. The protein extracts were prepared from *shb1-D* plants grown either in the dark or being transferred from dark to white light or blue light for 5 hours,

and performed immunoblot analysis with anti-SHB1 antibody (Figure 11A). The accumulation of SHB1 protein was not affected by either blue or white light treatment. SHB1 protein level was then examined in *shb1-D* and the six intragenic mutants grown under either white light or blue light condition. All six intragenic mutants accumulated comparable levels of SHB1 protein to *shb1-D*, and therefore, these point mutations in the SPX domain did not affect the stability of SHB1 protein (Figure 11A).

The intragenic mutations affect SHB1 localization was also examined. By using site-directed mutagenesis, all six mutated derivatives of SHB1:GFP as G81R:GFP, A94T:GFP, G124E:GFP, P156L:GFP, P156S:GFP, and R421S:GFP were generated. SHB1:GFP and six mutated SHB1:GFPs were transiently expressed in *Nicotiana benthamiana* leaves and the plants were kept either in the dark, blue light, or white light conditions. As shown in Figure 8B, SHB1:GFP and the six mutated SHB1:GFPs were all localized to the nucleus similarly either in the dark or under blue or white light, and the missense mutations in the SPX domain did not affect the nuclear localization of SHB1(Figure 11B).

To test whether these intragenic mutations in the SPX domain affect the association of SHB1 with the previous described protein complex, a similar superdex gel-filtration analysis were performed for protein extracts prepared from *shb1-D* or the six intragenic suppressors (*G81R*, *A94T*, *G124E*, *P156L*, *P156S*, and *R421S*). The wild type or mutated SHB1 proteins in various fractions were analyzed using anti-SHB1 antibody through the western blot. As shown in Figure 8C, wild type SHB1 appeared in fractions 10, 11, and 12 but the mutated SHB1 proteins all shifted to fractions 11, 12, and 13 of

lower molecular mass. This pattern was consistently observed in several repeated experiments and the six intragenic mutations apparently affect its association with the protein complex (Figure 11C).

Discussion

The SPX domain mediates the signaling activity of SHB1

The transgenic plants that overexpress the N-terminal SPX domain showed a similar hypocotyl elongation response as *shb1-D* or the transgenic plants that over-express full-length *SHB1* (Figure 2) (Kang and Ni, 2006). These transgenic plants also showed a similar response to *shb1-D* in the accumulation of anthcyonin and chlorophyll pigments and the regulation of *CAB3*, *PIF4* and *HFR1* expression under various light wavelengths (Figures 5 and 6). The SPX domain is therefore critical for SHB1 signaling and function. Further gel filtration analysis demonstrates that the SPX domain is still able to form a protein complex but at a much reduced molecular weight compared to that of the protein complex involving full-length SHB1 (Figure 7B). The size difference could not be simply explained by the loss of its EXS domain, and most likely due to the loss of the EXS domain and its associated proteins. However, this SPX domain-containing protein complex is fully functional as over-expression of this domain caused a long hypocotyl phenotype similar to that of *shb1-D* or the transgenic plants that overexpress full-length SHB1 (Figure 2). The formation of the SPX domain-containing protein complex is also independent of the endogenous SHB1 since we observed a similar gel

filtration profile of N320:GFP fusion protein in either wild type or *shb1* mutant background.

The EXS domain anchors SHB1 to the protein complex

In contrast, the transgenic lines that overexpress the C-terminal EXS domain showed a dominant-negative phenotype or a short hypocotyl phenotype under blue light, similar to that of the *shb1* knockout mutant (Figure 3) (Kang and Ni, 2006). The over-accumulation of the EXS domain in the *C225:GFP OE* transgenic lines did not affect the abundance of the endogenous SHB1 protein (Figure 4), and the EXS domain was still able to participate the formation of a protein complex of a smaller molecular mass (Figure 5B). The size shift may be due to the loss of the N-terminal SPX domain and a smaller protein that associates with the SPX domain (Figure 7B). The over-accumulation of the EXS domain interferes the assembly of the endogenous SHB1 into a larger protein complex and the release of the endogenous full-length SHB1 to a monomeric form (Figure 7C). The over-accumulated EXS domain may simply compete with the endogenous full-length SHB1 for a similar interacting protein within the protein complex, which may likely explain the dominant negative phenotype in the transgenic plants that overexpress the EXS domain (Figures 3 and 7B).

Intragenic mutations in SPX domain reduce the affinity of its association with the protein complex

The screening of *shb1-D* suppressor mutants that fully or partially suppress the long hypocotyl phenotype of *shb1-D* to wild type was conducted. This screen has allowed me to isolate such weak alleles or partial loss-of-function alleles within the *SHB1* coding region. The six mis-sense mutations identified from the intragenic revertants of *shb1-D* are all clustered within or nearby the SPX domain, suggesting that the SPX domain is critical for SHB1 function (Figure 8A). These mis-sense mutations do not affect either the stability or the sub-cellular localization of the SHB1 protein (Figure 11A and 11B). Rather the mutations partially altered the assembly of the SHB1-containing protein complex, and we observed a protein complex of smaller size (Figure 11C). Likely, the mis-sense mutated SHB1 proteins are still able to participate in the formation of a protein complex, but at much a reduced affinity to a particular SHB1 interacting component of the complex. This interacting component might often be lost from the complex, but has a critical role for the function of the SHB1-containing protein complex. At the biochemical level, the five amino acids in the SPX domain may either maintain a proper conformation of SHB1 or may be directly involved in a physical contact with the yet-unidentified protein component within the protein complex.

A model for SHB1 function in light signaling

Based on the experimental data, it is proposed that the SPX domain and EXS domain of SHB1 may contact two separate proteins within a protein complex since the sizes of the protein complex formed by the SPX domain and the EXS domain are quite different and SHB1 does not act as a homodimer (Figures 7B and 12A). Both domains

are required for the formation of a stable protein complex, whereas the N-terminal SPX domain is critical for SHB1 function and signaling activity (Figure 12B). This is largely due to the fact that the N-terminal SPX domain is biologically active in the absence of the EXS domain and the mis-sense mutations are all clustered within or nearby the SPX domain. However, the affinity of the SPX domain with its interacting protein is not high enough to prevent the assembly of the endogenous SHB1 into its native protein complex (Figure 7C). The EXS domain in the absence of the SPX domain is also able to participate the formation of a protein complex, but the complex is not functional due to the loss of the SPX domain (Figure 7B). The loss of the SPX domain, on the other hand, might dramatically alter the affinity of the EXS domain to its interacting component within the protein complex, and through a yet unknown mechanism, the over-accumulated EXS domain interferes with the participation of the endogenous SHB1 in its native protein complex (Figures 7C and 12C). This is probably why a shorter hypocotyl phenotype was observed from the transgenic lines that over-express the EXS domain, similar to that of the loss-of-function *shb1* mutant (Figure 3).

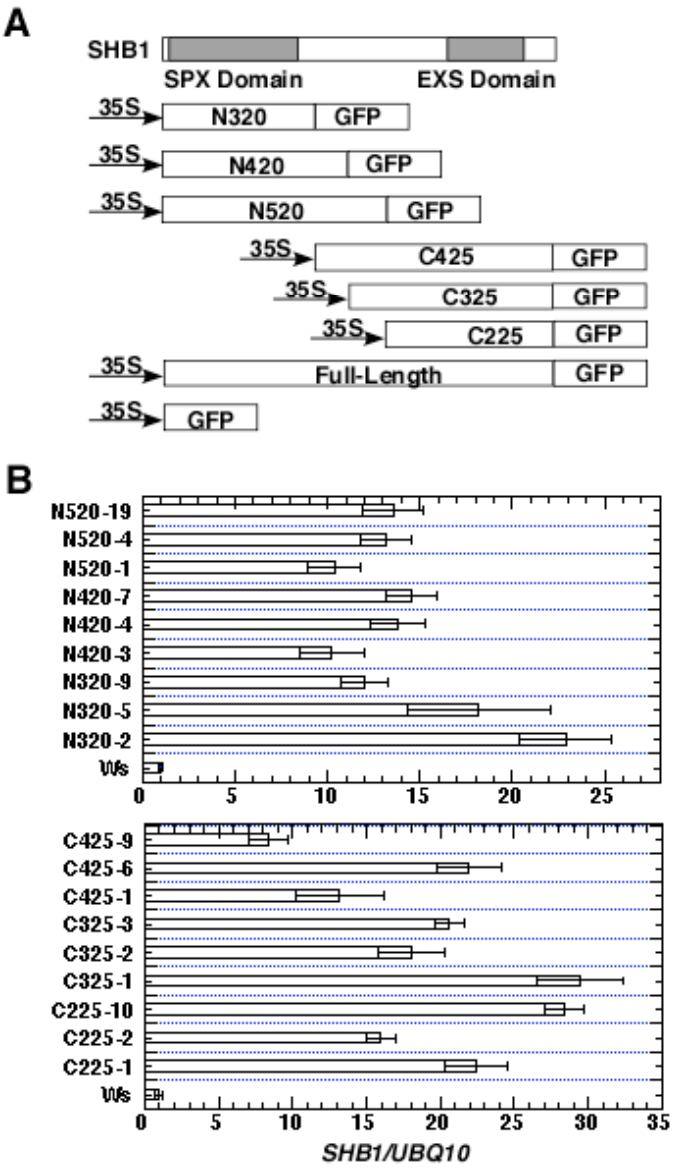

Figure 1. (A) Schematic diagram showing the full-length and different deletion derivatives of SHB1. All SHB1 truncations were fused with GFP at their C-termini under the control of CaMV 35S promoter. (B) Quantification of SHB1 transgene level through real-time RT-PCR. Expression of the truncated transcripts from SHB1 N-terminal deletion series (upper Panel) or C-terminal deletion series (lower panel) compared to Ws wild type through real time RT-PCR analysis. The expression levels of the truncated *SHB1* transgenes were normalized to that of *UBQ10.* Data are presented as means plus or minus the standard errors from three independent biological replicates.

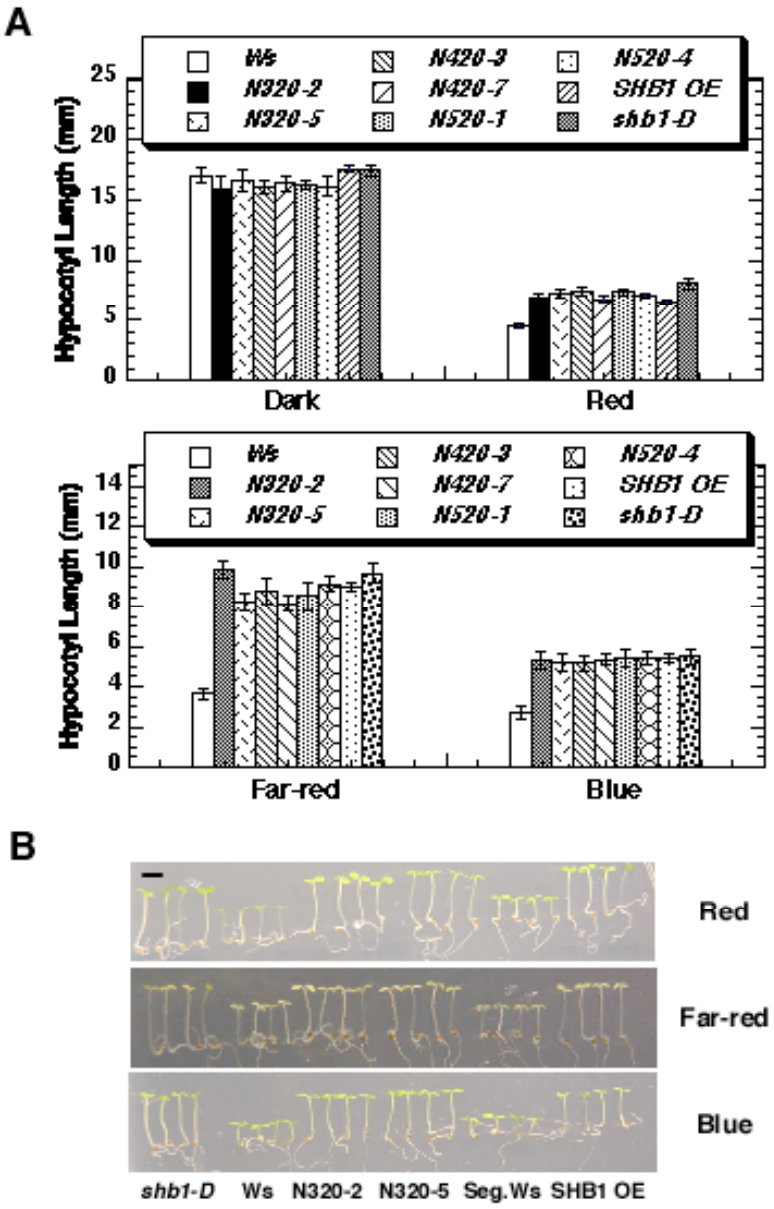

Figure 2. The N-terminal SPX domain is critical for SHB1 function. (A) Hypocotyl lengths of Ws, *shb1-D*, and transgenic plants that overexpress full-length SHB1 (*SHB1 OE*), N320:GFP (*N320:GFP OE*), N420:GFP (*N420:GFP OE*), or N520:GFP (*N520:GFP OE*) in the dark or under red light (15 μmol /m^2/s, upper panel), far-red light (10 pmol/m^2/s) or blue light (3 μmol /m^2/s) (lower panel). The means plus or minus the standard errors were calculated from at least 25 seedlings each replicate and three replicates total. (B) Representative images showing the long hypocotyl phenotype of the *N320-GFP OE, N420-GFP OE*, or *N520-GFP OE* transgenic lines under red, far-red, or blue light for 4 days after germination. Bar = 2 mm.

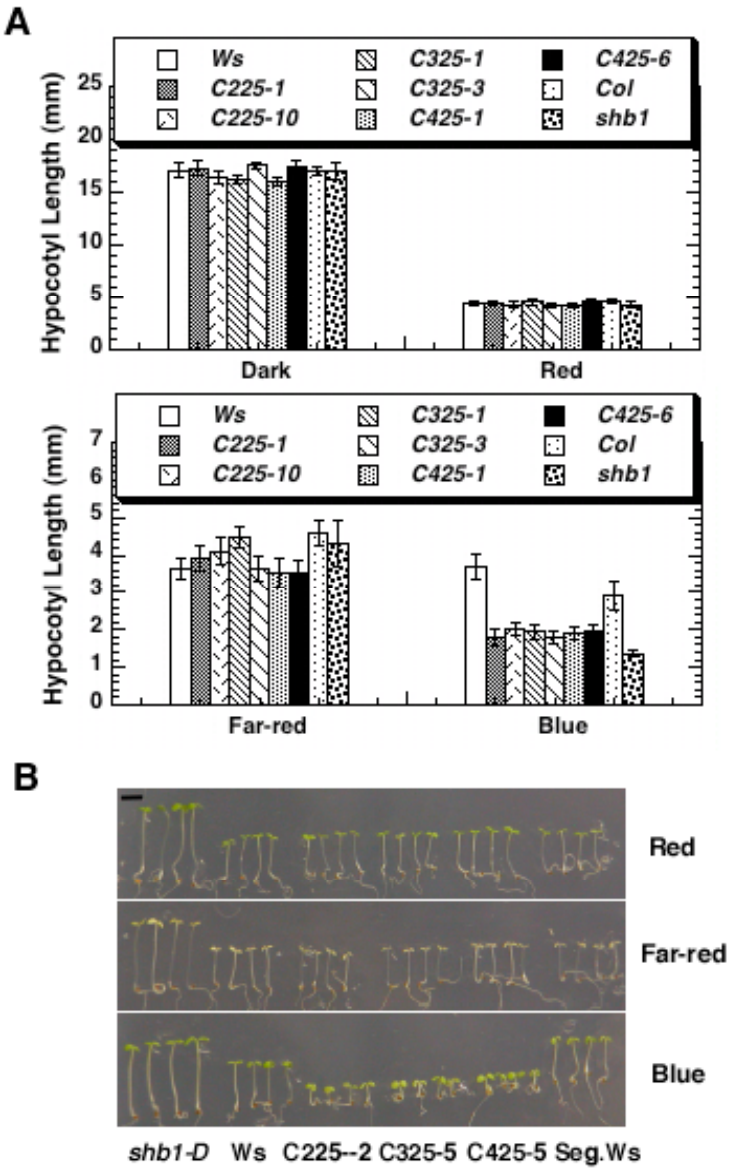

Figure 3. Over-expression of SHB1 C-terminal EXS domain created a short hypocotyl phenotype. (A) Hypocotyl lengths of Ws, Col, *shb1*, and transgenic plants that overexpress C225:GFP (*C225 OE*), C325:GFP (*C325 OE*), or C425:GFP (*C425 OE*) in the dark or under red light (upper panel), far-red light or blue light (lower panel) with intensities as specified in Figure 2A. The means plus or minus the standard errors were calculated from at least 25 seedlings each replicate and three replicates total. (B) Representative images showing the short hypocotyl

phenotype of the *C225:GFP, C325:GFP,* or *C425:GFP* transgenic plants under red, far-red, or blue light for 4 days after germination. Bar = 2 mm.

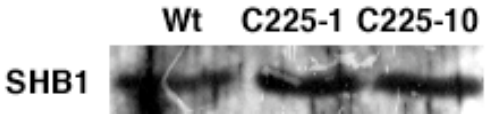

Figure 4. Over-expression of the EXS domain does not alter the accumulation of the endogenous SHB1 protein. Protein extracts were prepared from Ws or independent transgenic lines that overexpression C225:GFP in Ws background, separated on SDS-PAGE, and blotted with antisera against SHB1.

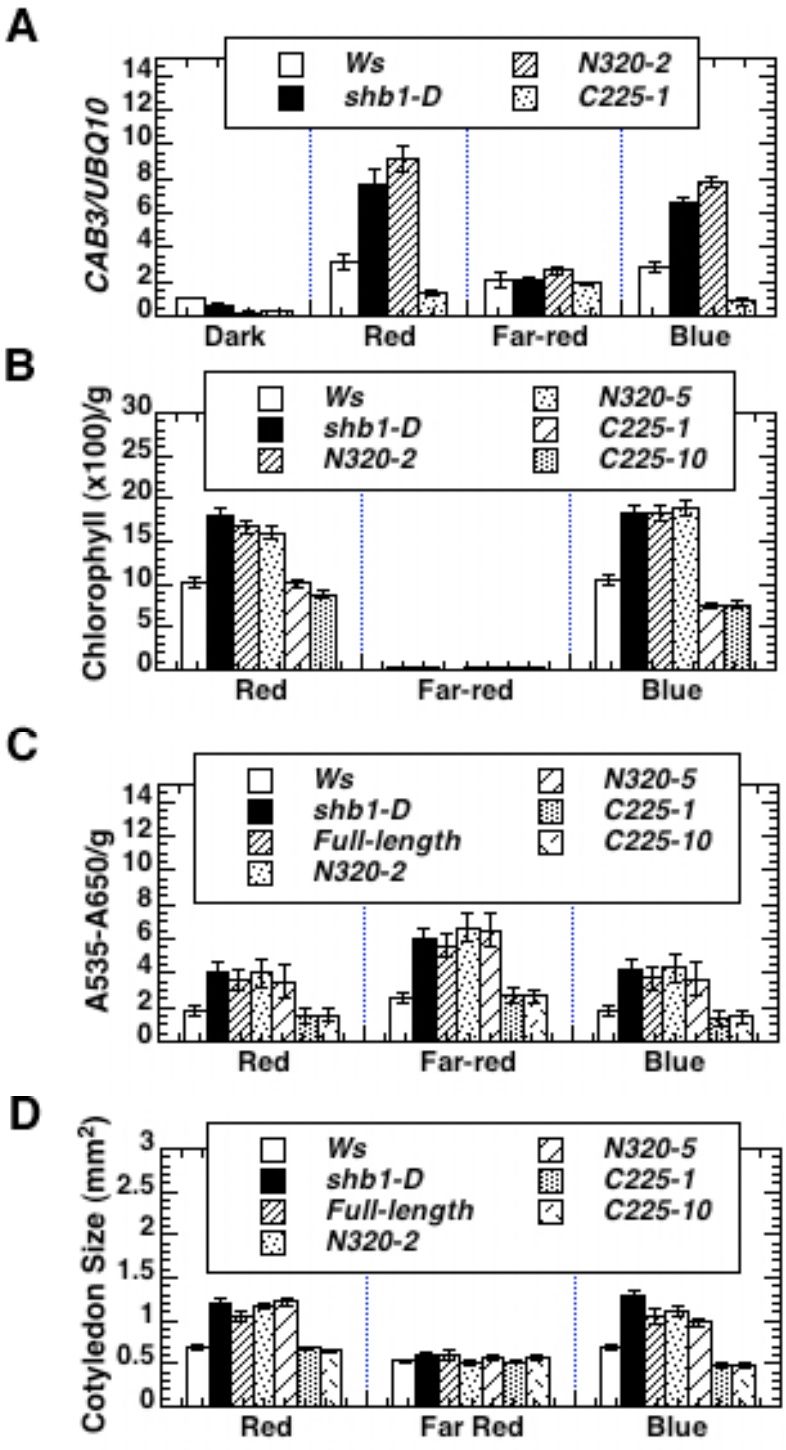

Figure 5. Over-expression of the SPX and EXS domains affects many other light responses. (A) Expression of *CAB3* assayed through real time RT-PCR analysis. Total

RNA was isolated from 5-day-old dark-grown seedlings without light treatment or being treated with red, far-red, or blue light for 4 hr. The expression levels of *CAB3* were normalized to that of *UBQ10*. (B) and (C) Quantification of the content of chlorophyll and anthocyanin in 5-day-old Ws, *shb1-D*, and the transgenic plants that expression *N320:GFP* (lines 2 and 5) or *N320:GFP* (lines 1 and 10) under red, far-red, or blue light. (D) Cotyledon size of 5-day-old Ws, *shb1-D*, and the transgenic plants that expression full-length SHB1, *N320:GFP* (lines 2 and 5) or *N320:GFP* (lines 1 and 10) under red, far-red, or blue light. The light intensities was as indicated in Figure 2A. Data were presented as means plus or minus the standard errors from three independent biological replicates.

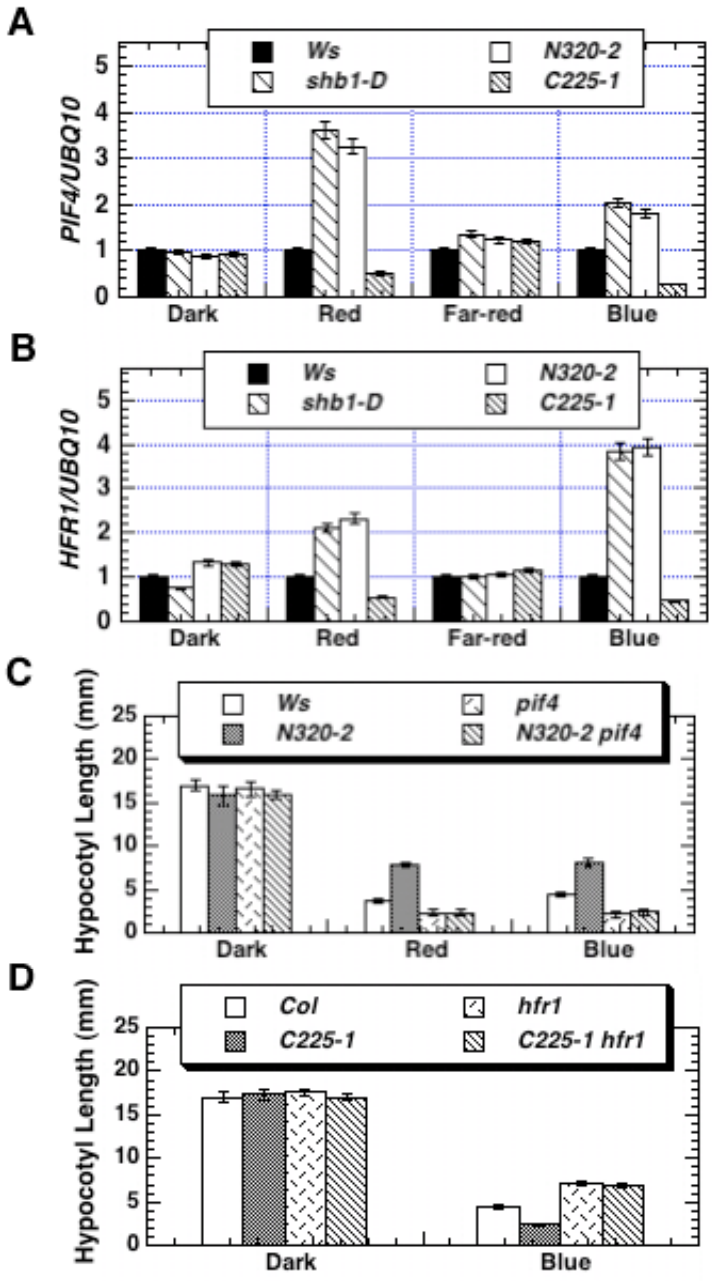

Figure 6. The expression of *PIF4* and *HFR1* was altered in transgenic plants that overexpression either the SPX or the EXS domain. The expression of *PIF4* (A) and *HFR1* (B) in Ws, *shb1-D*, or transgenic plants that express either *N320:GFP* (line 2) or *C225:GFP* (line 1). Total RNA was isolated from 5-day-old seedlings in the dark or being treated for 4 hr with red, far-red, or blue light. The expression levels of *PIF4* or

HFR1 were normalized to that of *UBQ10*. Data were presented as means plus or minus the standard errors from two independent experiments. (C) Hypocotyl elongation responses of Ws, *pif4*, or transgenic plants that express *N320:GFP* in either Ws or *pif4* background in the dark or under red or blue light. (D) Hypocotyl elongation responses of Col, *hfr1*, or transgenic plants that express *C225:GFP* in either Col or *hfr1* background in the dark or under blue light. The light intensities were as specified in Figure 2A. Data were presented as means plus or minus the standard errors from at least 25 seedlings.

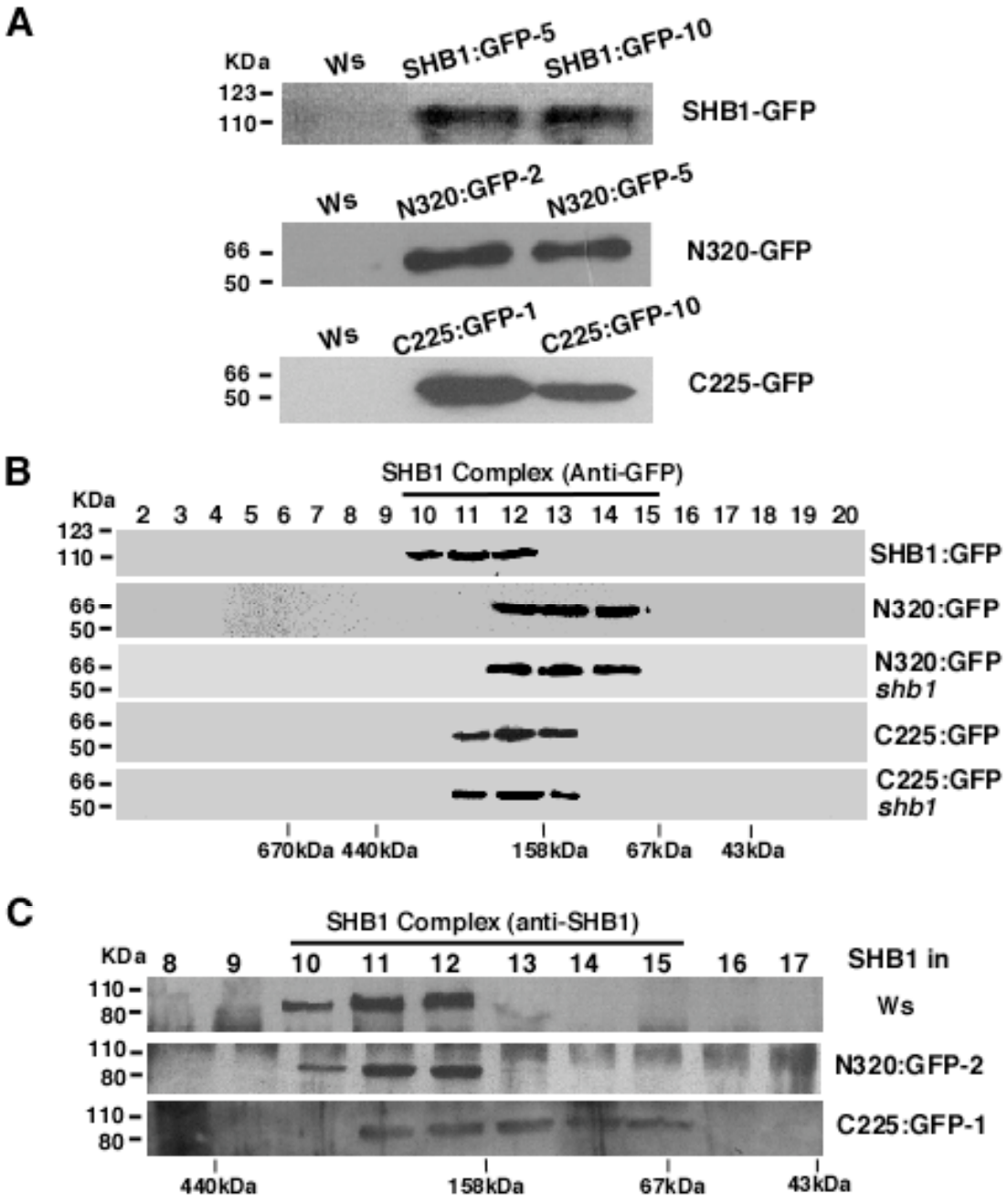

Figure 7. The SPX and EXS domains participate the formation of a protein complex of altered size. (A) The expression of SHB1:GFP, N320:GFP, and C225:GFP in two independent transgenic lines as immunoblotted with anti-GFP antibody. (B) Gel filtration profiles of SHB1:GFP (line 2), N320:GFP (line 2) in Ws or *shb1*, or N320:GFP

(line 1) in Ws or *shb1*. (C) Gel filtration profiles of the endogenous SHB1 in Ws and transgenic plants that overexpress either *N320:GFP* (line 2) or *N320:GFP* (line 1) in Ws background. Plant extracts from 7-day-old seedlings were fractionated on a Superdex-200 gel-filtration column. The various fractions were collected, separated on SDS-PAGE, and blotted with anti-GFP antibodies or antisera against SHB1. The Molecular mass standards of the gel filtration fractions were labeled at the bottom, and the molecular mass markers of the SDS-PAGE gel were labeled on the left.

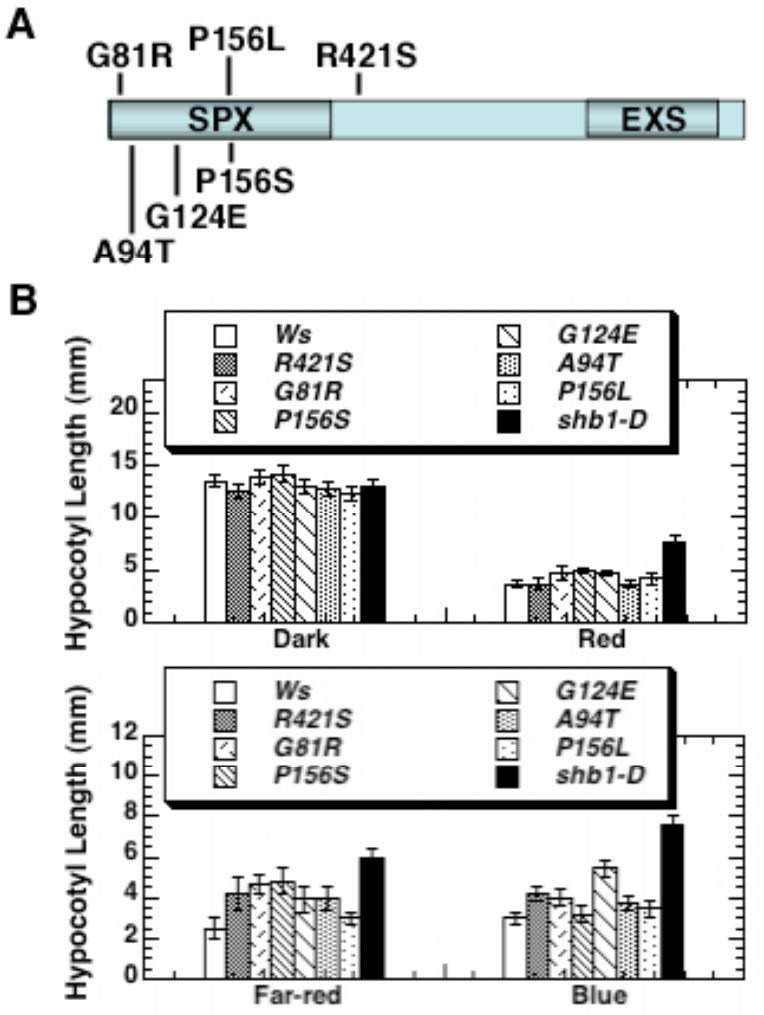

Figure 8. Six intragenic mis-sense mutations suppress the hypocotyl phenotype of *shb1-D*. (A) Diagram showing the location of the six mis-sense mutations within or nearby the SPX domain. (B) Hypocotyl elongation responses of Ws, *shb1-D*, and six SHB1 missense mutants in the dark or under red light (upper panel), far-red or blue light (lower panel) at intensities as specified in Figure 2A. The means plus or minus the standard errors were calculated from at least 25 seedlings.

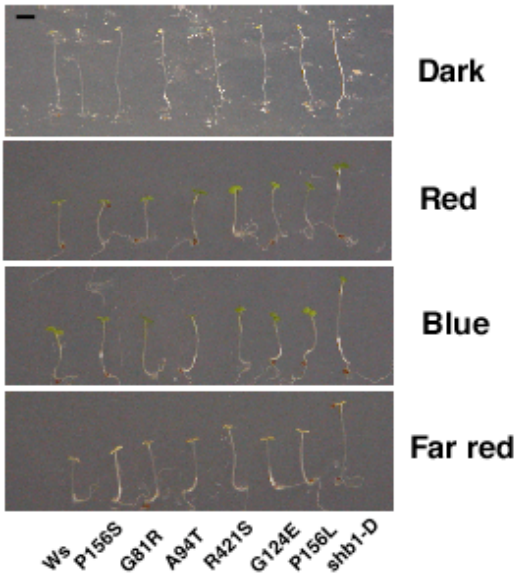

Figure 9. The phenotype of six intragenic mutants in *shb1-D* background. Visual presentation of the hypocotyl growth responses of Ws, *shb1-D*, and six mis-sense SHB1 mutants in the dark or under red, far-red, or blue light at intensities as specified in Figure 2A.

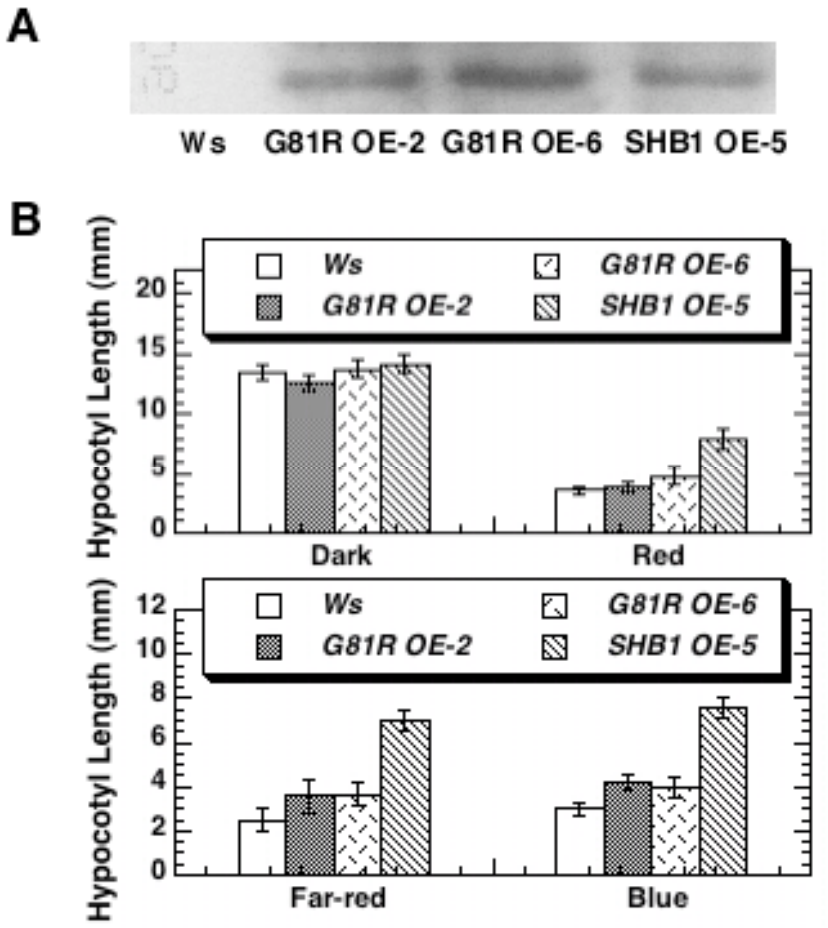

Figure 10. Over-expression of SHB1 with a G81R conversion fails to create a long hypocotyl phenotype. (A) Expression of SHB1:GFP in transgenic plant that overexpress wild type *SHB1:GFP* (line 5) or mutated *SHB1:GFP* G81R (lines 2 and 6) as immunoblotted with anti-GFP antibody. (B) Hypocotyl elongation responses of Ws, *SHB1 OE* transgenic line 5, and two independent transgenic plants that overexpress mutated *SHB1* G81R (lines 2 and 6) in the dark or under red light (upper panel), far-red or blue light (lower panel) at intensities as specified in Figure 2A. The means plus or minus the standard errors were calculated from at least 25 seedlings.

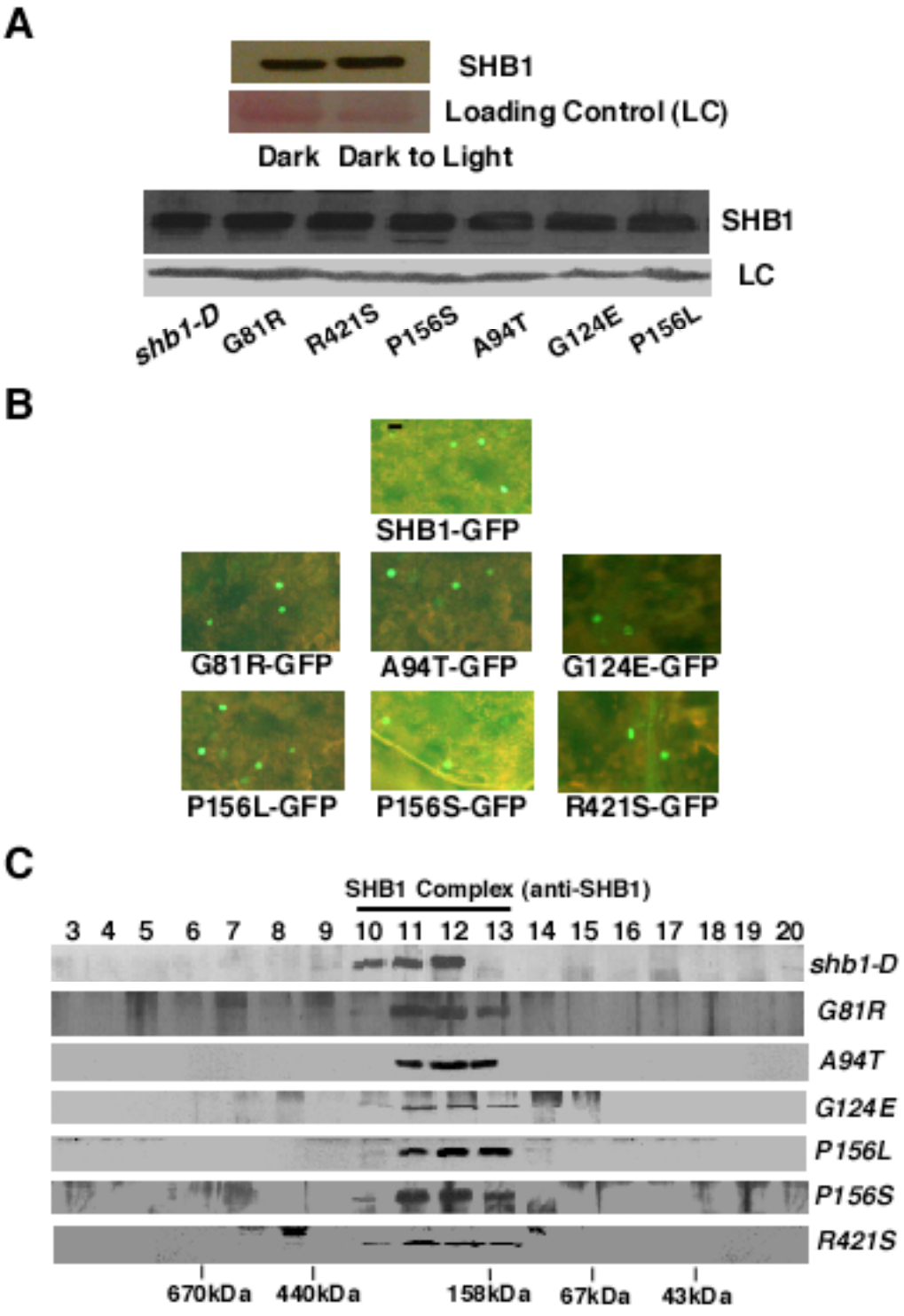

Figure 11. Mis-sense mutations within or nearby the SPX domain alter the association of SHB1 with a protein complex. (A) Accumulation of SHB1 in the dark or

under white light for 5 hr (upper panel). Mis-sense mutations did not affect the accumulation of SHB1 under white light (lower panel). Poncues S stain serves as loading control. (B) Mis-sense mutations in the SPX domain did not affect the nuclear localization of SHB1. Fluorescent images showing the subcellular localization of wild type SHB1:GFP and SHB1:GFP bearing the indicated mis-sense mutations in a transient *Nicotiana benthamiana* expression system. Bars =25 μm. (C) Mis-sense mutations in the SPX domain altered the association of SHB1 with a protein complex. Gel filtration profiles of wild type SHB1 or SHB1 bearing the six mis-sense mutations in the *shb1-D* locus. Plant extracts from 7-day-old seedlings were fractionated on a Superdex-200 gel-filtration column. The various fractions were collected, separated on SDS-PAGE, and blotted with antisera against SHB1. The Molecular mass standards of the gel filtration fractions were labeled at the bottom, and the molecular mass markers of the SDS-PAGE gel were labeled on the left.

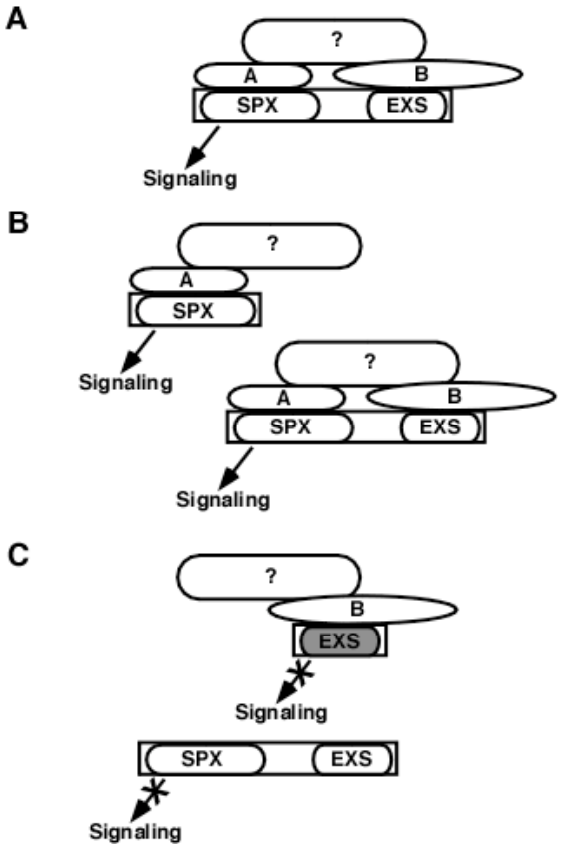

Figure 12. A working hypothesis is proposed for SHB1 function in light signaling. (A) Both the SPX and the EXS domains anchor SHB1 through two separate proteins to a protein complex. The interaction of the SPX with its counterpart mediates SHB1 signaling activity. (B) In the absence of the EXS domain, the SPX still associates with its counterpart and this association is active in signaling. The affinity of such association also allows the assembly of the endogenous SHB1 to its native protein complex. (C) In the absence of the SPX domain, the C-terminal EXS domain associates with its counterpart but this association does not generate signaling. The affinity of the over-accumulated EXS domain to its signaling counterpart might be dramatically altered due to the loss of the SPX domain, which, through a yet unknown mechanism, largely prevents the assembly of the endogenous SHB1 protein into its native protein complex.

Chapter III

Dual roles of SHB1 in photoperiodic and autonomous flowering

Introduction

In this chapter, I investigate the function of SHB1 in *Arabidopsis* flowering. The original overexpression allele, *shb1-D,* flowers early, whereas *shb1,* the knock-out allele, flowers late under both long days and short days. SHB1 positively regulates the expression of *CONSTANS* and the signal is propagated to cause increased *FT* and *SOC1* expression under long days**.** Under short days, it activates the expression of *LD* (*LUMINIDEPENDENS*) to suppress the expression of *FLC* and to allow the activation of *SOC1* in shoot apical meristem. SHB1 seems to play dual roles in the day-length pathway and autonomous pathway and defines a signal step that the two pathways interact.

Materials and Methods

Plant materials and flowering experiments

ld-3 in Wassilewskija (Ws) background were obtained from the *Arabidopsis* Biological Resources Stock Center (Ohio State University, Columbus). *flc-3* in the Columbia background was described previously (Michaels and Amasino, 1999) and *phyB-9*, *phyA-211*, *cry1-304*, *cry2-1,* and *co-2* were also described previously (Kang et al., 2007). Flowering experiments were conducted under either long days (16 h light/8 h dark) or short days (8 h light/16 h dark) under fluorescent cool white light at 22°C. Flowering time was determined as rosette leave numbers after bolting 1 cm. For

expression analysis of *CO*, *FT*, *SOC1*, *FLC* and *LD*, Ws, *shb1-D*, Col, and *shb1* seedlings were grown under long days or short days for 12 days and sampled at Zeitgeber times 12 and 16 (LD) or at Zeitgeber times 8 and 12 (SD) when *CO* and *FT* have the highest levels of expression.

Gene expression experiments and real-time RT-PCR analysis

For qRT-PCR analysis, total RNAs were isolated by using the SV total RNA isolation kit (Promega). SuperScript^{TM} III reverse transcriptase (Invitrogen) was used to synthesize the first-strand cDNA with oligo dT primer and 1 μg of total RNA at 50°C for 1 h. Random hexamers (Thermo Scientific, UK) were used to synthesis the first-strand cDNA for the analysis of *FLC* expression level (endogenous plus transgenes in the *FLC* transgenic plants). Quantitative PCR was then performed with Platinum SYBR Green qRT-PCR kit (Invitrogen) on Applied Biosystems 7500 Real Time PCR machine. The thermal cycling program was 50°C for 10 min and 95°C for 10 min, followed by 40 cycles of 95°C for 30s, 56°C for 30s, 72°C for 1 min and a one-cycle dissociation stage at 95°C for 15 s, 60°C for 1 min, and 95°C for 15 s. The primer pairs used in qRT-PCR were *FT*, 5'- GAGACCCTCTTATAGTAAGCA -3' and 5'-CTTCCTCCGCAGCCACTCA -3'; *SOC1*, 5'-AATATGCAAGATACCATAGATCGT -3' and 5'-TTCTTGAAGAACAAGGTAACCCAA -3'; *CO*, 5'-ACGCCATCAGCGAGTTCC -3' and 5'- AAATGTATGCGTTATGGTTAATGG -3'; *FLC*, 5'- AGTAGCCGACAAGTCACCTT -3' and 5'- GAGAGTCACCGGAAGATT -3'; *LD*, 5'- AACAGCAACAATATATGCAAC -3' and 5'-

ATATCCTGGATTGCTACTCAT -3'; *UBQ10*, 5'-AGGTACAGCGAGAGAAAGTAGCA -3' and 5'- TAGGCATAGCGGCGAGGCGT -3'. *UBQ10* was used as an internal reference. Data were calculated from three biological replicates and each biological replicate was examined in triplicate.

For tissue specific expression experiments, different tissues was harvested from plants and frozen immediately in liquid nitrogen. Seedling tissue includes 5-day light-grown seedlings; meristem tissue includes inflorescence meristem and shoot apex; floral tissue includes closed floral buds and flowers at different stages; Silique tissue includes siliques at 1 to 8 days after pollination; rosette and cauline leave tissue includes leaves of sizes 5 to 12 mm; and stem tissue includes internodes from 4-week-old plants. Roots were harvested from seedlings at 12 days after germination. RNA was extracted from two different biological samples for each tissue type. Primer pairs used for *SHB1* were 5'-CAGGTTCAAGCACTGAGGAGT -3' and 5'- TGCTTCCTCGGTTTAGAGTA -3'.

Double mutant analysis

To control the difference in flowering responses between different ecotypes, the entire F2 population was scored for flowering times under long days and short days and each was individually PCR-genotyped. Mean values plus or minus SEM for each genotype from the entire F2 population were calculated. To generate *shb1-D/co-2* double mutants, *shb1-D* (Ws) was crossed to *co-2* (Ler). For *shb1-D* genotyping, gene specific primer pairs were 5'- GAAGATACGGGTTTTGCAT -3' and 5'-GGGAAGCTTGGATGTCTTGAA -3', and the T-DNA specific primer for *shb1-D* was

5'- CATTTTATAATAACGCTGCGGACATCTAC -3'. The *co-2* locus was genotyped based on two pairs of markers described previously (Kang et al., 2007). To analyze the expression of *FT* and *SOC1* in the double mutants, F3 seedlings derived from several individual homozygous double mutants, single mutants or wild types, all in mixed background, were grown under either long days or short days for 12 days, and were sampled at Zeitgeber time 16 (LD) or 12 (SD).

shb1/flc-3 was generated by crossing *shb1*(Col) to *flc-3* (Col) and *flc-3* mutation was genotyped according to the previous report (Lee et al., 2000; Moon et al., 2005). *shb1/phyB-9* was generated by crossing *shb1*(Col) to *phyB-9* (Col). The *shb1* locus was PCR-genotyped and gene specific primer pairs for *shb1* were 5'-TAAGCAGCACGAGCTCAAAT -3' and 5'- TGCTTCCTCGGTTTAGAGTA -3'. The T-DNA specific primer for *shb1* is 5'- GGAACCACCATCAAACAGGAT -3'. *phyB-9* was genotyped based on its long hypocotyl under red light. The F2 populations for *shb1-D/phyB-9*, *shb1-D/phyA-211*, *shb1-D/cry2-1*, and *shb1/cry2-1* double mutants were previously generated (Kang et al., 2005). The *shb1-D* mutation was genotyped as described above, and *phyB-9* or *phyA-211* were back-genotyped in the F3 generation based on its dramatic hypocotyl phenotype under red or far-red light. *cry2-1* contains large deletions and homozygous *cry2* mutation was genotyped by using the following primers: cry2 5'-GGTTTAGAAGAGACCTAAGGAT-3' and 5'-CCAGATTCTTCCCTTCTGAT-3'.

Results

shb1 mutations affect flowering under both long-days and short-days

To explore if SHB1 also acts in other phases of *Arabidopsis* development, the flowering phenotypes of *shb1-D* and *shb1* were examined. Compared to Ws wild type, *shb1-D* and *SHB1* overexpression transgenic plants flowered early under both long-days and short-days (Figure 13). They have fewer rosette leaves compared to wild type when bolting (Figure 13A). By contrast, *shb1,* a loss-of-function allele, flowered late compared to Col wild type in both long and short days (Figure 13).

shb1 mutations affect the expression of two key photoperiodic flowering genes

The expressions of two key photoperiodic flowering pathway genes, *CO* and *FT,* were examined by Real-time RT-PCR analysis (Figure 14). The seedlings were sampled at Zeitgeber time (ZT) 12 and 16 in long days and 8 and 12 in short days when *CO* and *FT* were expressed at their peaks (Searle et al., 2006; Wigge et al., 2005). At Zeitgeber time (ZT) 16 under long-days, the expression of *CO* level was increased 2-fold in *shb1-D* and repressed 2-fold in *shb1* compared to wild type (Figure 14A). The expression of *FT*, a gene immediately downstream of CO, at ZT 16 h under long-days showed a similar scale of changes as that of *CO* in *shb1-D* and *shb1* mutants compared to wild type (Figure 14B). The expression of *SOC1*, a downstream readout for both photoperiodic and autonomous pathways was also examined at ZT 12h and 16h under long-days. Compared to wild type, the expression of *SOC1* was enhanced 2.5-fold in *shb1-D* and repressed 2-fold in *shb1* (Figure 14C).

At ZT 12 h under short-days, the *shb1* mutations also caused a 2-fold increase or decrease in the expression of *CO* (Figure 14A). In contrast, at ZT 8 under short-days, the expression of *FT* was enhanced up to 6 times in *shb1-D* and repressed more than 3 times in *shb1* (Figure 14B). The changes in the expression of FT may not be as significant as the level of FT transcript is very low under short days. The expression of *SOC1* was consistently enhanced 2.5-fold by *shb1-D* and repressed 2-fold by *shb1* at ZT 8 and 12 under short-days (Figure 14C). In contrast to transcriptional regulation, the levels of CO protein were not altered in Ws and *shb1-D* seedlings that were grown under long days for 10 days, transferred to blue light at Zeitgeber time 0 in the morning, and sampled at Zeitgeber time 12 or 16 when CO protein accumulates to the highest levels (data not shown).

shb1-D enhances flowering through CO and FT in long days

It remains unknown if the change in the expression of *SOC1*, a more reliable readout of the flowering response, is mainly caused by enhanced expression of *CO* and *FT* in *shb1-D* under long days. The double mutant of *shb1-D* (Ws) with *co-2* (L*er*) was constructed, and the flowering response and the expression of *FT* and *SOC1* in Ws, *shb1-D*, L*er*, *co-2,* Ws/L*er*, and *shb1-D*/*co-2* were examined (Figure 15). *shb1-D* was selected for this experiment since *shb1-D* has a stronger flowering phenotype over that of *shb1* and the flowering phenotype of *shb1-D* is opposite to that of *co-2*. To control the difference in flowering responses between crosses of different ecotypes, their flowering phenotypes were examined in a F2 segregating population. *shb1-D* contains a T-DNA

inserted 129 bp from the *SHB1* start codon and homozygous *shb1-D* will be genotyped by using a PCR strategy (Kang and Ni, 2006). *co-2* contains a point mutation and was genotyped by using two pairs of length polymorphic markers closely linked to the *co-2* locus (Kang et al., 2007). *shb1-D* flowers early under both long and short days, whereas *co-2* flowers late under long days but not short days (Figure 13, 15). The *shb1-D*/*co-2* double mutant flowered as late as *co-2* under long days, but showed an *shb1-D*-like early flowering phenotype under short days (Figure 15A, B).

Since the flowering response of *shb1-D* under long days is mainly operated through the CO signaling branch, *co-2* mutation may strongly block the activation of *FT* or *SOC1* expression by the *shb1-D* mutation. The expression of *FT* and *SOC1* in *shb1-D/co-2* double mutant was quantified compared with single mutants and wild types. At ZT 16 in long days, the activation of *FT* expression by the *shb1-D* mutation was totally impaired by the *co-2* mutation, however, at ZT 8 in short days, the activation of *FT* expression in *shb1-D* was only partially affected by the *co-2* mutation (Figure 15C). At ZT 16 in long days, the activation of *SOC1* by *shb1-D* mutation was also significantly suppressed by the *co-2* mutation (Figure 15C). However, at ZT 8 in short days, the induction of *SOC1* expression by *shb1-D* was barely affected by the *co-2* mutation (Figure 15C). Both genetic and expression analysis suggest that the function of SHB1 in flowering and the activation of *FT* or *SOC1* expression in long days requires a functional CO. In contrast, the flowering response of *shb1-D* in short days is barely dependent on the function of *CO*.

SHB1 acts in autonomous pathways by negatively regulating FLC expression

As the activation of *SOC1* expression by *shb1-D* was not significantly affected by the *co-2* mutation under short days, the flowering response of *shb1-D* may involve other components such as FLC, a major negative regulator in vernalization and autonomous pathway in *Arabidopsis*. The expression of *FLC* was determined through qRT-PCR and *FLC* transcript level was suppressed by 2-fold in *shb1-D* and increased 2-fold in *shb1* under both long-days and short-days (Figure 16A). The quantitative expression of *FLC* is tightly regulated and very sensitive for the floral initiation, and it has been shown that overexpression of *FLC* strongly suppressed the expression of both *FT* and *SOC1* (Hepworth et al., 2002; Michaels et al., 2005).

If the FLC signaling branch plays a minor role for the early flowering of *shb1-D* under long days, the expression of *FLC* at or slightly above the wild type level may not affect the activation of *SOC1* expression by the *shb1-D* mutation. In contrast, CO may not play a major role in short days and FLC is a strong flowering repressor, and the expression of *FT* and *SOC1* in short days may be regulated through the FLC signaling branch. Therefore, the expression of *FLC* at or slightly above the wild type level in the *shb1-D* background could largely block the early flowering response of *shb1-D* as well as the activation of *FT* or *SOC1* expression under short days.

Several independent transgenic lines that overexpress *FLC* in *shb1-D* mutant background were generated, and two lines had comparable level of *FLC* transcript to wild type level (Figure 16B). A third line contained a higher level of *FLC* transcripts than that of wild type (Figure 16B). Their flowering responses were then examined under both

long and short days (Figure 16C). The two transgenic plants with *FLC* expressed at the wild-type level in the *shb1-D* background showed a *shb1-D* like early flowering phenotype under long days, but a wild type-like flowering phenotype under short days (Figure 16C). The line that overexpresses *FLC* above the wild type level in *shb1-D* showed a late flowering phenotype under both long days, and much late flowering phenotype under short days (Figure 16C). The activation of *FT* expression by *shb1-D* was not largely affected in the two transgenic plants that express *FLC* at the wild type level at ZT 16 in long days, but was significantly altered comparable to *shb1-D* at ZT 12 in short days (Figure 16D). Furthermore, the activation of *SOC1* expression by *shb1-D* was partially suppressed under long days, but suppressed to wild type level under short days in the two transgenic plants that express *FLC* at the wild type level (Figure 16D). FLC apparently plays a more prominent role to mediate SHB1 function in short-day flowering, whereas CO may play a dominant role in SHB1 flowering under long days.

shb1/flc-3 double mutant was also constructed and their flowering responses were examined under long days and short days. Under long days, *shb1* flowered late and *flc-3* flowered slightly earlier than Col as previously reported (Figure 17A, Michaels and Amasino, 1999). The *flc-3* mutation only partially suppressed the late flowering phenotype of *shb1* in the double mutant (Figure 17A). In contrast, *flc-3* was completely epitatic to *shb1* under short days and *shb1/flc-3* showed a *flc-3* like early flowering phenotype (Figure 17A). Under short days, the *flc-3* mutation also totally suppressed the effects of the *shb1* mutation on the expression of either *FT* or *SOC1* (Figure 17B, C).

However, the *flc-3* mutation only partially suppressed the effects of the *shb1* mutation on the expression of *FT* and *SOC1* under long days (Figure 17B, C).

SHB1* acts upstream of *LUMINDEPENDENS

The expression of all known genes in autonomous flowering pathway upstream of *FLC* were investigated in *shb1-D* and *shb1* compared with wild type, and RT-PCR results demonstrated that SHB1 specifically and positively regulated the expression of *LUMINIDEPENDENS* (*LD*) but not all others under long-days and short-days (Figure 18A; data not shown). The expression of *LD* was increased by 2 fold in *shb1-D* compared to wild type and was reduced by half in *shb1* (Figure 18A). LD has been characterized as positive regulator upstream of *FLC* in the autonomous flowering pathway. *ld-3* mutant shows late flowering phenotype and *FLC* expression level is up-regulated in *ld-3* (Koornneef et al., 1991; Michaels and Amasino, 1999) . Interestingly, the tissue specific expression pattern of *SHB1* showed a large overlap with that of *LD*. *LD* transcript and protein are very abundant in shoot apices, floral bus, stems, and roots, and less abundant in leaves (Aukerman et al., 1999). The expression of *SHB1* was observed strong in flower buds (including floral organs, pollen grains, and prepollinated ovules) and seedlings, intermediate in seedlings, shoot apex, and developing siliques, and weak in cauline leaves (Figure 18B).

Furthermore, *ld* is epistatic to *shb1-D* and *shb1-D/ld-3* double mutant showed a *ld-3*-like flowering phenotype under both long-days and short-days (Figure 18C). The repression on the expression of *FLC* by *shb1-D* was totally reverted by the *ld-3* mutation,

and the expression of *FLC* in the *shb1-D/ld-3* double mutant is similar to that of the *ld-3* single mutants under long-days and short-days (Figure 18D).

SHB1 interacts with photoreceptors

To learn the function of SHB1 in photoperiodic flowering with respect to the photoreceptors, the genetic interaction of *shb1-D* with *phyA-211*, *phyB-9*, and *cry2-1* was analyzed under long days and short days (Figure 19). *shb1-D* flowered earlier than did Ws/Col wild type, whereas *phyA-211* flowered slightly later than did Ws/Col wild type under both long days and short days (Figure 19). *shb1-D/ phyA-211* showed an incomplete epistasis or an intermediate flowering phenotype of the *shb1-D* and *phyA-211* single mutants under both long days and short days, suggesting certain degree of interaction between SHB1 and phyA (Figure 19). *cry2-1* flowered much later that did Ws/Col wild type under long days, and flowered normally under short days (Figure 19). *shb1-D*/*cry2-1* showed a *cry2-1*-like late flowering phenotype under long days, and a *shb1-D*-like early flowering phenotype under short-days (Figure 19). Similarly, *shb1/cry2-1* showed a *cry2-1*-like flowering phenotype under long days and a *shb1*-like flowering phenotype under short days (Figure 20).

shb1 flowered notably later than did Col wild type, whereas *phyB-9* flowered much earlier than did Col under both long days and short days. *shb1*/*phyB-9* double mutant flowered as early as the *phyB-9* single mutant in both long days and short days (Figure 20). *shb1-D* flowered early under both long days and short days, whereas *phyB-9* flowered earlier than did *shb1-D* under long days but similarly as did *shb1-D* under short

days (Figure 20). *shb1-D*/*phyB-9* showed a *phyB-9*-like flowering phenotype under long days but an additive flowering phenotype under short-days (Figure 20).

Discussion

SHB1 activates CO and FT to control flowering under long days

As the *shb1-D* mutation affects the expression of both *CO* and *FLC*, It is aimed to sort out the contribution of SHB1 to the photoperiodic and autonomous pathways under different day-length conditions. The results suggest that SHB1 functions dually to channel the leave-derived photoperiod-mediated promotion signals and meristem-derived autonomous-mediated repression signaling to accommodate the final floral initiation. Day-length sensing and CO activation occurs in the leaves, and subsequently activates FT moves through pholem to shoot apical meristem where it physically interacts with FD to promote downstream gene expressions (An et al., 2004; Abe et al., 2005; Wigge et al., 2005; Corbesier et al., 2007). The expression of *SHB1* was also detected in leaves, and locally expressed SHB1 in leaves might function in *CO* activation and subsequent induction of *FT* and *SOC1* expression. Under long days, CO either binds to *SOC1* promoter to directly regulate its expression or upregulates the expression of *FT* and therefore, the expression of *SOC1* (Hepworth et al., 2002; Yoo et al., 2005). CO is epistatic to SHB1 under long days, and the activation of *FT* by SHB1 required the proper function of CO (Figure 15). SHB1 thus acts upstream of CO under long-day condition. In contrast, *shb1-D/co-2* double mutant showed a *shb1-D*-like flowering phenotype under short days (Figure 15). The activation of *FT* expression by SHB1 was only slightly

affected by the *co-2* mutation, and the activation of *SOC1* expression by SHB1 was barely affected by the *co-2* mutation under short days (Figure 15). SHB1 may deploy a different mechanism to regulate the expression of *SOC1* under short-days.

SHB1 regulates flowering through FLC under short days

Under short days, the activation of *FT* expression by SHB1 was operated through LD and FLC (Figure 16, 17). The expression of *FLC* was up-regulated by SHB1 and the activation of either *FT* or *SOC1* expression by SHB1 was diminished by elevating FLC level to wild type under short-days (Figure 16). Increased expression of *FLC* to wild type level in *shb1-D* background only partially affected the activation of either *FT* or *SOC1* expression (Figure 16D). Consistent with previous reports, *flc-3* mutant flowered slightly late under long days, but much later under short days (Figure 17A; Michaels et al., 2005). *shb1*/*flc-3* double mutant showed an intermediate flowering phenotype under long days but an *flc-3*-like flowering phenotype under short days (Figure 17A). Furthermore, the reduced expression of either *FT* or *SOC1* by the *shb1* mutation was reverted partially under long days but completely to level comparable to that of *flc-3* under short days.

SHB1 acts upstream of LD

The expression of *LD*, *FVE*, *FLD*, *FLK*, *FY*, *FCA* and *FPA* were examined in *shb1* mutants, and only the expression of *LD* was affected by the *shb1* mutations (Figure 18A). The effect of the *shb1-D* mutation on the expression of *FLC* requires a functional LD under both long days and short days (Figure 18D). It remains interesting if

overexpression of *LD* can mimic the phenotype of the gain-of-function allele *shb1-D* and its effects on *FLC* expression. Interestingly, the expression of *SHB1* overlaps with that of *LD* in shoot apex and floral organs (Figure 18B, Aukerman et al., 1999). Similarly, *FLC* is also expressed in shoot apical meristem in addition to leaves and root meristem (Sheldon et al., 1999), (Noh and Amasino, 2003) and (Bastow et al., 2004). The overlapping expression pattern of *SHB1* with that of *LD* and *FLC* in the shoot apex may suggest a close functional relation of these three genes. ChIP analysis indicated that SHB1 is not associated with the promoters of either *CO* or *LD* through (Figure 20). It is speculated that SHB1 may directly regulate the expression of genes upstream of CO and LD.

Chromatin modifications, including histone acetylation and methylation, play an important role in controlling *FLC* expression (He and Amasino, 2005; Domagalska et al., 2007). The *ld-3* mutation increased methylation of the *FLC* locus in triMeH3K4 in region IV, corresponding to the 5' UTR and the first exon (Lee et al., 1994). The histone H3 acetylation (H3Ac) was also increased in the regions around the translation initiation start, the first exon, and the 5' region around the first intron of the *FLC* locus in the *ld-3* mutant (Domagalska et al., 2007). Although the chromatin structure of the *FLC* locus was not examined in *shb1* mutants, it is very likely that SHB1 regulate the expression of *FLC* expression through LD and its effects on the chromatin structure of the *FLC* locus.

SHB1 functions downstream of phyB and cry2

The expression patterns of the clock input genes such as *ELF3* and the central oscillating genes such as *CCA1*, *LHY*, *ELF4, TOC1,* and *GIGANTEA (GI)* were not altered by *shb1* mutations compared with wild type (data not shown). *SHB1* transcripts did not show robust oscillation when entrained under 12h light/12h dark cycle and SHB1 might not involve in the circadian regulation of the flowering time (data not shown).

Phytochromes and cryptochromes regulate flowering through light quality in a circadian dependent or independent manners. phyB mediates red light repression of flowering under both long days and short days (Mockler et al., 2003; Valverde et al. 2004). phyA promotes flowering possibly through both phyB dependent and independent ways (Lin, 2000; Mockler et al., 2003; Valverde et al., 2004). In response to extended photoperiods, cry2-deficient *Arabidopsis* plants have a delayed flowering response through the regulation on either the abundance of CO transcripts or CO protein stability (Guo et al., 1998; Valverde et al., 2004). The genetic analysis demonstrated that the effects of *shb1* mutations on flowering require functional phyB under both long days and short days and functional cry2 under long days (Figure 19, 20). The interaction of SHB1 with phyA appeared more complex.

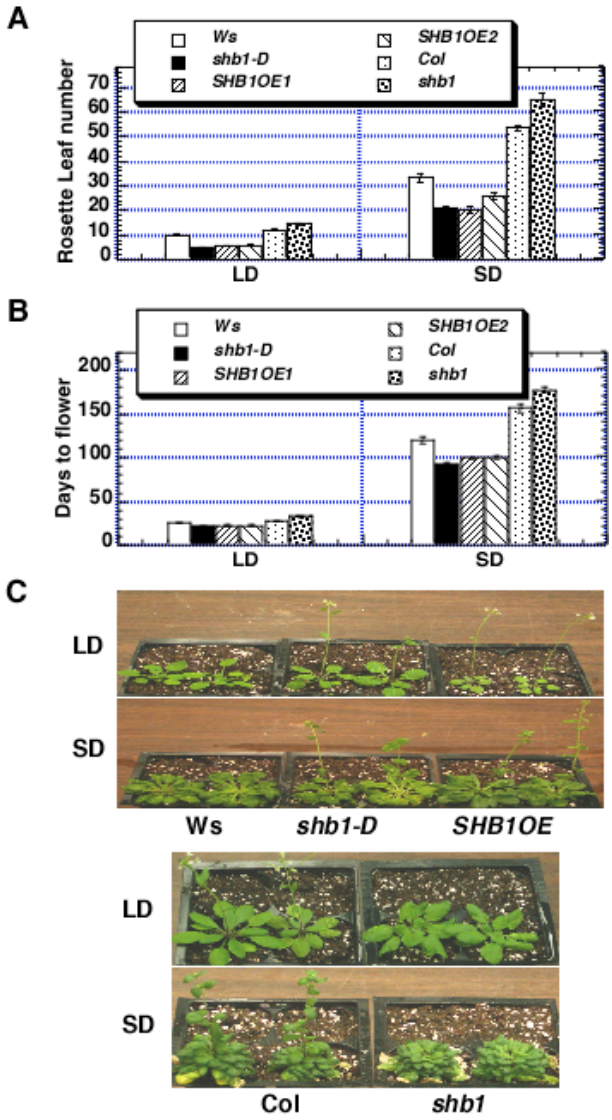

Fig. 13. *shb1* mutations affect flowering. (A) Rosette leaf numbers of Ws, *shb1-D*, and the transgenic plants that overexpress full-length SHB1 (*SHB1 OE*), Col, and *shb1* under LD (16 hr light/8 hr dark) or SD (8 hr light/16 hr dark). (B) Days to flowering of Ws, *shb1-D*, *SHB1 OE*, Col, and *shb1* under LD or SD. The means plus or minus the standard errors were calculated from at least 25 plants. (C) Ws, *shb1-D*, *SHB1OE* at 30 days after germination (LD) or at 100 days after germination (SD); Col and *shb1* at 35 days after germination (LD) or at 140 days after germination (SD).

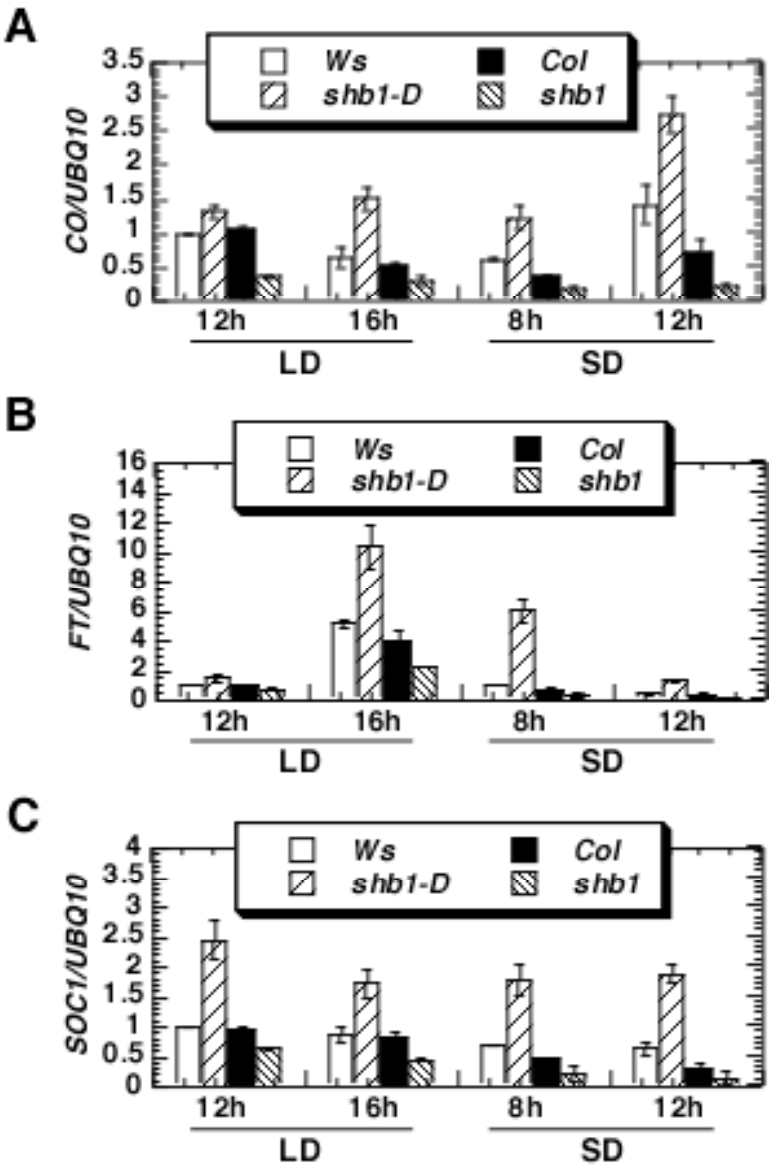

Fig. 14. *shb1* mutations affect the expression of *CO* (A), *FT* (B) and *SOC1* (C) under long days and short days through real time RT-PCR analysis. The expression of each gene is normalized to that of Ws at long-day ZT 12 h except for he expression of *FT* in short days, which is normalized to that of Ws at short-day ZT 8 h.

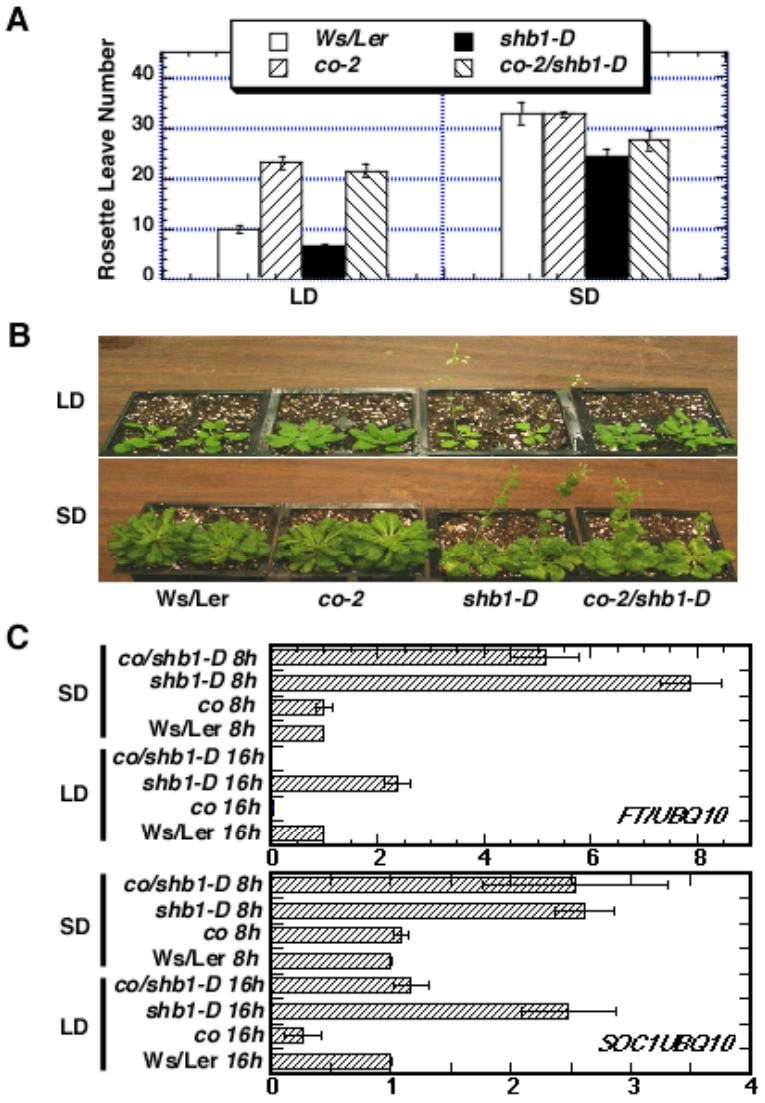

Fig. 15. *co-2* is epistatic to *shb1-D* under long days. (A) Rosette leaf number of wild type (Ws/Ler), *co-2* (Ws/Ler), *shb1-D* (Ws/Ler), and *shb1-D/co* (Ws/Ler) at bolting 1 cm. At least six independent lines from each genotype in a mixed Ws/ler background were used in the flowering experiment. Data are presented as means plus or minus the standard errors. (B) Ws/ler, *co-2* (Ws/ler), *shb1-D* (Ws/ler), and *shb1-D/co-2* (Ws/ler) at 30 days after germination (LD) or at 90 days after germination (SD). Expression of *FT* (C) and *SOC1* (D) in Wild type (Ws/ler), *co-2* (Ws/ler), *shb1-D* (Ws/ler), and *shb1-D/co-2* (Ws/ler) under LD and SD.

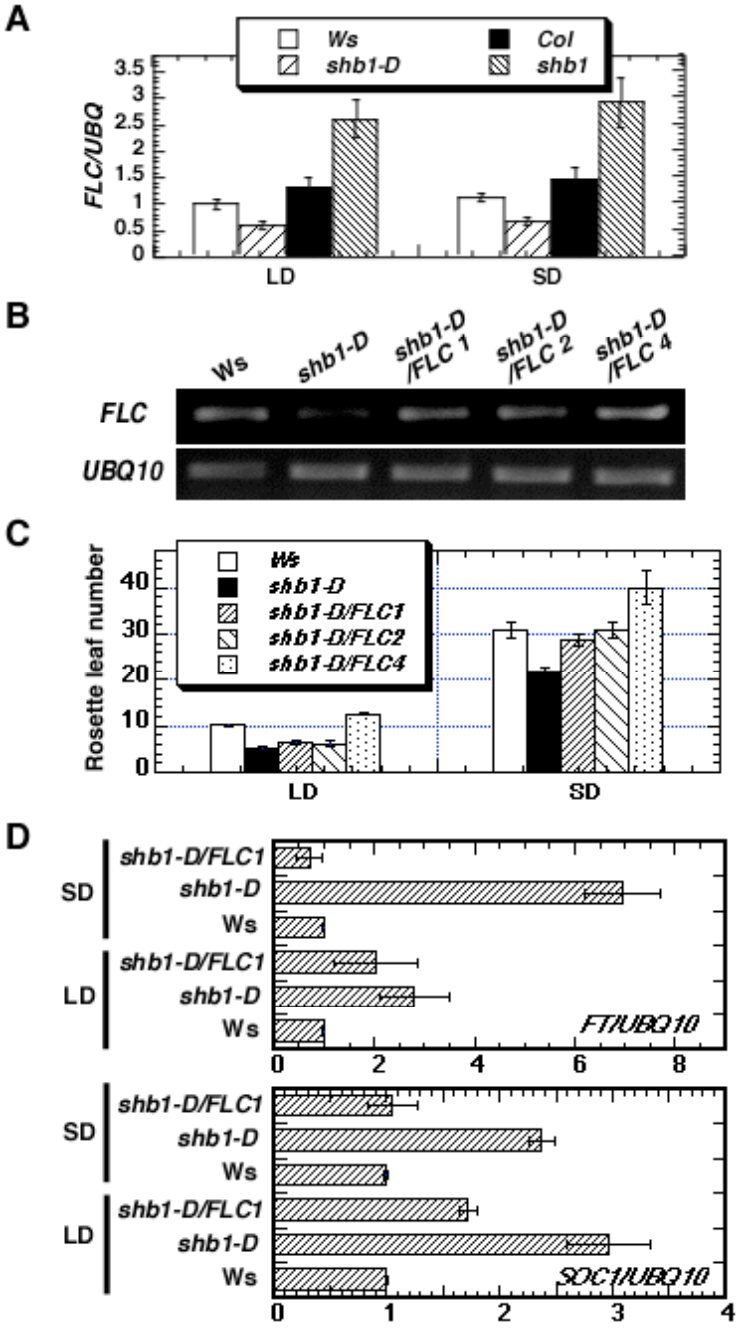

Fig. 16. *shb1* mutations affect the expression of *FLC*. (A) Real time RT-PCR analysis of *FLC* expression in Ws, *shb1-D*, Col, and *shb1* under LD and SD. (B) The expression of *FLC* in Ws, *shb1-D*, and several *FLC* transgenic lines in *shb1-D* background, including

the endogenous *FLC* transcripts and the transcripts of *FLC* transgene. (C) Rosette leaf number of Ws, *shb1-D*, and several *FLC* transgenic lines in *shb1-D* background under long days and short days. (D) Expression of *FT* and *SOC1* under LD and SD in Ws, *shb1-D*, and *FLC* transgenic lines in *shb1-D* background. The expression of each gene at different time points is normalized to that of Ws under long days.

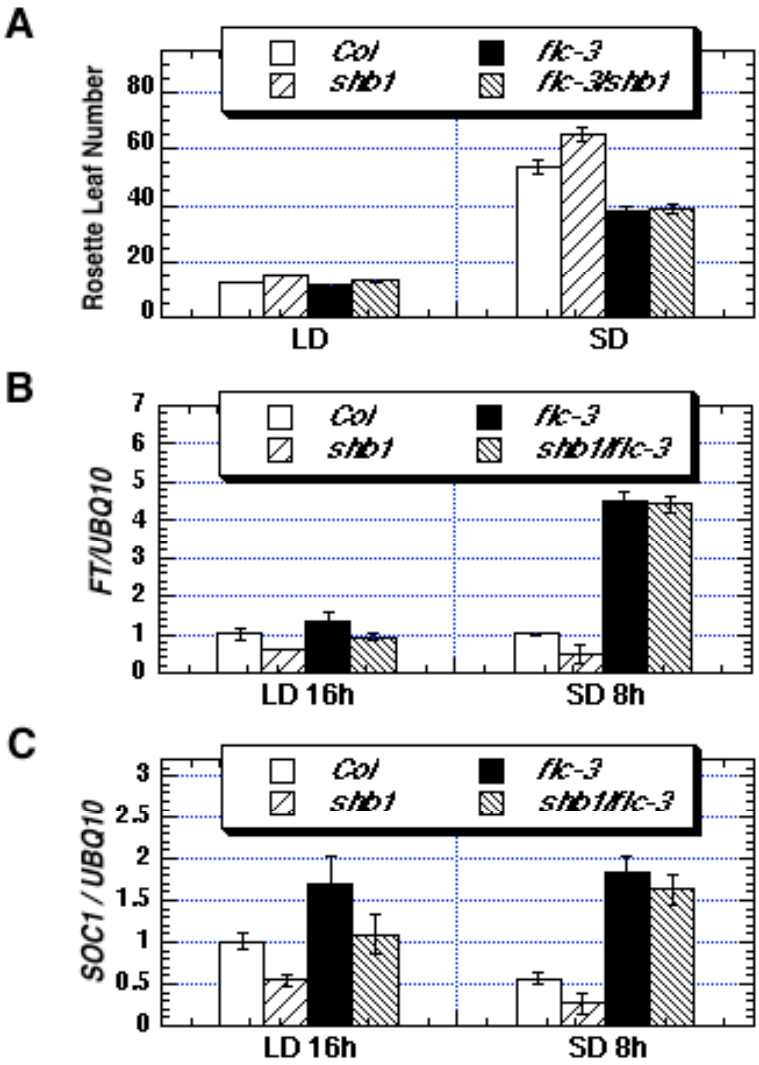

Fig. 17. *SHB1* acts upstream *FLC*. (A) Rosette leaf number of Col, *shb1*, *flc-3*, and *shb1*/*flc-3* under long days and short days. Expression of *FT* (B) and *SOC1* (C) in Col, *shb1*, *flc-3*, and *shb1*/*flc-3* under long days and short days through real time RT-PCR analysis. The expression of each gene is normalized to that of Ws at long-day ZT 12 h except for the expression of *FT* in short days, which is normalized to that of Ws at short day ZT 8 h.

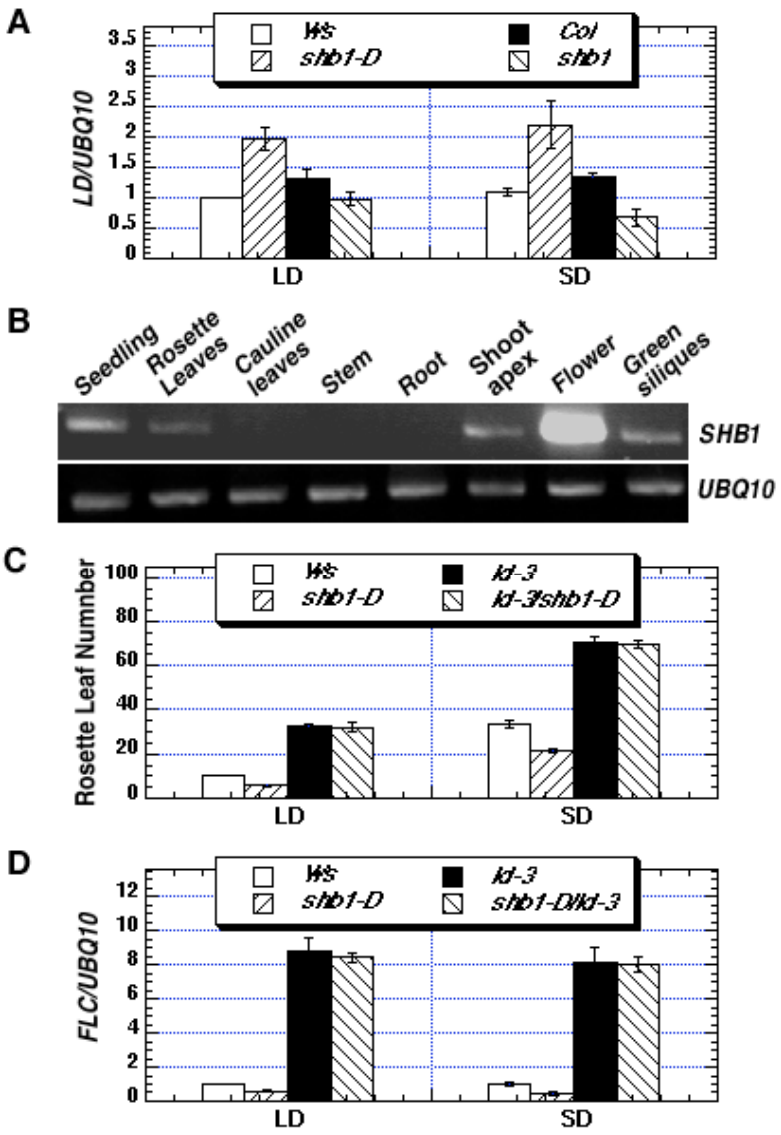

Fig. 18. SHB1 acts upstream of *LUMINIDEPENDENS* or *LD*. (A) Real time RT-PCR analysis of *LD* expression in Ws, *shb1-D*, Col, and *shb1* under LD and SD. (B) Expression of SHB1 in different tissue types through real-time RT-PCR analysis showed the organ-type specific expression pattern of *SHB1*. (C) Rosette leaf numbers of Ws, *ld-3*, *shb1-D*, and *shb1-D/ld-3* under LD and SD. (D) Expression of *FLC* in Ws, *ld-3*, *shb1-D*, and *shb1-D/ld-3* under LD and SD.

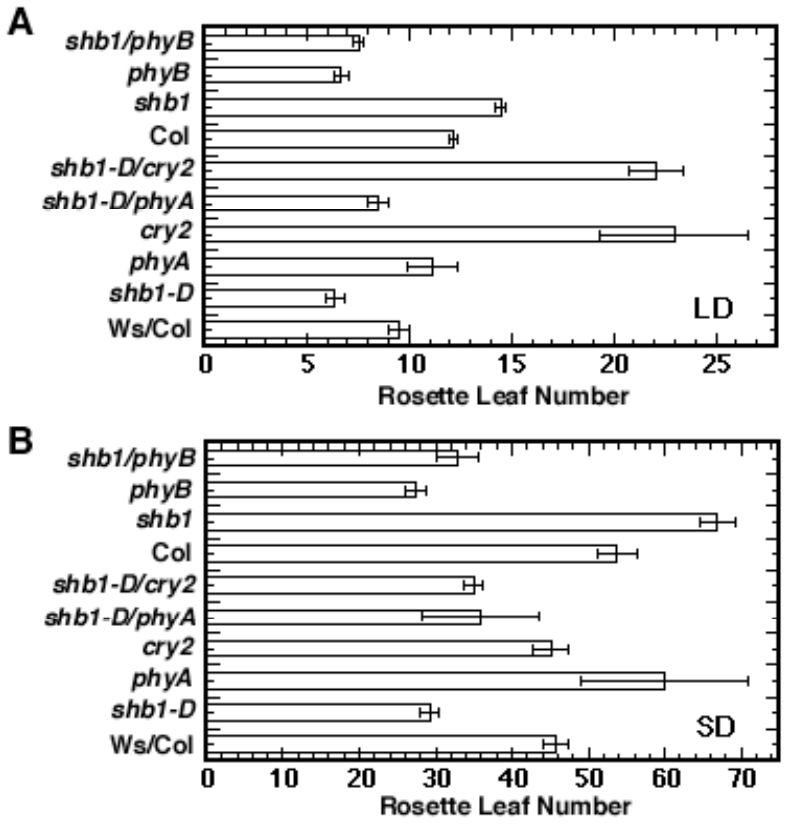

Fig. 19. SHB1 interacts genetically with photoreceptors. Rosette leaf numbers of Ws/Col, *shb1-D (W/C)*, *phyA-211 (W/C)*, *cry2-1 (W/C)*, *shb1-D*/*phyA-211 (W/C)*, *and shb1-D*/*cry2-1 (W/C)*, Col, *shb1, phyB-9, shb1*/*phyB-9* under long days (A) and short days (B) at bolting 1 cm.

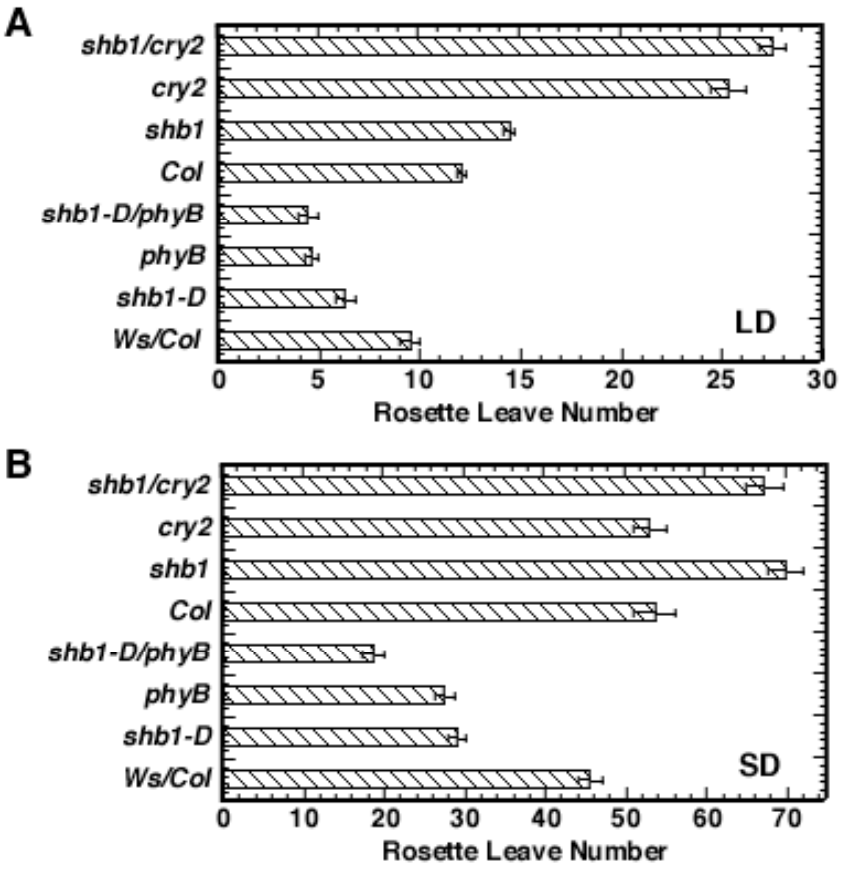

Fig. 20. Genetic interaction of *shb1-D* with *phyB-9* and *shb1* with *cry2-1*. Rosette leaf numbers of Ws/Col, *shb1-D* (Ws/Col), *phyB-9* (Ws/Col), *shb1-D*/*phyB-9* (Ws/Col), Col, *shb1*, *cry2-1*, and *shb1*/*cry2-1* under long days (A) and short days (B) at bolting 1 cm.

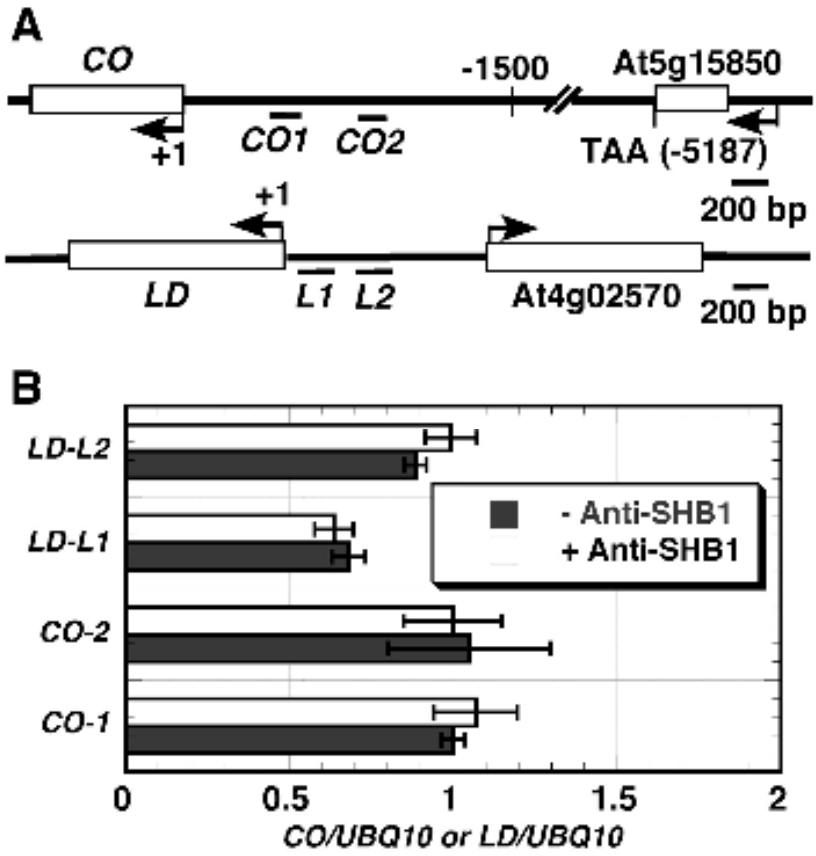

Figure 21. ChIP analysis of SHB1 over *CO* and *LD* promoters. (A) Schematic drawing of the *CO* and *LD* loci and different amplicons used for ChIP analysis. (B) Enrichment of *CO* and *LD* chromatin regions with anti-SHB1 antibody in wild type plants through real-time PCR analysis. Preimmune serum was used as mock control and the fold enrichment of the specific chromatin fragment was normalized to *UBQ10* amplicon and calculated for each amplicon by using the following equation: $2^{(Ct\ LD\ /\ L1\ MOCK - Ct\ LD\ /\ L1\ ChIP)\ /\ 2(Ct\ UBQ10\ MOCK - Ct\ UBQ10\ ChIP)}$. Means were calculated from two biological samples and each biological sample was examined with four PCR technical replicates. The calculated standard errors include technical error and biological error.

Chapter IV

SHB1 functions in seed development in *Arabidopsis*

Introduction

In this chapter, I demonstrate that SHB1 also has specific function in *Arabidopsis* seed development. The seed phenotype is not tightly related to its function in light signaling since other light signaling mutants do not have alterations in seed development. In addition, there were no particular enhancement of *shb1-D* or *shb1* seed size by red, far-red enriched, or blue light compared to white light. The seed development defects in gain- and loss-of-function *shb1* mutants indicate that SHB1 affects the endosperm proliferation and the timing of endosperm cellularization in the initial phase of seed development. SHB1 associates with *MINI3* and *IKU2* promoters as shown by chromatin immunoprecipitation (ChIP) analysis, which indicates SHB1 is involved in the direct transcription activation of *MINI3* and *IKU2* in the early seed development in *Arabidopsis*.

Materials and Methods

Plant materials and growth conditions

mini3-2 (SALK_050364), *iku2-4* (SALK_073260), and *ap2* (SALK_071140) are in Columbia (Col) background and were obtained from the *Arabidopsis* Biological Resources Stock Center (Ohio State University, Columbus). *shb1-D* and *shb1* mutants were backcrossed twice to wild type before phenotypic analysis. Plants were grown at 23°C under continuous light. All seeds from a single plant were harvested when the plant was mature and the last siliques on the inflorescence had elongated, turned brown, and

dried. Early at four-leaf stage, the younger plants or seedlings were also fitted with a plastic well to catch all seeds released by dehiscing siliques. These hand-harvested seeds were combined with those caught in the well, dried at 25°C for 7 days, and weighed.

Cytological experiments

Mature seeds of Ws, *shb1-D, SHB1 OE*, Col, *shb1*, Ws/Col, *mini3-2, iku2-4, mini3-2/shb1-D, iku2-4/shb1-D* were photographed under Nikon Eclipse E800 microscope with a Cool Cam color CCD camera (Cool Camera) and Imago Pro Plus version 3.0 software (Media cybermetics). Mature dried seeds of wild type and *shb1* mutants were also imbibed for 1 hr and dissected under a microscope to isolate mature embryos. The embryos was incubated in buffer that contains 50 mM sodium phosphate pH 7.0, 10 mM EDTA, 1% Triton X-100, and 1% DMSO at 37°C for 12 hr, fixed with FAA that contains 10% formalin, 5% acetic acid, 45% ethanol, and 0.01% Triton X-100 for 45 min, and dehydrated through an ethanol series (Ohto et al., 2005). The embryos were then treated for 1 h in Hoyer's solution that contains 3:0.8:0.4 of chloral hydrate:water:glycerol. Observations were made with a Zeiss 510 Meta laser scanning confocal microscope. Cotyledon area and average epidermal cell size from the central region of cotyledons were determined by using NIH IMAGE analysis software as described (Ohto et al., 2005). The area of cotyledon was calculated from 50 mature embryos. The cell size in the middle of cotyledon was also determined from 20 mature embryos by dividing the equal area of the image by the number of cells. Data are presented as the average of two independent experiments.

Scanning electron microscopy (SEM)

The mature embryos from mutant and wild type were released from the seed coats by applying gentle pressure, and fixed in FAA (10% formalin, 5% acetic acid, 45% ethanol, and 0.01% Triton X-100) at 4°C for 2 hours. After fixation, the samples were dehydrated through an ethanol series (70%, 85%, 95%, and 100%), each for 30 min. The embryos were then critical point dried using Autosamdri-814 Critical Point Dryer (Tousimis, USA). The individual embryos were mounted on SEM stubs, sputter-coated with gold with a Fullam Sputter-coater, and examined under a Hitachi S3500N Variable Pressure Scanning Electron Microscope (Tokyo, Japan) at an accelerating voltage of 5 k.

Protein, Carbohydrate, and fatty acids analysis

Total proteins were extracted from the same number of seeds from wild type and mutants as described (Heath et al., 1986). The content was determined by using Bio-Rad assay kit with BSA as standard. Total protein extracts from 200 seeds of wild type and mutants was also fractionated on 12% SDS-PAGE and stained with Coomassie blue as described (Ohto et al., 2005).

To extract total fatty acids, 100 seeds from wild type and mutants were homogenized in 500 ml 1 N HCl-methanol, and 200 ml hexane were added in each vial and heated for two hours at 85 °C (Larson and Graham, 2001). After heating, the solutions were cooled and 250 ml 0.9% KCl was added to partition the hexane phase that contained the fatty acid methyl esters. One ml aliquot of the hexane solution was then

analyzed by gas chromatography with flame ionization detection (GC-FID). Free fatty acid C21:0 (Sigma) was added as an internal control. The content of total fatty acids was estimated by comparing the total fatty acid methyl ester peak area to that of the C21:0 internal standard.

To extract total sugars and reducing sugars from mature seeds, one hundred seeds each of wild type and *shb1* mutants were also homogenized in 500 ml 80% ethanol, and the extracts were incubated at 70°C for 90 min (Focks and Benning, 1998). Following centrifugation, the supernatant was saved and the pellet was extracted twice again with 500 µl of 80% ethanol. The combined supernatants were evaporated, and the residue was dissolved in 100 µl of dH_2O and measured for reducing sugars by the Nelson-Somogyi assay (Nelson, 1944; Somogyi, 1952). The total sugar contents were measured by using phenol sulfuric acid carbohydrate assay against 1 mg/ml glucose-generated standard curve (Dubois et al., 1956).

Developmental alteration analysis

To examine the developmental alterations of *shb1* mutants, wild type and *shb1* mutant flowers were hand-pollinated, and the developing seeds were harvested at different days after pollination. The siliques were then cut into 2-mm length fragments, fixed, and dehydrated as described above. The segments were next cleared in Hoyer's solution overnight and examined by using an Olympus BX51 with differential interference contrast (DIC) optics. Data after 10 DAP were not collected as siliques were mature and preparation of clear seeds at these late developmental stages become difficult.

To investigate endosperm development, the siliques were fixed in FAA solution overnight at 4°C, dehydrated as described above, and embedded in EPON 812 (SERVA). Sections were stained with 0.1% (w/v) toludine blue O in distilled water. Stained sections were photographed by using an Olympus BH-2 microscope.

Real-time RT-PCR analysis

For qRT-PCR analysis, total RNAs were isolated using SV Total RNA isolation kit (Promega) from green siliques of wild type and various mutants. SuperScript^{TM} III reverse transcriptase (Invitrogen) was used to synthesize the first-strand cDNA with oligo dT primer and 1 μg of total RNA at 50°C for 1 h. Quantitative PCR was then performed with Platinum SYBR Green qRT-PCR kit (Invitrogen) on a Applied Biosystems 7500 Real Time PCR machine. The thermal cycling program was 50°C for 10 min and 95°C for 10 min, followed by 40 cycles of 95°C for 30 s, 56°C for 30s, 72°C for 1 min and a one-cycle dissociation stage at 95°C for 15 s, 60°C for 1 min, and 95°C for 15 s. The primers used in qRT-PCR were *MINI3*, 5'- TTTGATGATATTGCAACGGAA -3' and 5'- GATCCTTTGTGTCTTGCTTGT -3'; *IKU2*, 5'- CGTGTGAGACAAGCGTTAGC -3' and 5'- GAGGAGACTTGTCCGTGCAT -3'; *AP2*, 5'- ATTCGGCTAATTCGAAGCATAA -3' and 5'- AGAGGAGGTTGGAAGCCATT -3'; *SHB1*, 5'- CAGGTTCAAGCACTGAGGAGT -3' and 5'- TGCTTCCTCGGTTTAGAGTA -3'; *UBQ10*, 5'- AGGTACAGCGAGAGAAAGTAGCA -3' and 5'- TAGGCATAGCGGCGAGGCGT -3'. *UBQ10* was used as an internal reference. Data were calculated from three biological

replicates and each biological replicate was examined in triplicate.

Reciprocal crosses and double mutant analysis

The reciprocal crosses between Ws and *shb1-D* and between Col and *shb1* were made with flowers at identical positions (11th to 14th flowers) on secondary inflorescences. Seed weight and seed number per silique were determined from 4 separate inflorescences per plant and 4 to 5 plants total. A series of double mutants of *shb1-D* with small seed size mutants *mini3-2* and *iku2-4* were made and PCR-genotyped. Gene specific primers for *MINI3* are 5'- TGTCGTTGCAATCTCTCCA -3' and 5'- GATCCTTTGTGTCTTGCTTGT -3'. Gene specific primers for *IKU2* are 5'- TCTTTTTAATGCCACTAGCTT -3' and 5'- CGAACATTCCAAGAGACACA -3'. Gene specific primers for *SHB1* are 5'- TAAGCAGCACGAGCTCAAAT -3' and 5'- TGCTTCCTCGGTTTAGAGTA -3'. Gene specific primers for *AP2* are 5'- TAGGTGGATTTGACACTGCT -3' and 5'- AGAGGAGGTTGGAAGCCATT -3'. The T-DNA specific primer for *mini3-2, iku2-4*, *shb1*, and *ap2* is 5'- GGAACCACCATCAAACAGGAT -3'. For *shb1-D* genotyping, gene specific primers are 5'- GAAGATACGGGTTTTGCAT -3' and 5'- GGGAAGCTTGGATGTCTTGAA -3', and the T-DNA specific primer is 5'- CATTTTATAATAACGCTGCGGACATCTAC -3'.

SHB1::GUS construct and GUS staining

A 2886 bp *SHB1* promoter region was amplified with PCR by using forward primer 5′- CTAAGCTTCTTCGCGTTATATGACACAACG -3′ and reverse primer 5′- TGAATCTTGGCCTCTCTCTGTC -3′ that contain Hind III and Sal I restriction sites. The PCR fragment was digested with Hind III and Sal I, and inserted in-frame in front of GUS gene in pCAMBIA1391 plasmid. The constructs were transformed into Ws through floral dip method by using *Agrobacterium tumefaciens* GV3101 (Clough and Bent, 1998). Transgenic plants were selected on 25 mg/l hygromycin B medium (Roche, Germany). GUS staining was performed by using the method of Sieburth and Meyerowitz (1997) with some modifications. Tissues were gently fixed by incubation in 90% acetone on ice for 15 to 20 min, and rinsed with buffer that contains 50 mM $NaPO_4$ pH7.2, 0.5 mM $K_3Fe(CN)_6$, and 0.5 mM $K_4Fe(CN)_6$. Tissues were then transferred to staining solution that contains 50 mM $NaPO_4$ pH 7.2, 2 mM X-gluc (sigma), 0.5 mM $K_3Fe(CN)_6$, and 0.5 mM $K_4Fe(CN)_6$, vacuum infiltrated for 10 min, and incubated at 37°C overnight. After staining, tissues were hydrated with 70% ethanol for 1 hr and cleared in Hoyer's solution. Ovules were observed by using an Olympus BX51 with differential interference contrast (DIC) optics. Other tissues were photographed by using a dissection microscope.

In situ hybridization

Ws wild type flowers were hand-pollinated, and the developing seeds were harvested at different days after pollination. The harvested siliques were fixed in FAA overnight at 4 °C, embedded in paraplast (Sigma) after dehydration, and sectioned at 8

μm. A 379 bp fragment specific to the 5' end of *SHB1* gene was amplified with forward primer 5′- GAGGTTTGGGAAAGAGTTTGTGTC -3′ and reverse primer 5′- AGCTGTCTCCACTTTCAGCCTG -3′, and cloned into pGEM-T easy vector. Antisense and sense RNA probes were synthesized *in vitro* with digoxigenin-UTP by SP6 and T7 RNA polymerases (digoxigenin RNA labeling kit, Boehringer Mannheim). Sections were hybridized with 200 ng/ml probes at 42 °C overnight in hybridization solution that contains 50% formamide. Hybridization signals were detected by using anti-digoxigenin antibody conjugated to alkaline phosphatase (DIG Nucleic Acid Detection Kit, Boehringer Mannheim). Photographs were taken by using an Olympus BH-2 microscope.

Chromatin immunoprecipitation (ChIP) assays

ChIP assays were performed as described (Bowler et al., 2004; Sawa et al., 2007) with minor modification. Briefly, developing siliques and closed floral buds were fixed with 1% formaldehyde under vacuum. Chromatins were incubated with either anti-SHB1 antibody or anti-GFP antibody (Santa Cruz, CA) for 3 hr at 4°C and added with protein A/G agarose beads, that were pre-equilibrated with salmon sperm DNA, for another 2 hr at 4°C. Preimmune serum was used as negative controls. After washing twice with low salt buffer and high salt buffer, respectively, that contains 0.05% SDS and 0.5% Triton X-100 (Bowler et al., 2004), the immuno-complexes were eluted from the agarose beads twicw by using fresh prepared elution buffer at 65°C (Bowler et al., 2004). DNA was purified by phenol/chloroform extraction and recovered by ethanol precipitation in the presence of glycogen (Sawa et al., 2007). DNA pellet was re-suspended in 150 μl water

and 3 µl aliquots were used for q-PCR analysis. Quantitative PCR was performed as described under the real-time PCR analysis section. The primer pairs used in real-time PCR experiments were: MINI3/M1, 5'- CTCATTTTTGACAAATCCTT -3' and 5'- AACCGAAGTAGAAACCTAAA -3'; MINI3/M2, 5'- TTGTTTTCAATTTTTCACAT -3' and 5'- AACAAACGGTTATTTTTCTT -3'; MINI3/M3, 5'- TGATGGTATAGTACCGTGATCG -3' and 5'- TTGGTTGGACTGGTAGAGTCAG -3'; IKU2/IK1, 5'- TCTCCGGTCTCTCTTGATAA -3' and 5'- GTAGGCGAAACAACATAAGG -3'; IKU2/IK2, 5'- CCTTATGTTGTTTCGCCTAC -3' and 5'- TCTCTACGTCGGAAGGATTA -3'; UBQ10, 5'- TCCAGGACAAGGAGGTATTCCTCCG-3' and 5'- CCACCAAAGTTTTACATGAAACGAA-3'.

Results

shb1-D produces significantly enlarged seeds and shb1 reduces seed size

The average seed mass was analyzed by weighing mature dry seeds in batches of 100 for seed lots from independently propagated Ws, *shb1-D*, Col, and *shb1* lines or independent transgenic lines that overexpress either GFP or full-length SHB1::GFP. *shb1-D* and the *SHB1 OE* had significantly increased seed weight per 100 seeds or per silique compared to Ws wild type, whereas the *shb1* mutation reduced seed weight by 15% compared to Col wild type ($P < 0.01$, two-tailed Student's t-tests) (Figures 22 A, B). Data from over 20 lines indicate that the increase in the seed mass of *sbh1-D* was 1.5- to 1.7-fold over that of Ws wild type (Figure 22B). By contrary, the number of seeds per

silique and the number of siliques per plant were not changed for Ws and *shb1-D* (Figure 22C and Figure 23). All seeds from each plant were harvested and as shown in Figure 22D, the seed yield of *shb1-D* plant was increased compared to Ws wild type and the seed yield of *shb1* was notably reduced compared to Col ($P < 0.001$, two-tailed Student's t-tests). Therefore, the increase in seed yield of *shb1-D* is due to an increase in seed size but not seed number.

Seed enlargement of shb1-D is due to increases in cell size and cell number

Embryos from mature seeds were isolated and visualized, and the cotyledon area of *shb1-D* was 1.5-fold larger than that of Ws wild type (Figures 24A, B). The embryonic shoot or hypocotyl and embryonic root apex of *shb1-D* also appeared larger compared to Ws wild type (Figure 24A). I further addressed if the seed size increase of *shb1-D* is due to an increase in cell division or cell expansion. The averaged size of *shb1-D* cotyledon cells is 1.2-fold that of wild type (Figure 24B). The size of *shb1-D* hypocotyl cells also appeared larger than that of Ws wild type (Figure 24C), and an up-regulation of two expansins, A21 and R3 were detected, up to 4-fold in *shb1-D*. The epidermal cells of mature embryo were monitored under scanning electron microscopy (SEM), and counted the cell number from 3 columns in the central region of cotyledons or hypocotyl plus embryonic root of Ws and *shb1-D*. The average cell numbers of cotyledon and hypocotyl plus embryonic root in *shb1-D* were 1.23 and 1.29-fold, respectively, over that of Ws wild type (Figure 24D). Interestingly, the 1.2-fold increase in cell size and 1.23- to 1.29-fold increase in cell number accounted for 1.44- to 1.56-fold increase in embryo size of

shb1-D. These data demonstrate that both increased cell size and cell number contribute to the overall enlargement of mature embryo in the gain-of-function mutant *shb1-D*.

shb1-D seeds accumulate more proteins and fatty acids

The seed mass alterations in *shb1-D* and *shb1* may be due in part to an increase or a decrease in seed reserves. The protein extracts from 200 seeds each of Ws wild type or *shb1-D* were prepared and the content and spectrum of soluble proteins were examined. Two major classes of *Arabidopsis* seed storage proteins include the 12S cruciferins and the 2S albumins (Heath et al., 1986; Pang et al., 1988). The seeds of *shb1-D* or the SHB1 overexpression (*SHB1 OE*) plants accumulated 1.5-fold more proteins, when expressed as mg/100 seeds, over that of Ws wild type (Figure 25A). By contrast, the total protein was reduced more than 20% in *shb1* relative to Col wild type ($P < 0.01$, two-tailed Student's t-tests). No such difference in protein content was detected when expressed on the basis of seed weight and more protein is apparently due to the larger seeds but not a higher concentration of protein in the seed (Figure 26). The spectrum of the seed storage proteins or the relative proportion of 12S storage proteins to other proteins was not selectively affected by the *shb1-D* mutation, whereas the 2S albumin proteins were not retained in the 12% SDS-PAGE gel (Figure 25B). The content of reducing sugars and total soluble sugars was also measured in wild type and *shb1-D* mutant seeds. *shb1-D* and *SHB1 OEs* accumulated more reducing sugars and total soluble sugars per seed compared to Ws, and *shb1* mutant accumulated less sugars per seed compared to Col (Figure 27).

The content and composition of total fatty acid methyl-ester were measured in Ws

wild type and *shb1-D* mutant seeds. Like *Brassica napus*, *Arabidopsis* seeds contain a small number of fatty acid species representing about 80% of the total seed fatty acids (Downey 1983; James and Dooner, 1990; Taylor et al., 1995). As shown in Figure 25D, *shb1-D* accumulated more total fatty acids per seed due to increased seed size compared to Ws, and 20% reduction was observed in *shb1* relative to Col ($P < 0.01$, two-tailed Student's t-tests) (Figure 25D). By contrast, the fatty acid composition was not significantly altered in *shb1-D* and Ws or *shb1* and Col, such as the palmitic (C16:0), palmitoleic (C16: 1), stearic (C18:0), oleic (C18: 1), linoleic (C18: 2), linolenic (C18: 3), arachidic (C20:0), eicosenoic (C20: 1), behenic (C22:0), and erucic (C22:1) acids (Figure 25C).

Activation of SHB1 enlarges the seed cavity and delays endosperm cellularization and embryo development

To explore the developmental alterations of *shb1* mutants, cleared seeds of *shb1-D* or *shb1* along with their wild types were compared at different developmental stages (Figure 28). After hand-pollination, the developing seeds were harvested at different days after pollination (DAP). The embryo sac or seed cavity in *shb1-D* mutant was significantly enlarged compared to Ws wild type at 4 DAP and remained larger throughout the rest stages of embryogenesis. By contrast, *shb1-D* embryos were developmentally delayed compared to Ws at the early phase of seed development, but gradually catch up at the later phase of seed development to overtake wild type in the mature seed (Figure 22, 28). In *shb1* loss-of-function mutant, the size of the embryo sac

was similar or slightly smaller than that of Col from 4 to 9 DAP, but the embryo of *shb1* was smaller compared to Col at 9 DAP (Figure 28). Seeds produced by homozygous *shb1-D* mutants were longer, wider, and more pointed at the micropylar pole (Figure 29). At 5 DAP, wild-type seeds had reached the late heart stage of embryogenesis, the chalazal endosperm formed a compact rounded cyst, and the peripheral endosperm was cellularizing from the micropylar pole (Figures 28, 29). At the same time point, *shb1-D* seeds had globular to early heart stage embryos, the chalazal endosperm was long and enlarged, and peripheral endosperm did not undergo substantial cellulerization as that seen in Ws wild type (Figure 29).

SHB1 acts zygotically to control seed size

To learn the transmission of the parental *SHB1*, reciprocal crosses were performed between Ws wild type and *shb1-D* mutant or between Col and *shb1* with flowers at identical positions (11th to 14th flowers) on secondary inflorescences. Seed weights were determined from 5 inflorescences per plant and 4 to 5 plants total. If *SHB1* acts through the sporophyte genome to control seed mass, the effect of the dominant *shb1-D* mutation on seed mass will be observed only when maternal plants are homozygous or heterozygous in the *shb1-D* locus. As shown in Figure 30A, the dominant *shb1-D* allele regulates seed mass through embryo genome in these reciprocal cross experiments. *shb1-D* (+/-) F1 seeds of *shb1-D* pistils pollinated with Ws wild-type pollens were larger by weight than wild-type seeds but were very close to *shb1-D (-/-)* seeds of *shb1-D* pistils pollinated with *shb1-D* pollens. *shb1-D (+/-)* F1 seeds of Ws wild type pistils pollinated

with *shb1-D* pollens were also larger than wild type, but 12 percent smaller than *shb1-D (-/-)* seeds (Figure 30A). Apparently, maternal homozygous *shb1-D* mutants produced seeds consistently heavier than those from maternal wild type plants due to a gene dosage effect as the triploid endosperm arises from the maternal central cell that contains two identical haploid genomes. Therefore, SHB1 may also partially act through the endosperm genome to control seed mass.

The large seed phenotype was still visible in a segregating F2 population for the two different reciprocal crosses. The F2 seeds from selfed *shb1-D (+/-),* regardless of maternal or paternal origin, all showed 1.4-fold increase in seed weight compared to Ws wild type (Figure 30A). *shb1 (-/-)* F1 seeds of *shb1* pistils pollinated with *shb1* pollens showed 15% reduction or consistently smaller seeds ($P < 0.01$, two-tailed Student's t-tests) (Figure 30B). As *shb1* is recessive and has a relatively weak seed phenotype*, shb1 (+/-)* F1 seeds of either *shb1* pistil or Col wild type pistil produced seeds of the same weight to that of Col wild type (Figure 30B).

SHB1 regulates the expression of MINI3 and IKU2

Through real time RT-PCR analysis demonstrated that the *shb1-D* mutation enhanced and the *shb1* mutation reduced the expression of *MINI3* and *IKU2*, a WRKY family transcription factor gene and an LRR receptor kinase gene, but not that of *AP2*, a transcription factor gene involved in floral organ and seed development ($P < 0.001$, two-tailed Student's t-tests) (Figure 31A). The expression of *MINI3* in *shb1-D* green siliques was increased 3 times compared to Ws wild type, and the expression of *MINI3* in *shb1*

was reduced 40% compared to Col ($P < 0.001$, two-tailed Student's t-tests) (Figure 31B). More dramatic induction or reduction of *IKU2* expression, 10-fold and 6-fold, was observed in *shb1-D* and *shb1* mutants, respectively, over that of Ws or Col wild type (Figure 31B). In contrast, the expression of *SHB1* relative to *UBQ10* in Col, *mini3*, *iku2*, and *ap2* was not changed (Figure 31B). As reported by Luo et al. (2005), mutation in either *mini3* or *iku2* reduces seed size, and the expression of *IKU2* was reduced in the *mini3* mutant. In either *shb1-D* or *shb1* mutant, a stronger enhancement or reduction was observed for the expression of *IKU2* over that of *MINI3*, and SHB1 may regulate the expression of *IKU2* through an additional signaling component parallel to that of MINI3.

SHB1 acts upstream of *MINI3* and *IKU2*

To substantiate the observation that SHB1 may act upstream of MINI3 and IKU2, double mutant analysis was performed between *shb1-D*, which produces large seed, and either *mini3-2* (SALK_050364) or *iku2-4* (SALK_073260) which produce small seeds. As *shb1-D* and *mini3-2* or *iku2-4* are in different genetic background, the genetic analysis was conducted in a mixed Ws and Col background of all genotypes. The genotypes from a segregating F2 population were selected by PCR-genotyping and at least 10 individuals of each genotype were identified and used in the analysis. As shown in Figure 31C, mutation in *IKU2* diminished the large seed phenotype of *shb1-D* to *iku2-4* and *shb1-D*/*iku2-4* double mutant phenotypically resembled *iku2-4*, suggesting that IKU2 acts downstream of SHB1. The *mini3-2* mutation also significantly suppressed the large seed phenotype of *shb1-D* to that of *mini3-2* single mutant (Figure 31C). Same results were

also obtained by overexpressing *SHB1* in *mini3-2* and *iku2-4* mutants along with *SHB1* overexpression lines in Col background. The expression of *IKU2* in the *shb1-D*/*mini3-2* double mutant was also analyzed. Mutation in *MINI3* completely blocked the expression of *IKU2*, and reduced the activation of *IKU2* expression by the *shb1-D* mutation from scale 10 to scale 0.6 (Figure 31D).

SHB1 has overlapping expression pattern to MINI3 and IKU2

To explore SHB1 function, the expression pattern of a GUS reporter gene under the control of a native *SHB1* promoter was examined. GUS activity was observed in apical meristem of young seedlings, rosette leaves, inflorescence, floral organs, mature pollen grains, germinating pollens, and mature unfertilized ovules (Figures 32 A-F). The expression of *SHB1* overlaps with that of *MINI3* in floral buds, pollen grains, pollen tubes, and ovules (Figure 32; Luo et al., 2005). The expression of *SHB1* in developing seeds was also monitored by in situ hybridization. Within the developing siliques, *SHB1* has overlapping expression pattern with *MINI3* in developing and cellularized endosperm and in globular and early-heart embryo 12 to 96 hr post-fertilization (Figures 32 G-K; Luo et al., 2005). *SHB1* also has overlapping expression pattern with *IKU2* in endosperm, and the expression of *IKU2* was only detected in the endosperm but not in the embryo or elsewhere of the plant (Luo et al., 2005). In addition, *SHB1* expression was also detected in chalazal endosperm or posterior cyst, and in late heart-stage and torpedo-stage embryos, suggesting a role of SHB1 to promote embryo development in the second phase of seed development (Figure 32 G-J).

SHB1 associates with MINI3 and IKU2 promoters

To investigate how SHB1 regulates the expression of *MINI3* and *IKU2*, chromatin immunoprecipitation (ChIP) assay was performed with either anti-SHB1 or anti-GFP antibodies followed by quantitative polymerase chain reaction (q-PCR) analysis. Figure 33A showed the promoter regions and various amplicons in *MINI3* and *IKU2* promoters used for those analyses. Amplicon M3 that spans from -986 to -1216 in *MINI3* promoter was highly enriched with either anti-SHB1 or anti-GFP antibodies, and amplicon M1 that spans from +3 to -349 in *MINI3* promoter was also significantly enriched (Figures 33B and 33C). By contrast, amplicon M2 that spans from -399 to -620 in *MINI3* promoter was not enriched with or without antibodies (Figures 33B and 33C). Amplicon 1 that spans from -3 to -277 in *IKU2* promoter was moderately enriched and amplicon 2 that spans from -296 to -665 in *IKU2* promoter were enriched up to 15-fold (Figures 33B and 33C). We also performed ChIP analysis of the promoter sequences of *HSF15*, an endosperm-specific gene, and *LEAF COTYLEDON2* (*LEC2*; Stone et al., 2001), an embryo-specific gene, and neither of the promoter sequences was significantly enriched (Figure 34).

Discussion

SHB1 is limiting during seed development

SHB1 plays a direct and specific role in endosperm and embryo development as the sizes of many other organs such as leaves, stems, roots, carpel, petals, and sepals were not significantly affected by either *shb1-D* or *shb1* mutation. Although *SHB1* gain or

loss-of-function of mutants affects seed size, *shb1* has relatively weak phenotype with a 15% reduction in seed weight compared to a 1.5- to 1.6-fold increase in seed size of the *shb1-D* lines (Figure 22). The changes in the content of either proteins or fatty acids were also less dramatic in *shb1* than in *shb1-D* (Figure 25). The development of embryo sac and endosperm was not affected by the *shb1* mutation, but the embryo of *shb1* appeared smaller at 9 DAP (Figure 28). One possibility is that SHB1 is limiting for endosperm and seed enlargement since the expression level of SHB1 is much lower in developing seeds compared to that in shoot apex, rosette leaves, and flowers through semi-quantitative RT-PCR analysis (data not shown). Therefore, SHB1 activation has a much stronger effect on seed development than does the loss of SHB1. On the other hand, the weak seed phenotype in *shb1* may be due to redundant SHB1 homologs or developmental pathways that regulate seed size. For example, one of the SHB1 homologs, gi 3548806 or At2g03240, is expressed at the globular and heart stages of *Arabidopsis* embryo and shows detectable expression level in developing siliques (*Arabidopsis* eFP Browser, http://bbc.botany.utoronto.ca/efp/cgi-bin/efpWeb.cgi). The expression pattern of another SHB1 homolog, gi 3548805 or At2g03250, is not available in the public domain and deserves further studies.

SHB1 promotes endosperm enlargement at the early phase of seed development

The early phase of endosperm development in most species is marked by cell proliferation and growth to generate a large multinucleate cell and is defined as syncytial phase (Olsen 2001; Berger 2003). This syncytium is then partitioned into individual cells

by a specific type of cytokinesis called cellularization. Cellularization is initiated in the micropylar pole and occurs after the eighth mitotic cycle in the peripheral endosperm (Garcia et al., 2003). Endosperm development is essential to provide nutrient supplies to the subsequent embryo development and to enforce a space limitation (Brink and Cooper, 1947). As the initial endosperm enlargement affects the final seed size, endosperm may initiate a signal to regulate the subsequent embryo development (Miller and Chourey, 1992; Hong et al., 1996). The *mini3* and *iku* mutations cause a premature cellularization of the endosperm and a reduced proliferation of the cellularized endosperm (Garcia et al., 2003; Luo et al., 2005). IKU and MINI3 may regulate endosperm size through the timing of endosperm cellularization (Luo et al., 2005). I demonstrated in this study that SHB1 gain-of-function regulates a similar set of cellular responses to MINI3 and IKU2, such as endosperm proliferation and the timing of endosperm cellularization (Figures 29). More significantly, the activation of SHB1 significantly enlarges the embryo sac at 4 DAP, and the endosperms remain larger throughout the rest stages of the initial phase of seed development (Figure 28).

The posterior pole of the endosperm does not undergo cellularization and contains a multinucleate pool of cytoplasm, chalazal endosperm or cyst. The cyst is located above the placentochalazal area of the seed integument where vascular elements terminate and is of potential importance for transfer of maternal nutrients to the seed (Schultz and Jensen, 1971; Otegui et al., 2002). The overall size of the posterior pole in *iku* seeds is reduced and in a few *iku* seeds, cellularization reaches the posterior pole, suggesting that *iku* mutations cause a posterior displacement of the boundary between the peripheral

endosperm and the posterior pole (Garcia et al., 2003). In *shb1-D* mutant, the posterior cyst is significantly enlarged and may result in more than adequate supplies of nutrients from the maternal parent, contributing to the subsequent embryo development (Figure 29).

SHB1 regulates embryo cell proliferation and elongation at the second phase of seed development

The *mini3* and *iku* mutations also retard the embryo proliferation after the early torpedo stage and reduce the total number of cells at mature embryo but not the cell size (Garcia et al., 2003; Luo et al., 2005). Similarly, the *exs/ems* mutant produced smaller seeds due to a reduction in cell size but not cell number (Canales et al., 2002; Zhao et al., 2002). The effect of the *iku2* mutation on embryo development may be indirect as a consequence of their effects on the endosperm development at the initial phase of seed development. In addition, the expression of *IKU2* is limited to endosperm (Luo et al., 2005). Although endosperm may initiate a signal to regulate the subsequent embryo development, it still needs further validation. For example, it is still unknown if overexpression of *IKU2* promotes embryo development and leads to enlarged seeds. Although *MINI3* message can be detected in both endosperm and embryo, it remains unknown if MINI3 functions in embryo development in addition to its role in endosperm proliferation (Luo et al., 2005). In contrast, SHB1 activation causes active endosperm proliferation in the initial phase of seed development at the expenses of embryo development, but subsequently the embryo of *shb1-D* reaches its large mature size in a

delay of 2 to 3 days. At maturity, *shb1-D* mutation increases both embryo cell size and cell number (Figure 24). Therefore, SHB1 may activate other developmental pathways that control embryo cell division and cell expansion in addition to the MINI3-IKU2 pathway that regulates endosperm proliferation.

SHB1 regulates the expression of both MINI3 and IKU2

SHB1 is required for the proper expression of both *MINI3* and *IKU2* (Figure 31A). Double mutant analyses indicate that the effect of *shb1* mutations on seed development was largely dependent on MINI3 and IKU2 function (Figure 31C). SHB1 contains a N-terminal SPX domain and a C-terminal EXS domain (Kang and Ni, 2006). A major function of the SPX domain in SYG1 protein is to mediate protein-protein interactions (Spain et al., 1995). The similar region of the EXS domain contains several predicted trans-membrane helices, and however, SHB1 is localized to the nucleus (Kang and Ni, 2006). Thus, the EXS domain in SHB1 may have a distinct function from those in SYG1-like proteins. SHB1 protein does not contain DNA binding motifs that recognize specific elements in *MINI3* and *IKU2* promoters, and SHB1 does not directly bind to either *MINI3* or *IKU2* promoter. ChIP experiments indicate that SHB1 associates with MINI3 and IKU2 promoters in vivo (Figure 33). A similar function has been discovered for many other proteins such as FT, GI, and FKF1 (Wigge et al., 2005; Sawa et al., 2007).

FT does not contain DNA binding activity but associates with *AP1* promoters through a direct interaction with FD, a bZIP transcription factor, that directly binds to

AP1 promoter (Wigge et al., 2005). GIGANTEA (GI) and FKF1 also associate with *CONSTANS* (*CO*) promoters through a direct interaction with CYCLING DOF FACTOR 1 (CDF1), a Dof transcription factor, in a blue light dependent manner (Sawa et al., 2007). Similarly, SHB1 may interact with other proteins that are specific transcription factors for *MINI3* and *IKU2* promoters and achieve its regulation over the transcription of *MINI3* and *IKU2* genes during the initial phase of seed development (Figure 35A). It remains unclear if SHB1 acts in a similar way to regulate embryo cell proliferation and elongation during the second phase of seed development (Figure 35B). Future studies will be directed to identify the protein factors that may interact with SHB1 in the regulation of either endosperm development or embryo development.

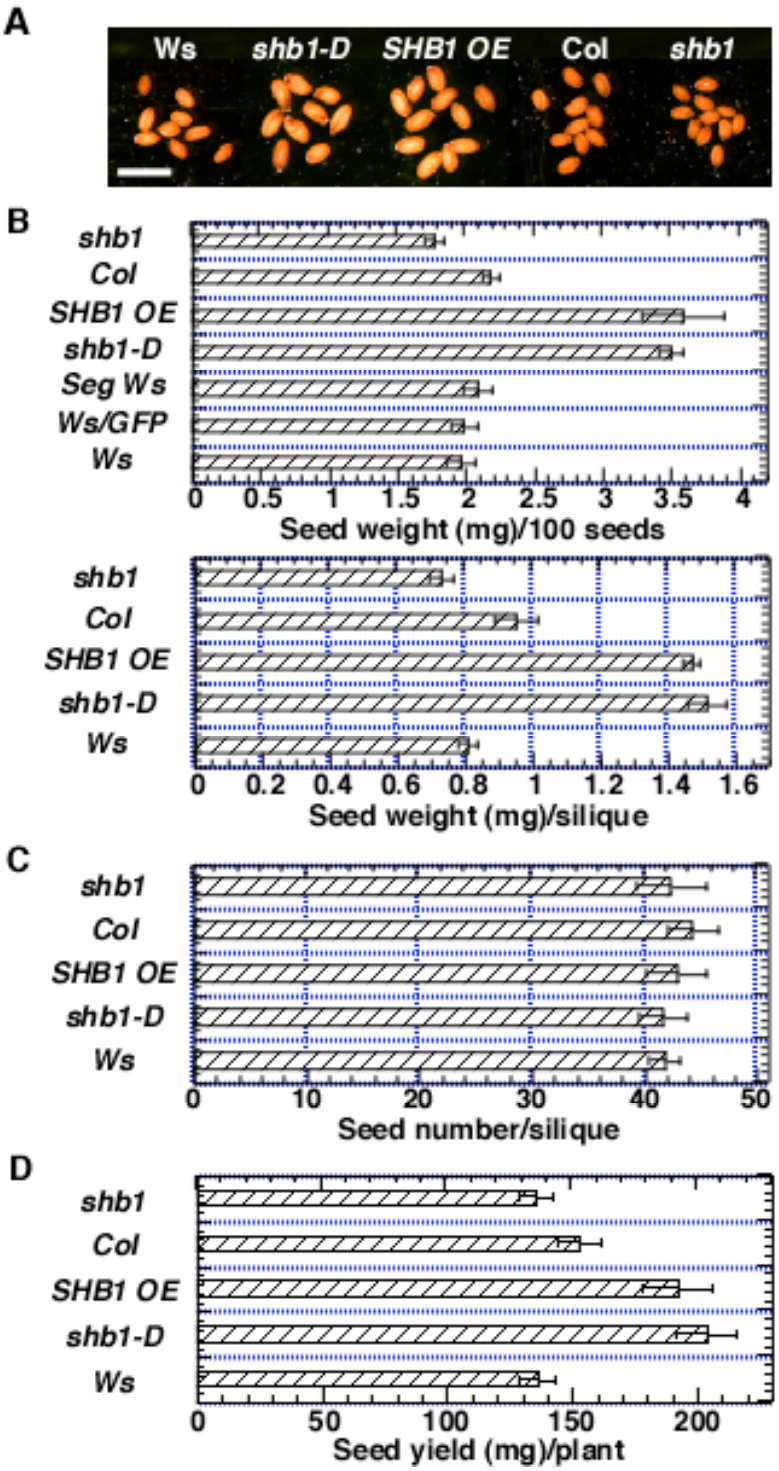

Figure 22. SHB1 regulates seed size. (A) Mature seeds of Ws, *shb1-D*, *SHB1* overexpression (*SHB1 OE*), Col, and *shb1*. Bar: 0.5 mm. (B) Averaged seed weight per

100 seeds (upper) or per silique (lower) for Ws, *shb1-D*, *SHB1 OE*, Col, and *shb1*. Data from segregating Ws plants or Ws plants that carry a GFP transgene are also shown as controls. (C) Seed number per silique for Ws, *shb1-D*, *SHB1 OE*, Col, and *shb1*. (D) Total seed yield for Ws, *shb1-D*, *SHB1 OE*, Col, and *shb1*. Data are means plus or minus standard errors from at least 6 independently propagated wild type and mutant lines or independent transgenic lines.

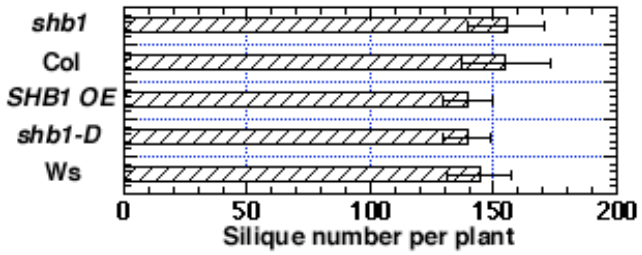

Figure 23. Numbers of siliques per Ws, *shb1-D*, SHB1 OE, Col, or *shb1* plant. Data are means plus or minus standard errors from at least 6 independently propagated wild type or mutant lines or independent transgenic lines.

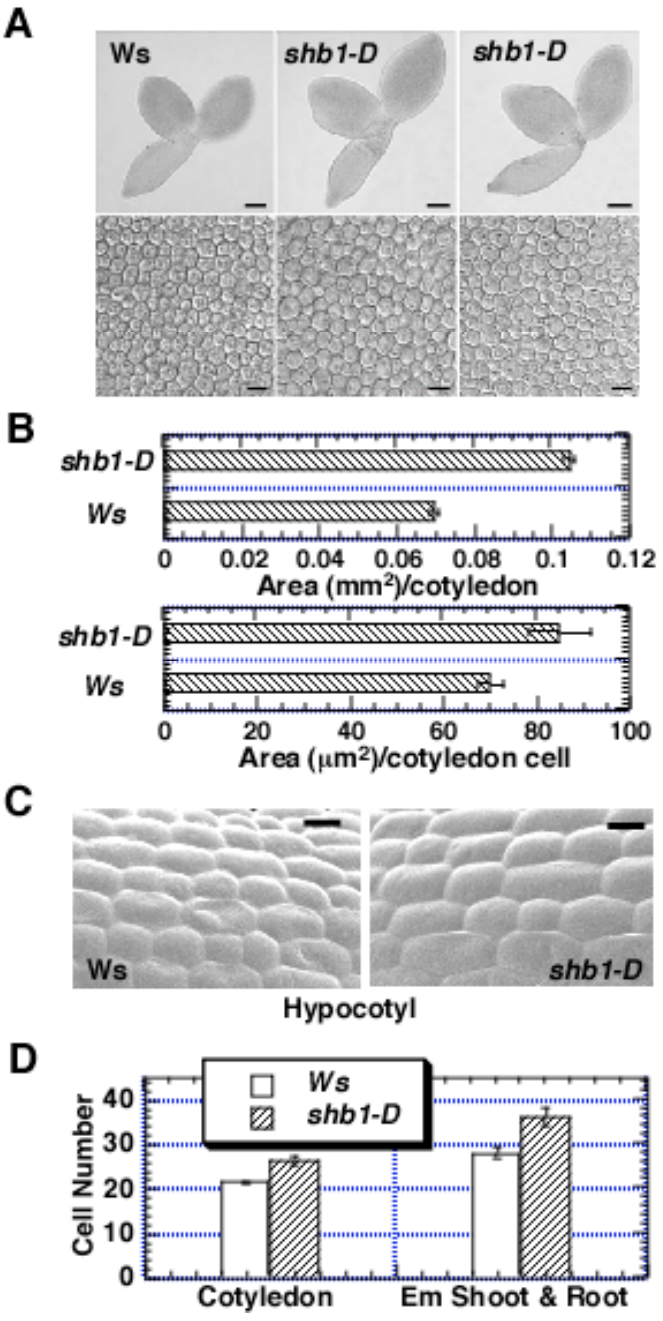

Figure 24. The increase in seed size of *shb1-D* is due to an increase in both cell size and cell number. (A) Mature embryos dissected from imbibed seeds of Ws (upper left) and *shb1-D* (upper right) plants. Bar: 100 mm. Epidermal cell layer from the central region of Ws (lower left) and *shb1-D* (lower right) cotyledons. Bar: 10 mm. (B)

Cotyledon area (upper) and cotyledon cell size (lower) of Ws and *shb1-D* plants. (C) Epidermal cell layer from the central region of Ws (left) and *shb1-D* (right) hypocotyls. Bar: 50 mm. (D) Average cell numbers from 3 columns in the central region of cotyledon or hypocotyl plus embryonic (Em) root in Ws and *shb1-D* plants.

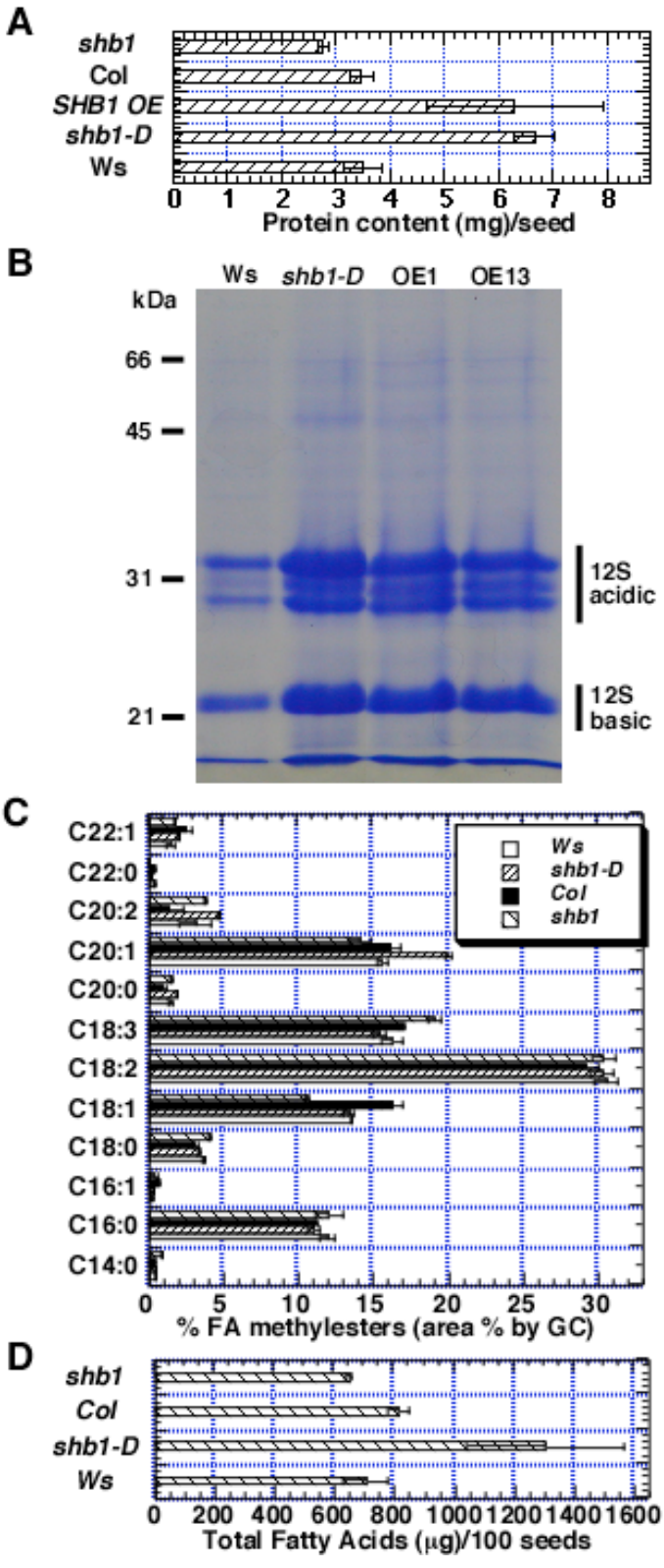
A
shb1
Col
SHB1 OE
shb1-D
Ws
0 1 2 3 4 5 6 7 8
Protein content (mg)/seed
B
Ws
shb1-D
OE1
OE13
kDa
66
45
31
21
12S acidic
12S basic
C
C22:1
C22:0
C20:2
C20:1
C20:0
C18:3
C18:2
C18:1
C18:0
C16:1
C16:0
C14:0
Ws
shb1-D
Col
shb1
0 5 10 15 20 25 30
% FA methylesters (area % by GC)
D
shb1
Col
shb1-D
Ws
0 200 400 600 800 1000 1200 1400 1600
Total Fatty Acids (µg)/100 seeds

Figure 25. *shb1-D* seeds contains higher protein and fatty acid content than do Ws seeds. (A) Total protein content per seed for Ws, *shb1-D*, *SHB1 OE*, Col, and *shb1*. (B) Spectrum of seed storage proteins in Ws, *shb1-D*, and *SHB1 OE*. Molecular standard ladder is shown to the left of the gel. (C) Relative fatty acid composition of each methyl-ester and (D) total fatty acid methyl-ester content per 100 seeds of Ws, *shb1-D*, Col, and *shb1*. Data are means plus or minus standard errors from at least 6 independently propagated Ws, mutant lines, or independent transgenic lines.

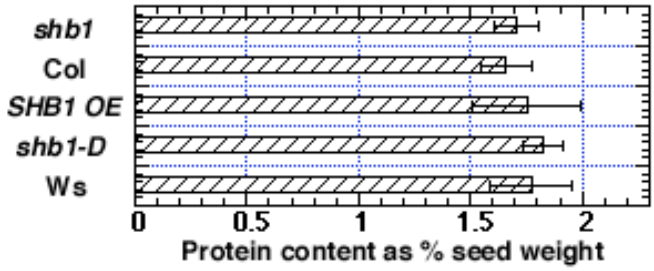

Figure 26. Protein contents calculated on the basis of seed weight for Ws, *shb1-D*, SHB1 OE, Col, or *shb1* plants. Data are means plus or minus standard errors from at least 6 independently propagated wild type or mutant lines or independent transgenic lines.

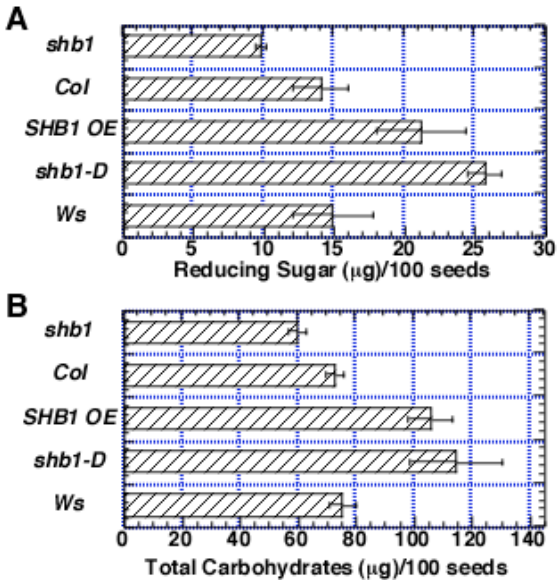

Figure 27. Reducing sugar (A) and total soluble sugar (B) contents per 100 seeds in Ws, *shb1-D*, *SHB1 OE*, Col, and *shb1*. Data are means plus or minus standard errors from at least 6 independently propagated wild type or mutant lines or independent transgenic lines.

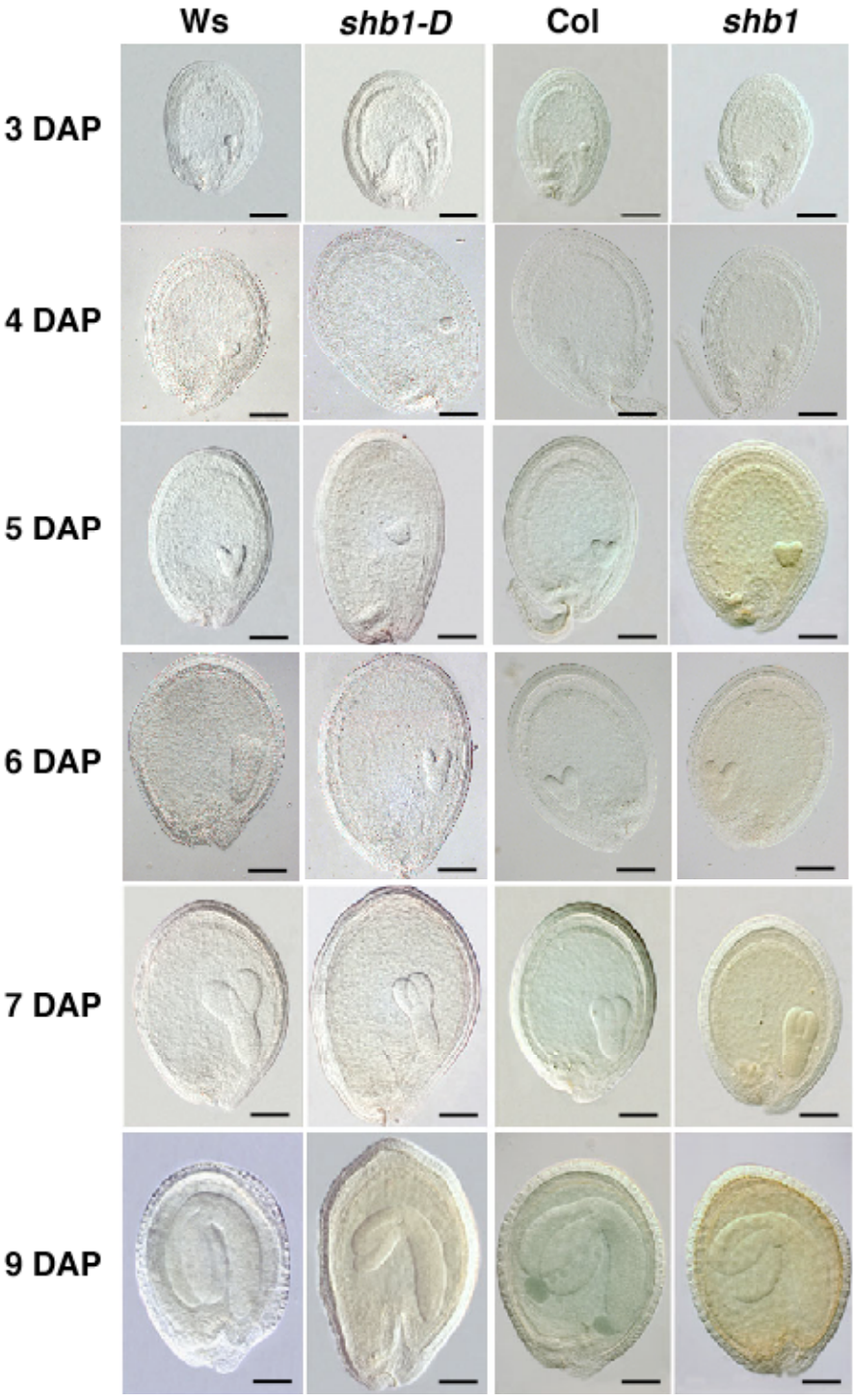

Figure 28. Seed development in wild type and *shb1* mutant plants. Cleared Ws, *shb1-D*, Col, and *shb1* seeds were imaged with differential contrast optics at 3, 4, 5, 6, 7, and 9 days after pollination (DAP). Scale bar: 50 mm.

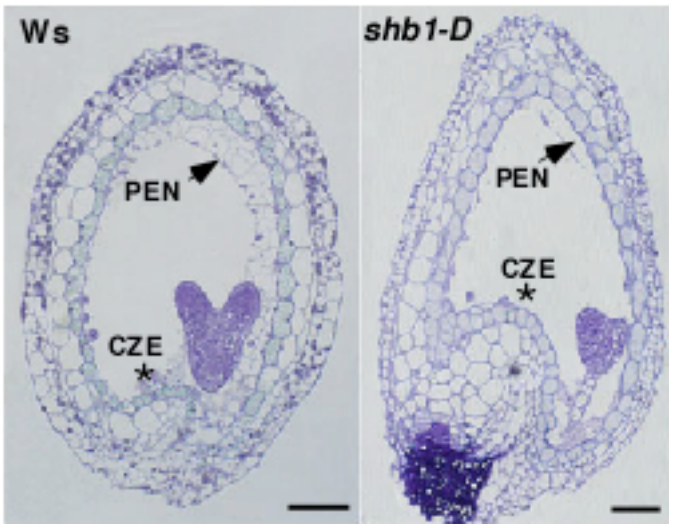

Figure 29. *shb1-D* mutation affects endosperm development and *SHB1* is transmitted zygotically. Five-day-old Ws seed at heart stage with cellularized peripheral endosperm and *shb1-D* seed at late-globular stage with uncellularized endosperm. PEN, the peripheral endosperm; CZE, the chalazal endosperm. Bar: 50 μm.

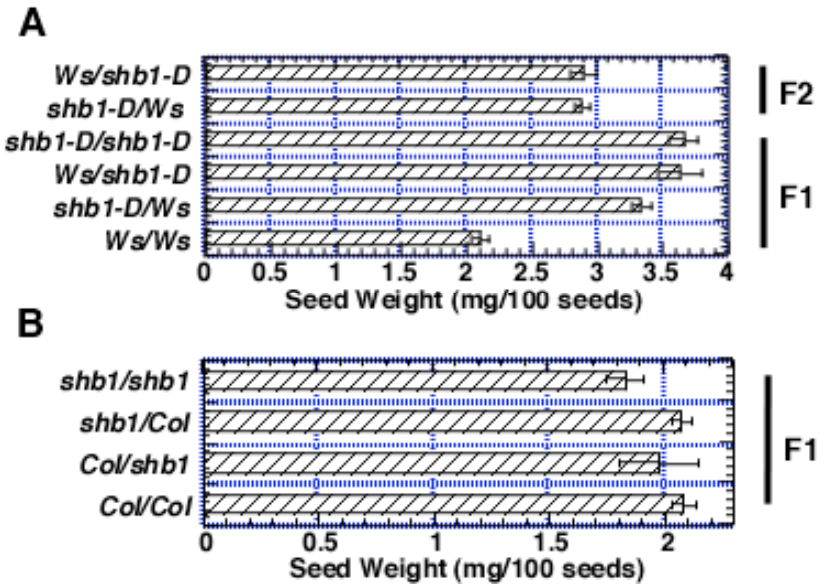

Figure 30. *SHB1* is transmitted zygotically. (A) F1 and F2 seed weight from reciprocal crosses between Ws and *shb1-D*. Ws/*shb1-D* indicates Ws pollen crossed to *shb1-D* pistil. (B) F1 seed weight from reciprocal crosses between Col and *shb1*. Data are presented as means plus or minus standard errors from at least 6 independently propagated Ws, Col, or mutant lines.

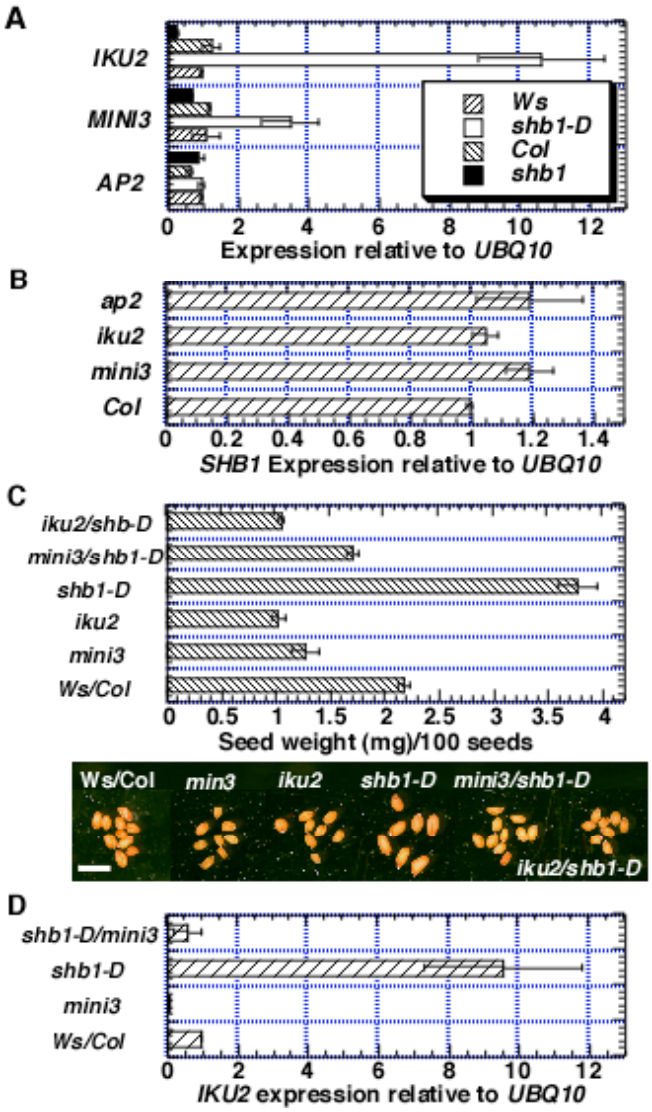

Figure 31. SHB1 regulates the expression of *MINI3* and *IKU2*. (A) Expression of *MINI3*, *IKU2*, and *AP2* in Ws, *shb1-D*, Col, and *shb1* through real time RT-PCR analysis. (B) Expression of *SHB1* in Col, *mini3*, *iku2*, and *ap2* through real time RT-PCR analysis. (C) Genetic interactions of *SHB1* with *MINI3* and *IKU2*. All genotypes are in a mixed Ws/Col background identified from a F2 segregation population, and at least 8 individuals were included in data calculation. The segregated wild type in the mixed Ws/Col background was used as control. (D) Expression of *IKU2* in Ws/Col, *mini3*, *shb1-D*, and *shb1-D/mini3* through real time RT-PCR analysis.

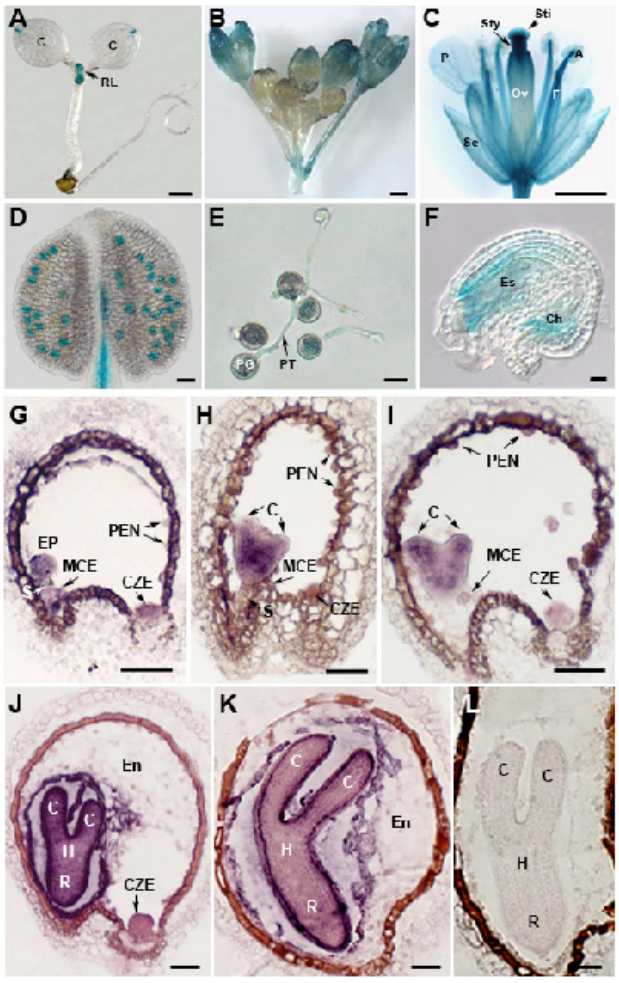

Figure 32. *SHB1* is expressed in endosperm and embryo. Expression of *SHB1::GUS* in (A) 8-day old seedling, (B) inflorescence, (C) flower, (D) mature pollen, (E) in vitro germinating pollens, and (F) unfertilized ovule. In situ hybridization of Ws with *SHB1* antisense probe at (G) early globular stage, (H) early heart stage, (I) heart stage, (J) torpedo stage, and (K) late torpedo stage or with *SHB1* sense probe at (L) torpedo stage. A, anther; C, cotyledon; Ch, chalazal end; CZE, chalazal endosperm; En, endosperm; EP, embryo proper; ES, embryo sac; F, filament; H, hypocotyl; MCE, micropylar endosperm; Ov, ovule; P, petal; PEN, peripheral endosperm; PG, pollen grain; PT, pollen tube; R, embryonic root; RL, rosette leaf; S, suspensor; Se, sepal; Sti, stigma; Sty, style. Scale bars: 1 mm for A to C, 25 mm for D) to F, 50 mm for G to L.

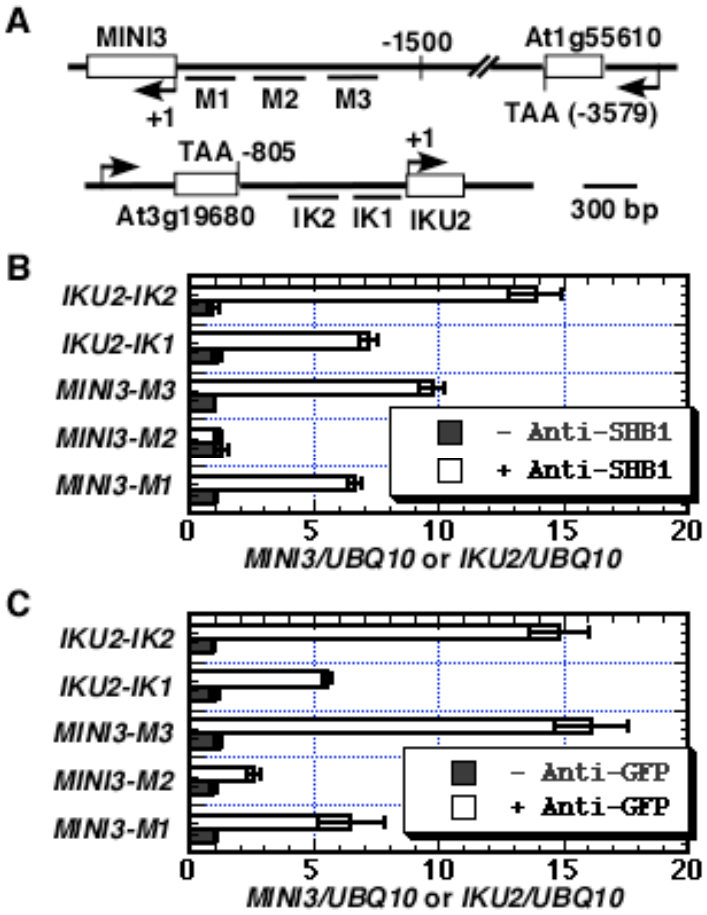

Figure 33. SHB1 associates with *MINI3* and *IKU2* promoters in vivo. (A) Schematic drawing of the *MINI3* and *IKU2* loci and 5 amplicons used for ChIP analysis. (B) Enrichment of particular *MINI3* and *IKU2* chromatin regions with anti-SHB1 antibody in wild type plants or anti-GFP antibody in SHB1:GFP transgenic plants (C) through real-time PCR analysis. Preimmune serum was used as mock control and the fold enrichment of the specific chromatin fragment was normalized to UBQ10 amplicon and calculated for each amplicon by using the following equation: $2^{(\text{Ct MINI3/M1 MOCK-Ct MINI3/M1 ChIP})} / 2^{(\text{Ct UBQ10 MOCK-Ct UBQ10 ChIP})}$. Data presented are the means of two independent ChIP experiments or biological samples with four PCR technical replicates for each biological sample plus or minus the standard errors.

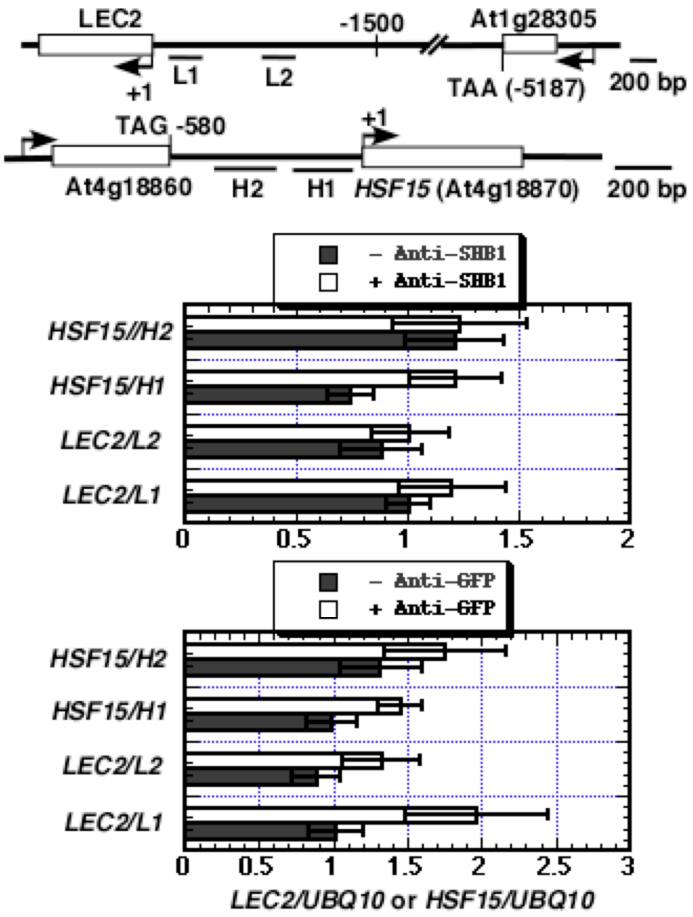

Figure 34. ChIP analysis of *HSF15* and *LEC2*. (A) Schematic drawing of the *LEC2* and *SHF15* loci and four amplicons (L1, L2, H1, and H2) used for ChIP analysis. (B) Enrichment of particular *LEC2* and *HSF15* chromatin regions with anti-SHB1 antibody in wild-type plants or with anti-GFP antibody in SHB1:GFP transgenic plants, as determined by real-time PCR analysis. *LEC2/L1* indicates the L1 amplicon in the *LEC2* promoter. Preimmune serum was used as a mock control and the fold enrichment of the specific chromatin fragment was normalized to the UBQ10 amplicon**.** Means were calculated from three biological samples and each biological sample was examined in triplicate. The calculated standard errors include technical error and biological error.

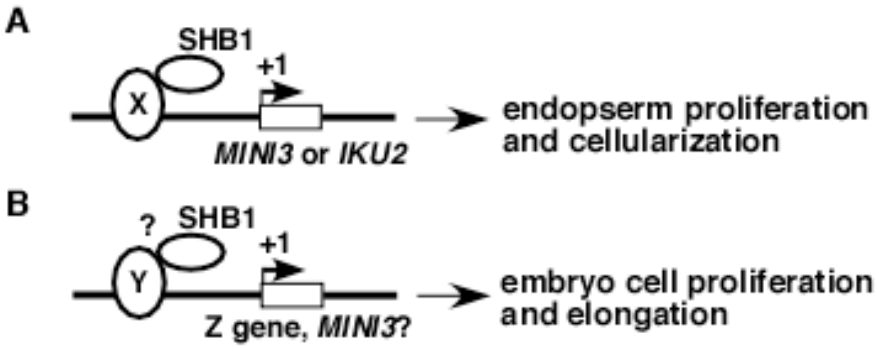

Figure 35. A working hypothesis suggests that SHB1 is recruited to the promoters of *MINI3* and *IKU2* by protein X and regulates the expression of key genes such as *MINI3* and *IKU2* that are required for endosperm proliferation and cellularization (A). It remains unknown if SHB1 deploys a similar mode of action to interact with protein Y and to present itself in the promoters of unknown targets such as Z gene or *MINI3* that are essential for embryo cell proliferation and elongation (B). *MINI3* is expressed in both endosperm and embryo in contrast to the unique expression of *IKU2* in the endosperm, and MINI3 may play additional roles in embryo development.

Bibliography

Abe, M., Kobayashi, Y., Yamamoto, S., Daimon, Y., Yamaguchi, A., Ikeda, Y., Ichinoki, H., Notaguchi, M., Goto, K., Araki, T. 2005. FD, a bZIP protein mediating signals from the floral pathway integrator FT at the shoot apex. Science 309, 1052–1056

Ahmad, M., and Cashmore, A.R. (1993). HY4 gene of A. thaliana encodes a protein with characteristics of a blue-light photoreceptor. Nature *366*, 162-166.

An, H., Roussot, C., Suárez-López, P., Corbesier, L., Vincent, C., Piñeiro, M., Hepworth, S., Mouradov, A., Justin, S., Turnbull, C., Coupland, G. 2004. CONSTANS acts in the phloem to regulate a systemic signal that induces photoperiodic flowering of Arabidopsis. Development 131, 3615-3626.

Aukerman, M.J., Lee, I., Weigel, D., and Amasino, R.M. 1999. The *Arabidopsis* flowering-time gene *LUMINIDEPENDENS* is expressed primarily in regions of cell proliferation and encodes a nuclear protein that regulates *LEAFY* expression. Plant J. 18, 195–203.

Bastow, R., Mylne, J.S., Lister, C., Lippman, Z., Martienssen, R.A., and Dean, C. 2004. Vernalization requires epigenetic silencing of FLC by histone methylation. Nature 427, 164-167.

Battini, J.L., Rasko, J.E., Miller, A.D. (1999). A human cell-surface receptor for xenotropic and polytropic murine leukemia viruses: possible role in G protein-coupled signal transduction. Proc Natl Acad Sci U S A *96*, 1385-1390.

Berger, F. (2003). Endosperm, the crossroad of seed development. Curr Opin Plant Biol *6*, 42–50.

Bowler, C. Benvenuto, G. Laflamme, P. Molino, D. Probst, A.V., Tariq, M. Paszkowski, J. (2004). Chromatin techniques for plant cells. Plant Journal *39*, 776-789.

Boisnard-Lorig, C., Colon-Carmona, A., Bauch, M., Hodge, S., Doerner, P., Bancharel, E., Dumas, C., Haseloff, J., and Berger, F. (2001). Dynamic analyses of the expression of the histone::YFP fusion protein in Arabidopsis show that syncytial endosperm is divided in mitotic domains. Plant Cell *13*, 495–509.

Brink, R.A., and Cooper, D.C. (1947). The endosperm in seed development. Bot. Rev. *13*, 423–541.

Boss, P.K., Bastow, R.M., Mylne, J.S., and Dean, C., 2004. Multiple pathways in the decision to flower: Enabling, promoting, and resetting. Plant Cell 16, S18–S31

Canales, C., Bhatt, A.M., Scott, R., and Dickinson, H. (2002). EXS, a putative LRR receptor kinase, regulates male germline cell number and tapetal identity and promotes seed development in Arabidopsis. Current Biology *12*, 1718–1727.

Cerdán, P.D., and Chory, J. 2003. Regulation of flowering time by light quality. Nature 423, 881-885.

Chou, M.L., and Yang, C.H. 1998. FLD interacts with genes that affect different developmental phase transitions to regulate *Arabidopsis* shoot development. Plant J. 15, 231-242.

Clough, S.J., and Bent, A.F. (1998). Floral dip: a simplified method for *Agrobacterium*-mediated transformation of *Arabidopsis thaliana*. Plant J *16*, 735–743.

Corbesier, L., Vincent, C., Jang, S., Fornara, F., Fan, Q., Searle, I., Giakountis, A., Farrona, S., Gissot, L., Turnbull, C., Coupland, G. 2007. FT protein movement contributes to long-distance signaling in floral induction of Arabidopsis. Science 316, 1030-1033.

Domagalska, M.A., Schomburg, F.M., Amasino, R.M., Vierstra, R.D., Nagy, F., and Davis, S.J. 2007. Attenuation of brassinosteroid signaling enhances *FLC* expression and delays flowering. Development 134, 2841-2850.

Downey, R.K. (1983). High and low erucic acid rapeseed oils, eds. Kamer, J., Sauer, F., and Pigden, W., (Academic, New York).

Dubois, M., Gilles, K.A., Hamilyon, J.K., Rebers, P.A., and Smith, F. (1956). Colorimetric method for determination of sugars and related substances. Anal. Chem. *28*, 350-356.

Duek, P.D., and Fankhauser, C. (2003). HFR1, a putative bHLH transcription factor, mediates both phytochrome A and cryptochrome signaling. Plant J *34*, 827-836.

Fairchild, C.D., Schumaker, M.A., Quail, P.H. (2000). HFR1 encodes an atypical bHLH protein that acts in phytochrome A signal transduction. Genes Dev *14*, 2377-2391.

Focks, N. and Benning, C. (1998). *wrinkled1*: a novel, low-seed-oil mutant of Arabidopsis with a deficiency in the seed-specific regulation of carbohydrate metabolism. Plant Physiol *118*, 91-101.

Garcia, D., Fitz Gerald, J.N., and Berger, F. (2005). Maternal control of integument cell elongation and zygotic control of endosperm growth are coordinated to determine seed size in Arabidopsis. Plant Cell *17*, 52–60.

Garcia, D., Saingery, V., Chambrier, P., Mayer, U., Jurgens, G., and Berger, F. (2003). Arabidopsis *haiku* mutants reveal new controls of seed size by endosperm. Plant Physiol *131*, 1661–1670.

Genoud, T., Santa Cruz, M.T., Kulisic, T., Sparla, F., Fankhauser, C., Métraux, J.P. (2008). The protein phosphatase 7 regulates phytochrome signaling in Arabidopsis. PLoS ONE *3*, e2699.

Gray, W.M., del Pozo, J.C., Walker, L., Hobbie, L., Risseeuw, E., Banks, T., Crosby, W.L., Yang, M., Ma, H., Estelle, M. (1999). Identification of an SCF ubiquitin-ligase complex required for auxin response in Arabidopsis thaliana. Genes Dev *13*, 1678-91.

Guo, H., Mockler, T., Duong, H., Lin, C. (2001). SUB1, an Arabidopsis Ca2+-binding protein involved in cryptochrome and phytochrome coaction. Science *291*, 487-490.

Guo, H., Yang, H., Mockler, T., and Lin, C. 1998. Regulation of flowering time by *Arabidopsis* photoreceptors. Science 279, 1360–1363.

Hamburger, D., Rezzonico, E., MacDonald-Comber Petetot, J., Somerville, C., Poirier, Y. (2002). Identification and characterization of the Arabidopsis PHO1 gene involved in phosphate loading to the xylem. Plant Cell *14*, 889-902.

Hardtke, C.S., Gohda, K., Osterlund, M.T., Oyama, T., Okada, K., Deng, X.W. (2000). HY5 stability and activity in arabidopsis is regulated by phosphorylation in its COP1 binding domain. EMBO J *19*, 4997-5006.

Hardwick, K.G., Lewis, M.J., Semenza, J., Dean, N., Pelham, H.R. (1990). ERD1, a yeast gene required for the receptor-mediated retrieval of luminal ER proteins from the secretory pathway. EMBO J *9*, 623-630.

Heath, J.D., Weldon, R., Monnot, C., and Meinke, D.W. (1986). Analysis of storage proteins in normal and aborted seeds from embryo-lethal mutants of Arabidopsis thaliana. Planta *169*, 304-312.

Helliwell, C.A., Wood, C.C., Robertson, M., Peacock, W.J., and Dennis, E.S. 2006. The Arabidopsis FLC protein interacts directly *in vivo* with *SOC1* and *FT* chromatin and is part of a high-molecular-weight protein complex. Plant J. 46, 183-192.

Hepworth, S.R., Valverde, F., Ravenscroft, D., Mouradov, A., and Coupland, G. 2002. Antagonistic regulation of flowering-time gene *SOC1* by CONSTANS and FLC via separate promoter motifs. EMBO J. 21, 4327-4337.

He, Y., and Amasino, R.M. 2005. Role of chromatin modification in flowering-time control. Trends Plant Sci. 10, 30-35.

Hong, S.K., Kitano, H., Satoh, H., and Nagato, Y. (1996). How is embryo size genetically regulated in rice? Development *122*, 2051–2058.

Hutchison, C.E., Li, J., Argueso, C., Gonzalez, M., Lee, E., Lewis, M.W., Maxwell, B.B., Perdue, T.D., Schaller, G.E., Alonso J.M., Ecker J.R., and Kieber J.J. (2006). The Arabidopsis histidine phosphotransfer proteins are redundant positive regulators of cytokinin signaling. Plant Cell *18*, 3073-3087.

Huq, E., and Quail, P.H. (2002). PIF4, a phytochrome-interacting bHLH factor, functions as a negative regulator of phytochrome B signaling in Arabidopsis. EMBO J *21*, 2441-2450.

Huq, E., and Quail, P.H. (2005). Phytochrome signaling. In Handbook of Photosensory Receptors, W. R. Briggs and J.L. Spudich, eds (WILEY-VCH, Weinheim, Germany), pp. 151-170.

Imaizumi, T., Schultz, T.F., Harmon, F.G., Lindsey A. Ho, L.A., and Kay, S.A. 2005. FKF1 F-Box protein mediates cyclic degradation of a repressor of CONSTANS in *Arabidopsis*. Science 309, 293-297.

Imaizumi, T., Tran, H.G., Swartz, T.E., Briggs, W.R., Kay, S.A. 2003. FKF1 is essential for photoperiodic-specific light signaling in. *Arabidopsis.* Nature 426**,** 302–306.

Ishii, Y., and Kondo, S. (1975). Comparative analysis of deletion and base-change mutabilities of Escherichia coli B strains differing in DNA repair capacity (wild-type, uvrA-, polA-, recA-) by various mutagens. Mutat Res *27*, 27-44.

James, D.W., and Dooner, H.K. (1990). Isolation of EMS-induced mutants in Arabidopsis altered in seed fatty-acid composition. Theor. Appl. Genet *80*, 241-245.

Jofuku, K.D., Omidyar, P.K., Gee, Z., and Okamuro, J.K. (2005). Control of seed mass and seed yield by the floral homeotic gene APETALA2. Proc. Natl. Acd. Sci. USA *102*, 3117-3122.

Johnson, C.S., Kolevski, B., Smyth, D.R., (2002). TRANSPARENT TESTA GLABRA2, a trichome and seed coat development gene of Arabidopsis, encodes a WRKY transcription factor. Plant Cell *14*,1359-1375.

Kang, I.H., Steffen, J.G., Portereiko, M.F., Lloyd, A., and Drews, G.N. (2008). The AGL62 MADS domain protein regulates cellularization during endosperm development in *Arabidopsis.* Plant Cell 20, 635-647.

Kang, X., Chong, J., Ni, M. (2005). HYPERSENSITIVE TO RED AND BLUE 1, a ZZ-type zinc finger protein, regulates phytochrome B-mediated red and cryptochrome-mediated blue light responses. Plant Cell *17*, 822-835.

Kang, X., and Ni, M. (2006). *Arabidopsis* SHORT HYPOCOTYL UNDER BLUE 1 contains SPX and EXS domains and acts in cryptochrome signaling. Plant Cell *18*, 921-934.

Kang, X., Zhou, Y., Sun, X., and Ni, M. 2007. HYPERSENSITIVE TO RED AND BLUE 1 and its C-terminal regulatory function control *FLOWERING LOCUS T* expression. Plant J. 52, 937-948.

Kim, Y., Schumaker, K.S., Zhu, J.K. (2006). EMS mutagenesis of Arabidopsis. Methods Mol Biol *323*, 101-103.

Koornneef, M., Hanhart, C.J., and van der Veen, J.H. 1991. A genetic and physiological analysis of late flowering mutants in *Arabidopsis thaliana*. Mol. Gen. Genet. 229, 57-66.

Larson, T.R., and Graham, I.A. (2001). A novel technique for the sensitive quantification of acyl CoA esters from plant tissues. Plant Journal *25*, 115-125.

Lee, H., Suh, S.S., Park, E., Cho, E., Ahn, J.H., Kim, S. G., Lee, J.S., Kwon, Y.M., Lee, I. 2000. The AGAMOUS-LIKE 20 MADS domain protein integrates floral inductive pathways in. Arabidopsis. Genes Dev. 14, 2366–2376.

Lee, I., Aukerman, M.J., Gore, S.L., Lohman, K.N., Michaels, S.D., Weaver, L.M., John, M.C., Feldmann, K.A., and Amasino, R.M. 1994. Isolation of *LUMINIDEPENDENS*: a gene involved in the control of flowering time in *Arabidopsis*. Plant Cell 6, 75-83.

Lim, M.H., Kim, J., Kim, Y.S., Chung, K.S., Seo, Y.H., Lee, I., Kim, J., Hong, C.B., Kim, H.J., and Park, C.M. 2004. A new *Arabidopsis* gene, *FLK*, encodes an RNA binding protein with K homology motifs and regulates flowering time via FLOWERING LOCUS C. Plant Cell 16, 731-740.

Lin, C. 2000. Photoreceptors and regulation of flowering time. Plant Physiol. 123, 39-50. Michaels, S.D., and Amasino, R.M. 1999. *FLOWERING LOCUS C* encodes a novel MADS domain protein that acts as a repressor of flowering. Plant Cell 11, 949-956.

Lin, C., Yang, H., Guo, H., Mockler, T., Chen, J., Cashmore, A.R. (1998). Enhancement of blue-light sensitivity of Arabidopsis seedlings by a blue light receptor -cryptochrome 2. Proc. Natl. Acad. Sci. USA *95*, 2686-2690.

Liu, H., Yu, X., Li, K., Klejnot, J., Yang, H., Lisiero, D., Lin, C. (2008). Photoexcited CRY2 interacts with CIB1 to regulate transcription and floral initiation in Arabidopsis. Science *322*, 1535-1539.

Luo, M., Dennis, E.S., Berger, F., Peacock, W.J., and Chaudhury, A. (2005). MINISEED3 (MINI3), a WRKY family gene, and HAIKU2 (IKU2), a leucine-rich repeat (LRR) KINASE gene, are regulators of seed size in Arabidopsis. Proc. Natl. Acd. Sci. USA *102*, 17531-17536.

Michaels, S.D., and Amasino, R.M. 2001. Loss of FLOWERING LOCUS C activity eliminates the late-flowering phenotype of FRIGIDA and autonomous pathway mutations but not responsiveness to vernalization. Plant Cell 13, 935-941.

Michaels, S.D., Himelblau, E., Kim, S.Y., Schomburg, F.M., Amasino, R.M. 2005. Integration of flowering signals in winter-annual. Arabidopsis. Plant Physiol. 137, 149–156.

Miller, M.E., and Chourey, P.S. (1992). The maize invertase-deficient miniature-1 seed mutation is associated with aberrant pedicel and endosperm development. Plant Cell *4*, 297-305

Mockler, T.C, Yang, H.Y., Yu, X.H., Parikh, D., Cheng, Y.C., and Lin, C. 2003. Regulation of photoperiodic flowering by *Arabidopsis* phototeceptor. Proc. Natl. Acd. Sci. USA 100, 2140-2145.

Mockler, T.C., Yu, X., Shalitin, D., Parikh, D., Michael, T.P., Liou, J., Huang, J., Smith, Z., Alonso, J.M., Ecker, J.R., Chory, J., and Lin, C. 2004. Regulation of flowering time in *Arabidopsis* by K homology domain proteins. Proc. Natl. Acad. Sci. USA 101, 12759-12764.

Moon, J., Lee, H., Kim, M. and Lee, I. 2005. Analysis of flowering pathway integrators in Arabidopsis. Plant Cell Physiol. 46, 292–299.

Mouradov, A., Cremer, F., Coupland, G. 2002. Control of flowering time: Interacting pathways as a basis for diversity. Plant Cell 14, Suppl, S111–S130

Mφller, S.G., Kim, Y.S., Kunkel, T., Chua, N.H. (2003). PP7 is a positive regulator of blue light signaling in Arabidopsis. Plant Cell *15*, 1111-1119

Neef, D.W., and Kladde, M.P. (2003). Polyphosphate loss promotes SNF/SWI- and Gcn5-dependent mitotic induction of PHO5. Mol. Cell Biol *11*, 3788-3797.

Neff, M.M., Fankhauser, C., and Chory, J. (2000). Light: an indicator of time and place. Genes Dev *14*, 257–271.

Nelson, N. (1944). A photometric adaptation of the Somogyi method for the determination of glucose. J. Biol. Chem. *153*, 375-380.

Noh, Y.S. and Amasino, R.M. 2003. PIE1, an ISWI family gene, is required for FLC activation and floral repression in. Arabidopsis. Plant Cell 15, 1671–1682.

Ohto, M., Fischer, R.L., Goldberg, R.B., Nakamura, K., and Harada, J.J. (2005). Control of seed mass by APETALA2. Proc. Natl. Acd. Sci. USA *102*, 3123-3128.

Olsen, O.A. (2001). Endosperm development: cellularization and cell fate specification. Annu Rev Plant Phys Plant Mol Biol *52*, 233–267.

Onouchi, H., Igeno, M.I., Perilleux, C., Graves, K., Coupland, G. 2000. Mutagenesis of plants overexpressing CONSTANS demonstrates novel interactions among Arabidopsis flowering-time genes. Plant Cell 12, 885-900.

Otegui, M.S., Capp, R., and Staehelin, L.A. (2002). Developing seeds of Arabidopsis store different minerals in two types of vacuoles and in the endoplasmic reticulum. Plant Cell *14*, 1311–1327.

Pang, P.P., Pruitt, R.E., and Meyerowitz, E.M. (1988). Molecular cloning, genomic organization, expression and evolution of 12S seed storage protein genes of Arabidopsis thaliana. Plant Mol. Biol *11*, 805-820.

Riefler,M., Novak, O., Strnad, M., and Schmülling, T. (2006). Arabidopsis cytokinin receptor mutants reveal functions in shoot growth, leaf senescence, seed size, germination, root development, and cytokinin metabolism. Plant Cell *18*, 40-54.

Putterill, J., Robson, F., Lee, K., Simon, R., and Coupland, G. 1995. The *CONSTANS* gene of *Arabidopsis* promotes flowering and encodes a protein showing similarities to Zinc finger transcription factor. Cell 80, 847-857.

Samach, A., Onouchi, H., Gold, S. E., Ditta, G. S., Schwarz-Sommer, Z., Yanofsky, M. F., and Coupland, G. 2000. Distinct roles of CONSTANS target genes in reproductive development of *Arabidopsis*. Science 288, 1613-1616.

Sawa, M. Nusinow, D.A., Kay, S.A., Imaizumi, T. (2007). FKF1 and GIGANTEA complex formation is required for day-length measurement in Arabidopsis. Science *318*, 261-265.

Schneider, K.R., Smith, R.L., O'Shea, E.K. (1994). Phosphate-regulated inactivation of the kinase PHO80-PHO85 by the CDK inhibitor PHO81. Science *266*, 122-126.

Schomburg, F.M., Patton, D.A., Meinke, D.W., and Amasino, R.M. 2001. *FPA*, a gene involved in floral induction in *Arabidopsis*, encodes a protein containing RNA-recognition motifs. Plant Cell 13, 1427-1436.

Schruff ,M.C., Spielman, M., Tiwari, S., Adams, S., Fenby, N., and Scott, R.J. (2006). The AUXIN RESPONSE FACTOR 2 gene of Arabidopsis links auxin signalling, cell division, and the size of seeds and other organs. Development *133*, 251-261.

Schultz, P., and Jensen, W.A. (1971). *Capsella* embryogenesis: the chalazal proliferating tissue. J Cell Sci *8*, 201–227.

Scott, R.J., Spielman, M., Bailey, J., and Dickinson, H.G. (1998). Parent-of-origin effects on seed development in Arabidopsis thaliana. Development *125*, 3329–3341.

Searle, I., and Coupland, G. 2004. Induction of flowering by seasonal changes in photoperiod. EMBO J. 23, 1217-1222.

Searle, I., He, Y., Turck, F., Vincent, C., Fornara, F., Kröber, S., Amasino, R.A., Coupland, G. 2006. The transcription factor FLC confers a flowering response to vernalization by repressing meristem competence and systemic signaling in *Arabidopsis*. Genes Dev. 20, 898-912.

Shalitin, D., Yang, H., Mockler, T.C., Maymon, M., Guo, H., Whitelam, G.C., Lin, C. (2002). Regulation of Arabidopsis cryptochrome 2 by blue-light-dependent phosphorylation. Nature *417*, 763–767.

Shalitin, D., Yu, X., Maymon, M., Mockler, T., and Lin, C. (2003). Blue light–dependent in vivo and in vitro phosphorylation of Arabidopsis cryptochrome 1. Plant Cell *15*, 2421–2429.

Sheldon, C.C., Burn, J.E., Perez, P.P., Metzger, J., Edwards, J.A., Peacock, W.J., and Dennis, E.S. 1999. The *FLF* MADS box gene: a repressor of flowering in *Arabidopsis* regulated by vernalization and methylation. Plant Cell 11, 445-458.

Sieburth, L.E. and Meyerowitz, E.M. (1997). Molecular dissection of the *AGAMOUS* control region shows that cis elements for spatial regulation are located intragenically. Plant Cell *9*, 355-365.

Somogyi, M. (1952). Notes on sugar determination. J. Biol. Chem. *195*, 19-23.
Sundaresan, V. (2005). Control of seed size in plants. Proc. Natl. Acad. Sci. USA *102*, 17887-17888.

Spain, B.H., Koo, D., Ramakrishnan, M., Dzudzor, B., Colicelli, J. (1995). Truncated forms of a novel yeast protein suppress the lethality of a G protein α subunit deficiency by interacting with the β subunit. J Biol. Chem. *270*, 25435-25444.

Stone, S.L., Kwong, L.W., Yee, K.M., Pelletier, J., Lepiniec, L., Fischer, R.L., Goldberg, R.B., and Harada, J.J. (2001). *LEAFY COTYLEDON2* encodes a B3 domain transcription factor that induces embryo development. Proc. Natl. Acad. Sci. USA 98, 11806–11810.

Suárez-López, P., Wheatley, K., Robson, F., Onouchi, H., Valverde, F., and Couplant, G. 2001. *CONSTANS* mediates between the circadian clock and the control of flowering in *Arabidopsis*. Nature 410, 1116-1120.

Tailor, C.S., Nouri, A., Lee, C.G., Kozak, C., Kabat, D. (1999). Cloning and characterization of a cell surface receptor for xenotropic and polytropic murine leukemia viruses. Proc. Natl. Acad. Sci. USA *96*, 927-932.

Taylor, D.C., Giblin, E.M., Reed, D.W., Hogge, L.R., Olson, D.J., and MacKenzie, S. L. (1995). Stereospecific analysis and mass-spectrometry of triacylglycerols from Arabidopsis thaliana (L) heynh Columbia seed. J. Am. Oil Chem. Soc *72*, 305-308.

Tepperman, J.M., Zhu, T., Chang, H.S., Wang, X., Quail, P.H. 2001. Multiple transcription-factor genes are early targets of phytochrome A signaling. Proc Natl Acad Sci U S A. 98, 9437-9442.

Valverde, F., Mouradov, A., Soppe, W., Ravenscroft, D., Samach, A., and Coupland, G. 2004. Photoreceptor regulation of CONSTANS protein in photoperiodic flowering. Science 303, 1003-1006.

Wang, Z., Hu, H., Huang, H., Duan, K., Wu, Z., Wu, P. (2009). Regulation of OsSPX1 and OsSPX3 on expression of OsSPX domain genes and Pi-starvation signaling in rice. J Integr Plant Biol. 51:663-674.

Wanger, D., Quail, P.H. (1995). Mutational analysis of phytochrome B identifies a small COOH-terminal-domain region critical for regulatory activity Proc. Natl. Acad. Sci. USA *92*, 8596-8600.

Ward, J.M., Cufr, C.A., Denzel, M.A., Neff, M.M. (2005). The Dof transcription factor OBP3 modulates phytochrome and cryptochrome signaling in Arabidopsis. Plant Cell *17*, 475-485.

Wigge, P.A., Kim, M.C., Jaeger, K.E., Busch, W., Schmid, M., Lohmann, J.U., and Weigel, D. 2005. Integration of spatial and temporal information during floral induction in *Arabidopsis*. Science 309, 1056-1059.

Xiao, W., Brown, R.C., Lemmon, B.E., Harada, J.J., Goldberg, R.B., and Fischer, R.L. (2006). Regulation of seed size by hypomethylation of maternal and paternal genomes. Plant Physiol *142*, 1160–1168.

Yang, Y.L., Guo, L., Xu, S., Holland, C.A., Kitamura, T., Hunter, K., Cunningham, J.M. (1999). Receptors for polytropic and xenotropic mouse leukaemia viruses encoded by a single gene at Rmc1. Nat. Genet *21*, 216-219.

Yanovsky, M.J., and Kay, S.A. 2002. Molecular basis of seasonal time measurement in *Arabidopsis*. Nature 419, 308-312.

Yoo, S.K., Chung, K.S., Kim, J., Lee, J.H., Hong, S.M., Yoo, S.J., Yoo, S.Y., Lee, J.S., Ahn, J.H. 2005. CONSTANS activates SUPPRESSOR OF OVEREXPRESSION OF CONSTANS 1 through FLOWERING LOCUS T to promote flowering in. Arabidopsis. Plant Physiol. 139, 770–778.

Zhang, W., Ito, H., Quint, M., Huang, H., Noël, L.D., Gray, W.M. (2008). Genetic analysis of CAND1-CUL1 interactions in Arabidopsis supports a role for CAND1-mediated cycling of the SCF^{TIR1} complex. Proc Natl. Acad. Sci. U S A *105*, 8470-8475.

Zhang, X.N., Wu, Y., Tobias, J.W., Brunk, B.P., Deitzer, G.F., Liu, D. (2008). HFR1 is crucial for transcriptome regulation in the cryptochrome 1-mediated early response to blue light in Arabidopsis thaliana. PLoS ONE *3*, e3563.

Zhao, D.Z., Wang, G.F., Speal, B., and Ma, H. (2002). The excess microsporocytes1 gene encodes a putative leucine-rich repeat receptor protein kinase that controls somatic and reproductive cell fates in the Arabidopsis anther. Genes Dev *16*, 2021-2031.

Zhou, Y., and Ni, M. (2009). SHORT HYPOCOTYL UNDER BLUE1 truncations and mutations alter its association with a signaling protein complex. *submitted*

Zhou, Y., and Ni, M. (2009). SHB1 plays dual roles in photoperiodic and autonomous flowering. Developmental Biology *331*, 50-57.

Zhou, Y., Zhao, X.Y., Kang, X., Zhang, X.S., Ni, M. (2009). SHORT HYPOCOTYL UNDER BLUE1 associates with *MINISEED3* and *HAIKU2* promoters in vivo to regulate *Arabidopsis* seed development. Plant Cell *21*, 1-12.